BMR JOURNAL of Australian Geology & Geophysics

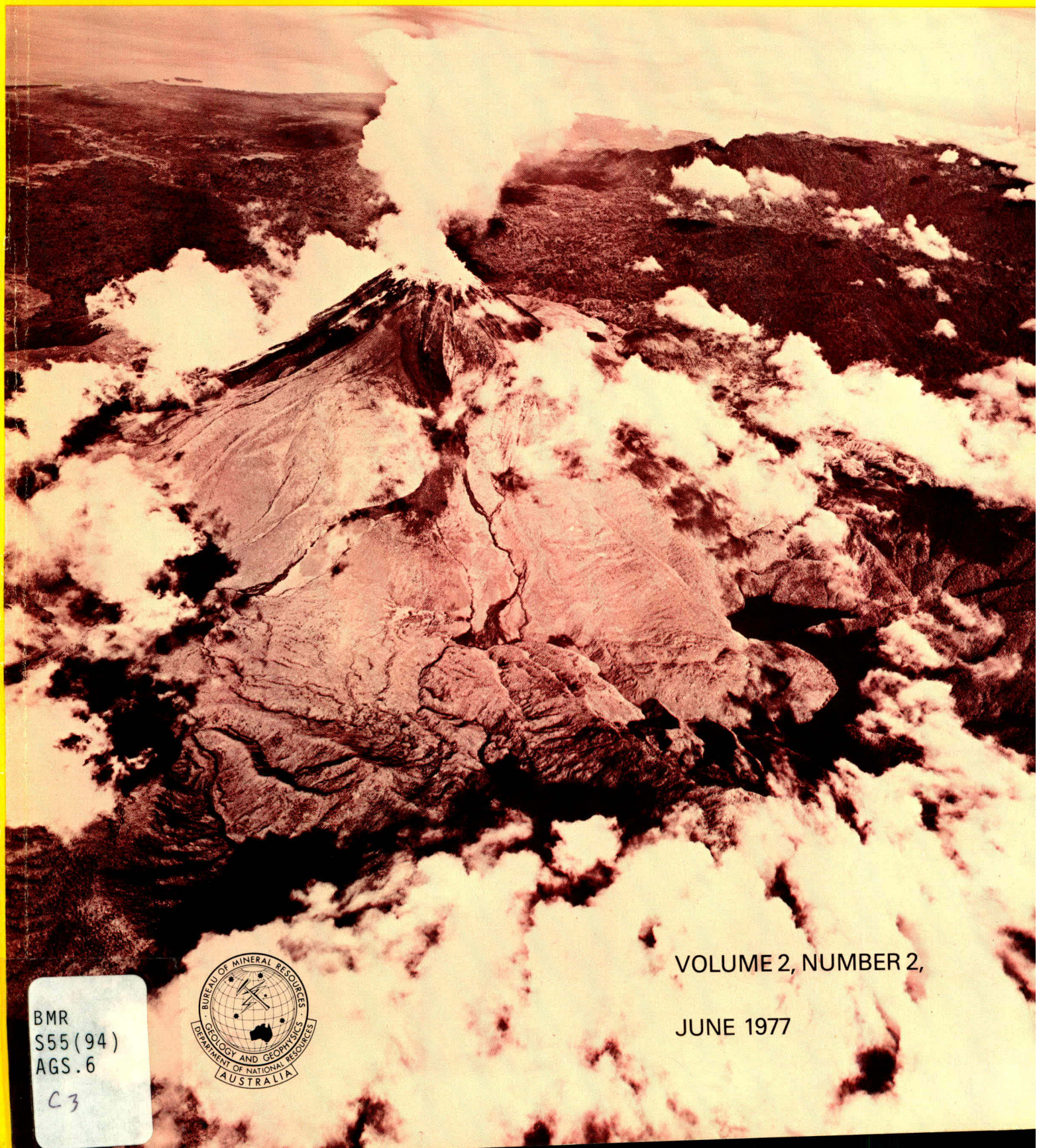

VOLUME 2, NUMBER 2,

JUNE 1977

Department of National Resources, Australia

Minister: The Rt Hon. J. D. Anthony, M.P.

Secretary: J. Scully

Bureau of Mineral Resources, Geology and Geophysics

Director: L. C. Noakes

Editor, BMR Journal: J. F. Truswell

The BMR Journal of Australian Geology and Geophysics is a quarterly journal of research and related activities. Contributions are from officers of the BMR, from BMR officers working in collaboration with others, or requested work sponsored by the BMR. In addition to articles the Journal may include shorter notes and discussion of papers published in it. Discussion of papers is invited from anyone.

Annual subscription to the Journal is at the rate of $10 (Australian). Individual numbers, if available, cost $3. Subscriptions, etc., made payable to the Receiver of Public Moneys in Australian dollars, should be sent to the Director, Bureau of Mineral Resources, Geology & Geophysics, P. O. Box 378, Canberra, A.C.T. 2601, Australia. The Journal can also be obtained from the offices of the Department of National Resources in Sydney and Melbourne.

Other matters concerning the Journal should be sent to the Director, marked for the attention of the Editor, BMR Journal.

B M R JOURNAL

of Australian Geology and Geophysics

Volume 2, Number 2

June 1977

AUSTRALIAN GOVERNMENT PUBLISHING SERVICE
CANBERRA 1977

Front cover:

Oblique aerial photograph of Bagana volcano, taken on 24 April 1971.

Bagana is considered to be the most consistently active volcano in Papua New Guinea and its 1370 m cone may have built up since the end of the Pleistocene.

Bagana is described in a paper in

JOHNSON, R. W. (Editor), 1976—VOLCANISM IN AUSTRALASIA; a collection of papers in honour of the late G. A. M. Taylor, G. C. *Elsevier. Amsterdam.*

Photograph: Qasco Pty. Ltd.

ISSN 0312-9608

Printed by Kerton Bros (S.A.) Pty Ltd, Edwardstown, S.A.

The late Cainozoic sequence of southeast South Australia and Pleistocene sea-level changes

*P. J. Cook[1], J. B. Colwell, J. B. Firman[2], J. M. Lindsay[2], D. A. Schwebel[3], & C. C. Von der Borch[3].**

A recent drilling program in southeast South Australia has provided new insight into the late Cainozoic sequence of that area. Uplift of the region occurred during the Pleistocene, related in part to volcanic activity in the Mount Gambier-Mount Burr area. This, together with eustatic sea-level changes, resulted in the development of a regressive sequence, which over a period of 690 000 years or less, led to a 100 km seaward progradation of the shore-line between Naracoorte and Robe. The sequence is made up of a ridge-forming sandy facies comprising beach and very shallow marine sands at the base, and aeolian sands at the top. These sediments are separated by a fine-grained interdunal facies deposited initially under bay or estuarine conditions, grading into lagoonal and finally saline lacustrine conditions at the top. The sequence between Naracoorte and Robe holds great promise as a location for establishing Pleistocene sea-level changes. The current program suggests at least 20 major high sea-level stands during the past 690 000 years.

Introduction

The late Cainozoic sediments of southeast South Australia have been the subject of a number of studies since late in the nineteenth century when Clark (1896) and Tate (1898) first described them. Subsequent work by Sprigg (1952a, b, 1958), Hossfeld (1950), Blackburn (1966a, b) and Firman (1967, 1969, 1973) has added considerably to our knowledge of the area. These authors are generally agreed that the beach-dune sequence west of Naracoorte is regressive, with the sand ridges having formed as shoreline accumulations during high sea-level stands in the Pleistocene. Several of these authors pointed out the potential that the area has for elucidating Pleistocene sea-level changes. Sprigg (1952a, b) in particular attempted to determine a sea-level curve using the relative elevation of the sand ridges and the Milankovitch astronomical theory. However, these and all other attempts have suffered both from the lack of absolute ages on any of the dunes and also from incomplete information on the Pleistocene stratigraphy. In an attempt to provide detailed stratigraphic information and also material suitable for dating high sea-level stands, the Bureau of Mineral Resources, the Geological Survey of the South Australian Department of Mines, and the Department of Marine Geology in Flinders University undertook a detailed study of the coastal sequence between Robe and Naracoorte (Fig. 1). The original intention was to drill a continuously cored hole on every ridge and every intervening flat between Naracoorte and the coast. Subsequently, it was decided also to drill a number of holes off the main traverse line to provide information on the attitude of the Oligo-Miocene Gambier Limestone surface. In addition, a number of holes were drilled in the Bordertown-Keith area because it was suspected that some of the sand ridges in that area were not represented in the Robe-Naracoorte area. All drill sites were subsequently accurately levelled. This publication briefly summarizes the general stratigraphic results obtained from this program. Subsequent publications will provide extended discussions on the regional stratigraphy, mineralogy, absolute chronology and palaeontology of the sediments.

1. Research School of Earth Sciences, Australian National University, Canberra, A.C.T.
2. Geological Survey of South Australia, Department of Mines, Adelaide, South Australia.
3. Department of Marine Geology, Flinders University, South Australia.

* Except for P. J. Cook, names are in alphabetical order.

Tectonic-volcanic activity

The tectonic setting of southeast South Australia has been largely responsible for creating an environment favourable for the preservation of a unique record of sea-level changes.

Prominent faults disrupt Mesozoic strata, but throws on faults diminish through the Cainozoic sediments. The only important fault affecting late Cainozoic sedimentation in the Naracoorte area is the Kanawinka Fault (or faults if the structure is complex), which trends northwest parallel to the Naracoorte Ranges (Figs. 1 and 2) and which has exercised structural control on the distribution of the East Naracoorte Range. This fault system terminates in crystalline basement west of Bordertown. Evidence from the displacement of the top of the *Victoriella conoidea* zone of the Gambier Limestone suggests that the total throw on this fault system at Naracoorte is about 40 m (Fig. 2). The fault system further to the southeast broadly marks the boundary between Cainozoic sequences of the Murray Basin to the north and east, and those of the Gambier Embayment in the Otway Basin to the south and west. Recent work by Singleton *et al.* (1976) suggests that there was movement on the Kanawinka Fault between about 2.2 and 1.7 m.y. and it is likely that there has also been further movement since.

Volcanic activity in the region has occurred throughout the Cainozoic, though there were periods of maximum volcanicity in the Palaeocene-Eocene and Plio-Pleistocene (Abele, 1976; Singleton and Joyce, 1969; Wellman, 1974). Volcanism has occurred during development of the beach-dune sequence (Sprigg, 1952b) and Holocene ash falls of 4830 years BP (Ferguson & Rafter, 1957) and 1410 ± 90 years BP (GAK—609:1956) (Blackburn, 1966b) have been recorded. Legend suggests that volcanism was witnessed in the region by ancestors of the modern aboriginal (Smith, 1880).

Broad regional upwarping occurred during the Plio-Pleistocene. Volcanism also took place at this time in the Mount Gambier-Mount Burr area. Topographic contours on the Penola 4-Mile Sheet (Sprigg *et al.*, 1951) and the elevation of the surface of the Gambier Limestone (which represents the base of the subsequent regressive sequence), indicate that uplift is related to these volcanic centres (Fig. 2) —though the precise nature of this correlation is uncertain. As other workers (Hossfeld, 1950; Sprigg, 1952; Kenley, 1976) have indicated, there is a broad northeast-trending culmination, with a prolonged history of pre-Pliocene movement in the region. In the gently upwarped Robe-Naracoorte area, sand ridges have been stranded at

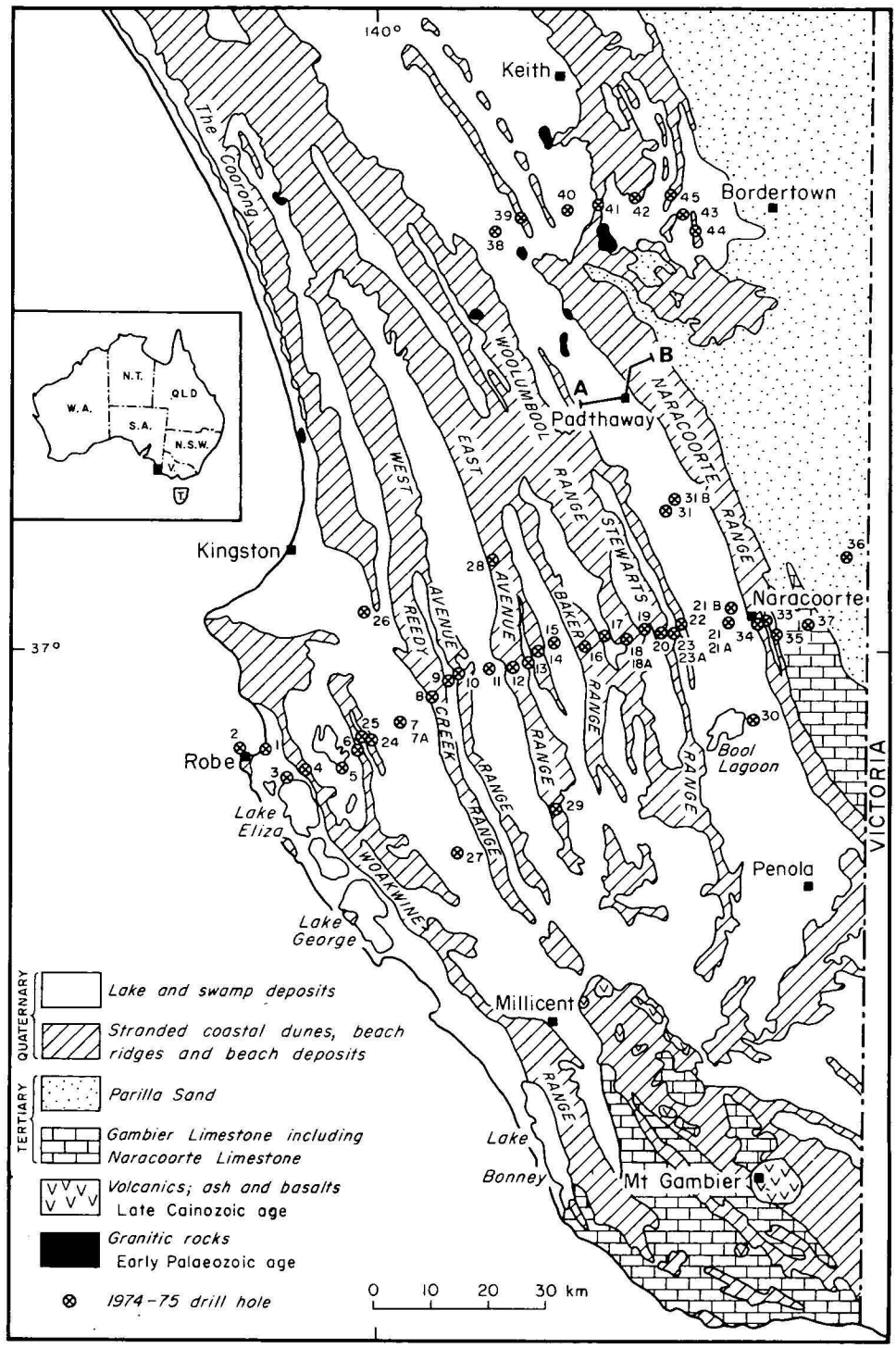

Figure 1. The geology of southeast South Australia. Location of holes drilled during the 1974-75 program are also shown.

successively greater elevation, suggesting monotonic uplift throughout the Pleistocene.

The Pre-Pleistocene sequence

West of Naracoorte the Cainozoic sequence is typical of the Murray Basin rather than the Gambier Embayment of the Otway Basin. Late Pliocene Parilla Sand is close to ground surface and overlies early Pliocene Loxton Sands (Fig. 3). The eroded edge of the sequence along the Kanawinka Scarp (that formed a barrier to the inland penetration of the Pleistocene sea) is veneered by a silicified ferruginous crust of late Pliocene or early Pleistocene age (Kenley, 1971; Firman, 1973; Gill, 1973; Abele *et al.*, 1976) which slopes down towards the coastal plain.

There is a marked unconformity at the base of the Pleistocene sequence throughout much of the region. To the north of Naracoorte, in the Keith-Bordertown area, Pleistocene sediments overlie Lower Palaeozoic granites, Knight Group or Buccleuch Beds (Eocene), Ettrick Formation or Gambier Limestone (Oligo-Miocene), or Pliocene sands (Fig. 3). West of the Naracoorte area, Pleistocene sediments overlie a Pliocene sand, whereas further south they rest on Oligo-Miocene Gambier Limestone. All of these units,

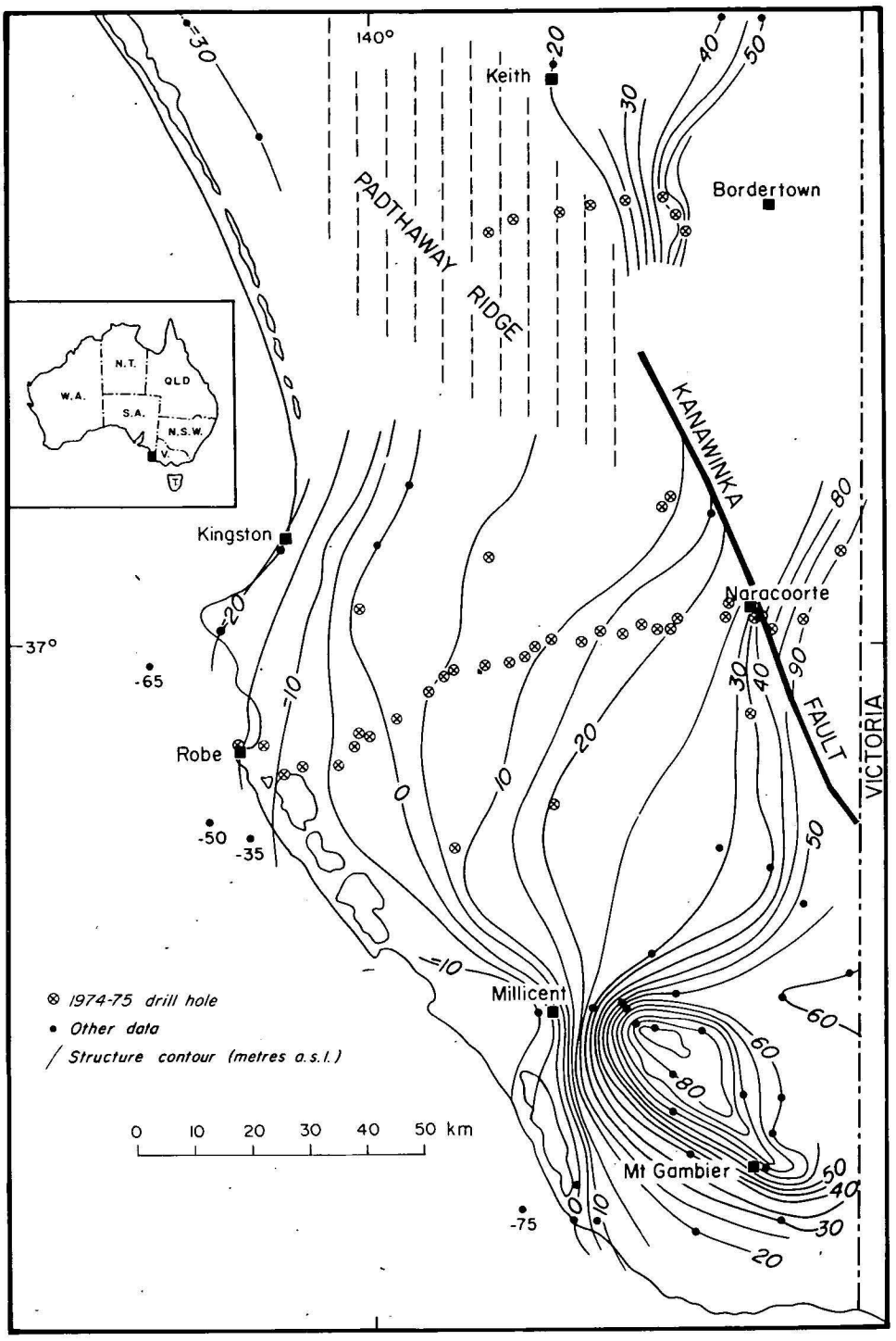

Figure 2. Elevation of the upper surface of the Gambier Limestone (including the Naracoorte Limestone east of Naracoorte).

except for the Pliocene sand, have been discussed in some detail by previous authors including Ludbrook (1961, 1969), Lawrence (1966) and Firman (1973), and need not be considered here. The relationship of these various units is shown in Figure 3.

The Pliocene sand in southeastern South Australia was little known prior to the present program, although a possible correlative is recorded by Kenley (1971), and Abele *et al.*, (1976), from western Victoria. It does not outcrop in the Robe-Naracoorte area, and its unconsolidated nature made sampling difficult by the previously used percussion drilling method. It is present throughout the eastern half of the area where it is up to 17 m thick, and comprises light grey, muddy in part, micaceous (muscovitic), moderately sorted mostly unconsolidated calcareous quartz sand. At the base, there is commonly a conglomerate with chert pebbles up to 2 cm in diameter.

Whole and fragmentary shells are abundant in the basal few metres. Benthonic foraminifera are mostly *Ammonia beccarii* (Linne) and species of *Elphidium*, *Discorbis*, and miliolids. The planktonic foraminifera include *Globorotalia puncticulata* (Deshayes), and *Globigerina foliata* (Bolli), which would suggest an early Pliocene age according to ranges given by Blow (1969). Also near the base of the sand,

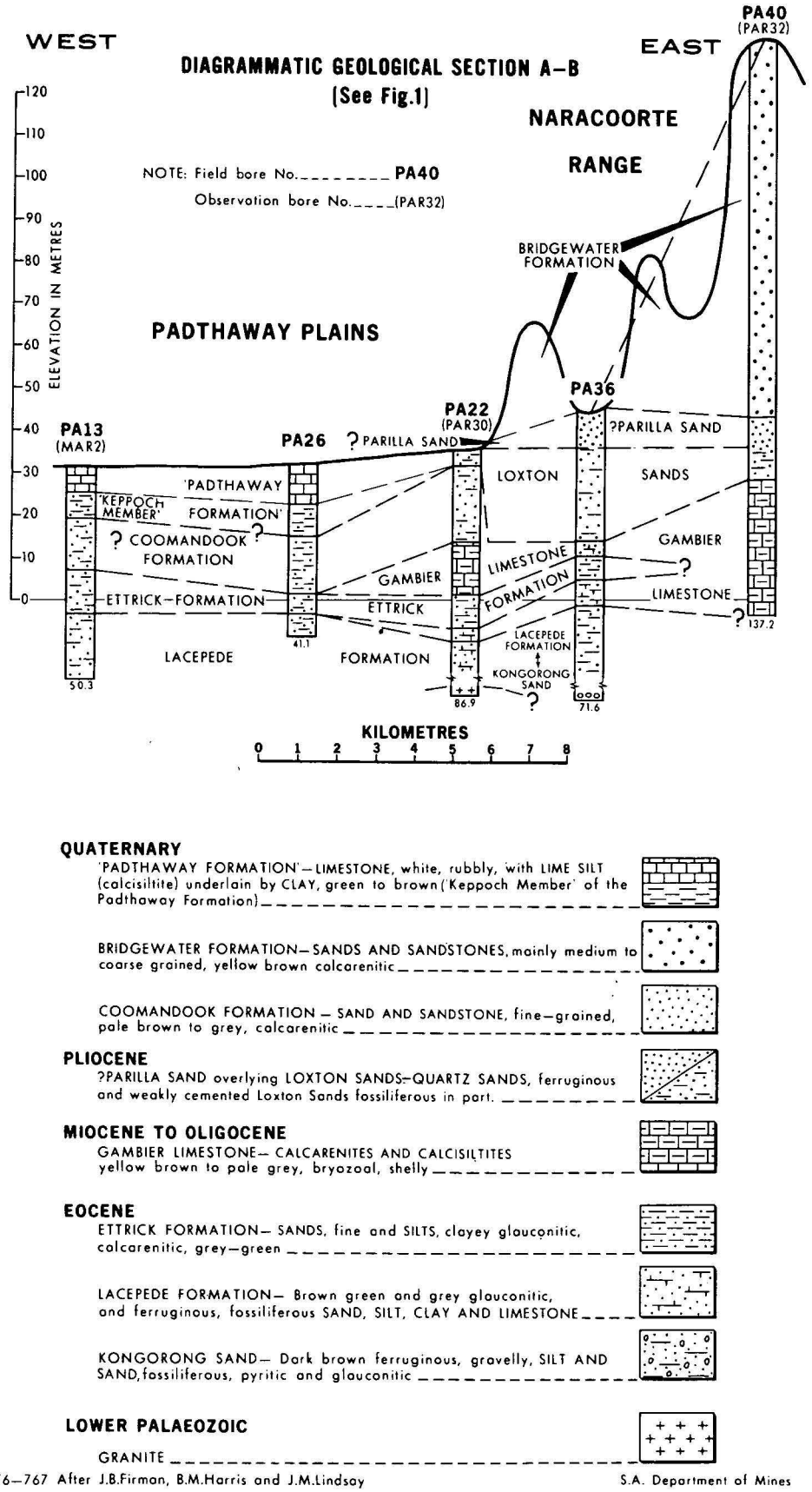

QUATERNARY

'PADTHAWAY FORMATION'—LIMESTONE, white, rubbly, with LIME SILT (calcisiltite) underlain by CLAY, green to brown ('Keppoch Member' of the Padthaway Formation)

BRIDGEWATER FORMATION—SANDS AND SANDSTONES, mainly medium to coarse grained, yellow brown calcarenitic

COOMANDOOK FORMATION — SAND AND SANDSTONE, fine–grained, pale brown to grey, calcarenitic

PLIOCENE

?PARILLA SAND overlying LOXTON SANDS–QUARTZ SANDS, ferruginous and weakly cemented Loxton Sands fossiliferous in part.

MIOCENE TO OLIGOCENE

GAMBIER LIMESTONE— CALCARENITES AND CALCISILTITES yellow brown to pale grey, bryozoal, shelly

EOCENE

ETTRICK FORMATION— SANDS, fine and SILTS, clayey glauconitic, calcarenitic, grey–green

LACEPEDE FORMATION— Brown green and grey glauconitic, and ferruginous, fossiliferous SAND, SILT, CLAY AND LIMESTONE

KONGORONG SAND— Dark brown ferruginous, gravelly, SILT AND SAND, fossiliferous, pyritic and glauconitic

LOWER PALAEOZOIC

GRANITE

76—767 After J.B.Firman, B.M.Harris and J.M.Lindsay S.A. Department of Mines

Figure 3. Diagrammatic geological section A—B (see Fig. 1 for location) to illustrate stratigraphic relationships in the Padthaway area of southeast South Australia.

benthonic foraminifera *Crespinella umbonifera* (Howchin & Parr), and *Fabularia howchini* (Schlumberger) support an early Pliocene age—the former not being known from above early Pliocene Loxton Sands in the Murray Basin (Ludbrook, 1961), and the latter having been described from the Kalimnan Stage, early Pliocene. The fauna indicates that the sand was deposited under shallow marine conditions. At least the basal part of this unit seems to correlate with the early Pliocene Loxton Sands of Ludbrook (1961, 1963). More precise correlations must await more detailed biostratigraphic studies in progress by J. M. Lindsay, but spatial relationships suggest that the unit in the Naracoorte area comprises downfaulted and eroded Pliocene sands at the base, overlain by Pleistocene sands.

The Pleistocene sequence

As a result of the drilling program between Robe and Naracoorte it is possible to now draw up a detailed stratigraphic cross-section for the Pleistocene sequence (Fig. 4). This section demonstrates that uplift continued throughout much of the Pleistocene, leading to progressive uplift of succeeding sand ridges. With the exception of the Kanawinka Fault, based on the *Victoriella conoidea* datum level, there appears to have been only minor faulting of the Gambier Limestone and younger sediments in this area. The Gambier Limestone in particular shows a very uniform seaward dip throughout. The amount of erosion which occurred prior to the deposition of the Pleistocene sequence is uncertain. The lack of Pliocene sand west of Reedy Creek Range is probably a consequence of one or more periods of erosion in the area. Work in progress by Colwell indicates some of the heavy minerals in the Pleistocene sands are likely to have been derived from the Pliocene sand.

The Pleistocene sequence considered overall is a sporadic regressive sequence in which repeated eustatic sea-level fluctuations have been imprinted on the gently uplifting coastal plain. Two main facies are apparent: a coarser beach-dune (sand ridge) facies separated laterally by finer estuarine-lagoonal and lacustrine (inter-ridge flat) facies.

Beach-Dune Facies

Sediments of this facies form the sand ridges of the region, rising up to 50 m above the adjacent plain. They are equivalent to the calcareous aeolianites which Boutakoff (1963) assigned to the Bridgewater Formation. There is a marked unconformity at the base of this unit throughout much of the region. The calcarenites contain on average about 50 percent carbonate; however, the carbonate abundance is variable, ranging from less than 10 up to 100 percent. Ridges to the east of Reedy Creek Range were found to be significantly less calcareous than those to the west. This is possibly due to the contribution of sediment to these older ridges from the quartzose Pliocene sand eroded from the western end of the section. However, increasing age of ridges to the east may also be responsible for the variations in carbonate content. The calcarenites are composed of fine to very coarse, rounded and fragmentary, skeletal carbonate grains, together with fine to medium, moderately rounded to well rounded, detrital grains (mainly quartz with minor feldspar and trace amounts of heavy minerals). Calcareous intraclasts derived from older indurated calcarenites contribute to the calcareous component in places. Sparry calcite forms the cement in the majority of the sands.

Cross-bedding is a common feature both in outcrops (mainly road cuttings and drainage channels) and in cores.

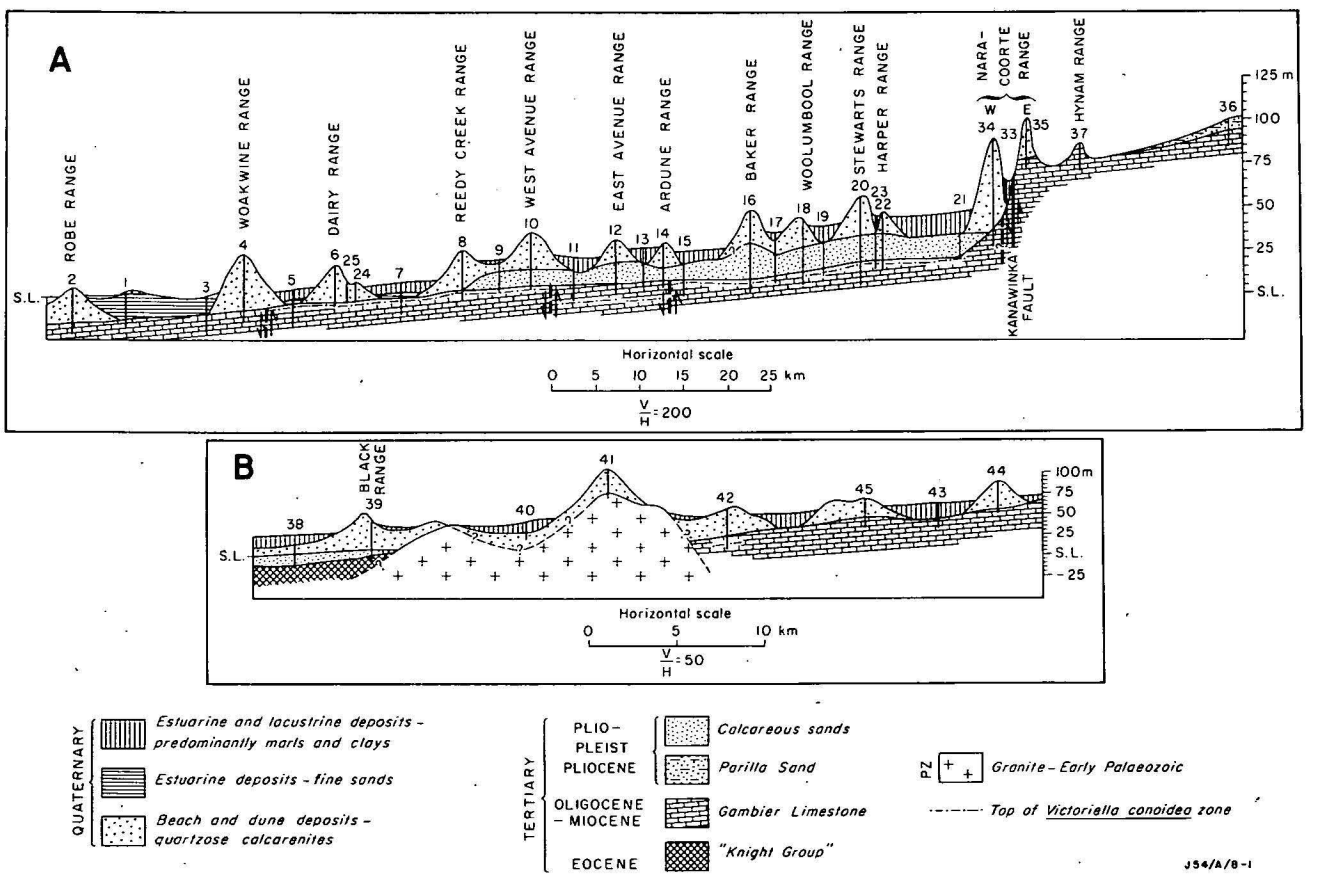

Figure 4. Sections through beach ridge sequence in (A) the Robe-Naracoorte area and (B) the Bordertown area.

A notable feature of the cross-bedding is that it is commonly more gently dipping at the base of the sequence. This, together with the downward increase of shelf-derived skeletal material, suggests that the lower part of the sequence was deposited in a beach or near-beach environment, whereas the upper part of the sequence was deposited under aeolian conditions. Clearly, the identification of this beach-aeolian interface is important in the determination of the altitude of a high sea-level stand.

The calcarenites range from pale grey (especially near the base) to light brown at the top. This simple pattern is complicated in the West Naracoorte Range by the presence of four well-defined iron-rich red-brown horizons, believed to be palaeosols. The absence of soils within the four sand ridges to the east of the Black Range in the Bordertown area (Figs. 1, 4) supports the thesis that the West Naracoorte Range is a composite feature which divides into its four component ridges north of Padthaway (Fig. 1).

The Woakwine Range is also a composite feature, and the presence of indurated surfaces marked by gravels and reefal molluscan faunas indicate five separate periods of beach-dune formation (Schwebel, in prep). Calcretes which are believed to have been deposited on erosional surfaces are also present within beach-dune sands in places. Firman (1973) reports a calcrete (probably Ripon Calcrete) in the Naracoorte Range at the contact between lower and upper sand units, which he equates with the lower and upper members of the Bridgewater Formation.

Estuarine-Lagoonal and Lacustrine Facies

These facies, which underlie the flat swampy areas between the ranges, become increasingly, though somewhat irregularly, thicker from west to east, reaching a maximum thickness of about 13 m in drill-hole 21 (Fig. 4). The sediments are predominantly calcareous muds, with variable amounts of calcite, aragonite and dolomite. These carbonates are characteristically pale grey and white, and have poorly developed bedding. Intraclastic breccias (probably associated with periods of dessication) are common. Coquinas and scattered individuals of the gastropod *Coxiella striata* (Reeve) (=*Coxiella confusa* (Smith)) indicate saline conditions. These calcilutites and dololutites are entirely of lagoonal or estuarine origin. In places, green to olive grey non-calcareous and poorly calcareous muds of bay or estuarine origin are present in the lower part of the sequence. Estuarine sediments (the "Anadara Beds" of Sprigg, 1952; Glanville Formation of Firman, 1973), which occur between the Woakwine and Reedy Creek Ranges, are composed mainly of the bivalves *Anadara trapezia* (Deshayes) and Katelyina sclarina (Lamarck), and some *Ostrea sinuata* (Lamarck).

The estuarine-lagoonal and lacustrine facies do not necessarily follow a pattern of a landward increase in age. This is for two reasons: firstly, because inter-dune lacustrine calcilutites, dololutites and peat deposits are being deposited inland at the present day (von der Borch, 1977); and secondly, because of the gentle gradient of the coastal plain, a small rise in sea-level (such as that represented by the "Anadara Beds"), may inundate topographically low areas behind sand ridges inland from the current coastline. Nevertheless, as a general rule, the sediments at the base of the various flats may reasonably be assumed to become progressively older to the east.

Dating of the Pleistocene sequence

Absolute age dating of the estuarine-lagoonal and lacustrine sediments has been undertaken to a limited extent. Radiocarbon ages of 22 000 ± 600 years BP and 26 600 ± 800 years BP were obtained on lacustrine calcilutites at depths of 2.3 m and 2.9 m respectively in drill-hole 21 (Fig. 4). Blackburn (1966b) has also carried out radiocarbon dating on shell material from the sediments to the west of the Reedy Creek Range. These results support a relatively young age for the surficial sediments between the Robe and Woakwine Ranges. A sample of the mollusc *Anadara trapezia* from the Lake Hawdon area gave an age of 24 950 ± 300 years BP. This must be regarded as an absolute minimum age—its true age is probably significantly greater. Other molluscs dated from the same area have ages in excess of the radio carbon dating range. The estuarine sediments of the flat between the Reedy Creek and Woakwine Ranges must then be considered to be undatable by radiocarbon methods. However, C^{14} dates on superficial dolomite mud from an ephemeral lake on one of the innermost inter-dune flats near Naracoorte gave an age of 1320 years (von der Borch, 1977) indicating that carbonates are probably still forming from groundwaters which seasonally discharge into some of the inland lakes.

The uranium series dating method offers a possible dating tool for the period less than 250 000 years. Attempts have been made by Gill (1974), and Gill & Amin (1975), to date molluscan material using this technique. They believe that it is possible to recognize a high sea level of 107 000 years age at Port Fairy. However, the results of Kaufman *et al.* (1971), indicate that uranium series dating of molluscs is generally unreliable, and that estimates of age must be regarded with extreme caution. A more promising approach may be the uranium series dating of aragonitic marls. Schwebel is currently undertaking this work following the approach outlined by Kaufman (1971), who obtained acceptable Th^{230}/U^{234} ages from the Dead Sea Basin aragonitic marls.

The age of the sand ridges has been a controversial question for some time. Crocker & Cotton (1946) considered that the sequence was deposited in the early Pleistocene. Others such as Hossfeld (1950) considered that the sequence was deposited entirely in the late Pleistocene, but Boutakoff (1963) suggested that the Bridgewater Formation in western Victoria was deposited during most of Quaternary time. Firman (1969) subdivided the sequence overlying late Pliocene marine sediments in South Australia into three units (with time connotations) referred to the lower, middle and upper Pleistocene, the Bridgewater and associated calcretes of the Naracoorte area and along the coastal margin forming the middle Pleistocene sequence. Subsequently the beach-dune facies and associated calcrete between Robe and Naracoorte were assigned by Firman (1973) to the upper member of the Bridgewater Formation. Sprigg (1952, Fig. 42) suggested from his correlations with the Milankovich Curves that the sequence to the west of the West Naracoorte Range was 540 000 years or less in age.

Fossils are abundant within the beach-dune sediments of the Robe-Naracoorte area. However, most are strongly abraded and none are biostratigraphically diagnostic. The present program was in part initiated in the hope of obtaining aragonite which could then be dated by uranium-series dating, and the search for suitable material is proceeding at the present time. Magnetostratigraphy, which has been applied to the sequence to a limited extent, has shown that all the calcarenites are normally polarized, with the exception of those of the East Naracoorte Range which are reversely polarized (Idnurm, pers. comm.). The implication of this is that the East Naracoorte Range formed during the Matuyama Reversed Polarity Epoch and is therefore older than about 690 000 years BP, whereas all the dunes to the west formed during the Brunhes Normal

Polarity Epoch and are therefore 690 000 years BP or younger.

Discussion

The main purpose of this paper is to elucidate the nature of the Pleistocene sequence in southeast South Australia. The data are clearly inadequate at the present time to allow us to precisely define a Pleistocene sea-level curve such as Chappell & Veeh (1977) have attempted. However, the information obtained from the drilling program shows that the section between Robe and Naracoorte is undoubtedly suitable for this purpose, provided material for absolute age dating can be obtained.

If the West Naracoorte Range is represented by four discrete ridges in the Bordertown area, and the Woakwine Range is a composite of five separate dune-forming events, then there are at least 20 separate strandline features, each representing a separate high sea-level stand between Naracoorte and the present-day coast. Palaeomagnetic evidence suggests that all these features were formed within the last 690 000 years.

Figure 4 shows the presence of three topographically defined groups of ridges and flats: (i) Robe Range to Reedy Creek Range; (ii) Reedy Creek Range to Baker Range; (iii) Baker Range to the West Naracoorte Range (and the range just to the west of Bordertown). The East Naracoorte Range is probably the sole remaining representative of a fourth sequence, but the interposing of the Kanawinka Fault makes it impossible to establish a relative chronology of the East and West Naracoorte Ranges, except that the East Naracoorte Range is older, with an age of greater than 690 000 years.

The division between the first and second group of ridges appears to have been particularly significant, as not only is there a major change in altitude, but to the west of the Reedy Creek Range there is also a marked increase in carbonate content of sands and almost complete erosion of the Pliocene sand. The third group is distinguished only by its higher elevation, corresponding in part to the greater length of time available for the deposition of lacustrine-swamp deposits. The reason for the development of the three groups of ridges and associated interdunes is uncertain at present. Their altitudinal differences are clearly not attributable to Pleistocene faulting because of the lack of corresponding faulting in the underlying Gambier Limestone as indicated by the elevation of the top of the *Victoriella conoidea* zone. To some extent the difference in level between the three topographically defined areas is due to differences in elevation of interdune deposits rather than of beach-dune deposits. The change in altitude may result from changes in the rate of uplift, producing differential elevations, though the regularity of the dip of the Gambier surface does not support this. Alternatively, the altitude differences may result from three periods of rapidly fluctuating sea level being separated by two prolonged periods of relatively stable sea level.

Conclusions

(i) An early Pliocene marine sand was deposited on Gambier Limestone in parts of southeast South Australia. It is recognized in several localities west of the Kanawinka Fault, but has been locally removed by Pleistocene erosion west of Reedy Creek Range.

(ii) Uplift of the region continued throughout the Plio-Pleistocene. At times there was associated volcanic activity in the Mount Gambier-Mount Burr region.

(iii) The entire sequence of dunal-interdunal sediments between Naracoorte and Robe (a distance of approximately 100 km) was deposited during the Pleistocene (during the last 690 000 years).

(iv) The sequence, which comprises a beach-dune facies, and estuarine-lagoonal and lacustrine facies, is essentially regressive. However, it may not be quite the regular regression previously assumed by some authors, as a number of dunes appear to be composite sand ridges reflecting more than one sea-level change. In addition, the altitudinal grouping of the sand ridges and intervening flats may also be a consequence of fluctuations in the rate of sea-level changes.

(v) During the last 690 000 years there have been at least 20 high sea-level stands.

Acknowledgements

The work of Mr L. Pain of BMR in both the field and the laboratory made a most valuable contribution to the program. The drilling section of BMR undertook their work despite frequently adverse conditions. Radiocarbon ages were provided by the Radiocarbon Laboratory of the University of New South Wales. Levelling of drill sites was undertaken by the Australian Survey Office and the South Australian Department of Mines. Drs J. M. A. Chappell, H. A. Jones and G. E. Wilford offered editorial comments. Firman and Lindsay publish with the permission of the Director of the South Australian Department of Mines. Work by Schwebel and von der Borch was supported by a Flinders University Research Grant. Von der Borch also received financial assistance from the Australian Research Grants Commission.

References

ABELE, C., 1976—Tertiary-Introduction; *in* J. G. DOUGLAS & J. A. FERGUSON (Editors), GEOLOGY OF VICTORIA. *Geological Society of Australia Special Publication* **5,** 177-90.

ABELE, C., KENLEY, P. R., HOLDGATE, G. & RIPPER, D., 1976—Otway Basin, *in* J. G. DOUGLAS & J. A. FERGUSON (Editors), GEOLOGY OF VICTORIA. *Geological Society of Australia Special Publication* **5,** 198-299.

BLACKBURN, G., 1966a—Soil distribution and geomorphology of constructional coastal lowlands. *Transactions of the 9th International Congress of Soil Science,* 623-30.

BLACKBURN, G., 1966b—Radiocarbon dates relating to soil development, coast-line changes and volcanic ash deposition in South East South Australia. *Australian Journal of Science,* **29,** 50-52.

BLOW, W. H., 1969—Late middle Eocene to Recent planktonic foraminiferal stratigraphy; *in* P. BRONNIMANN & H. H. RENZ (Editors), *Proceedings of the 1st International Conference on Planktonic Microfossils,* Geneva 1967, **1,** 199-422.

BOUTAKOFF, N., 1963—The geology and geomorphology of the Portland area. *Geological Survey of Victoria—Memoir* **22.**

CHAPPELL, J. R. & VEEH, H. H., in press—Quaternary uplift and sea level changes in Portugese Timor and Atauro Island. *Geological Society of America—Bulletin.*

CLARKE, E. V., 1896—Notes on the geology of the Ninety Mile Desert. *Transactions of the Royal Society of South Australia,* **20,** 110-17.

CROCKER, R. L. & COTTON, B. C., 1946—Raised beaches of southeast South Australia. *Transactions of the Royal Society of South Australia,* **70,** 64-72.

FERGUSSON, G. T. & RATTER, T. A., 1957—New Zealand C^{14} age measurement—No. 3. *New Zealand Journal of Scientific Technology,* **38B,** 732-33.

FIRMAN, J. B., 1967—Late Cainozoic stratigraphic units in South Australia. *Geological Survey of South Australia—Quarterly Geological Notes* **22,** 4-7.

FIRMAN, J. B., 1969—Quaternary Period; *in* L. W. PARKIN (Editor), HANDBOOK OF SOUTH AUSTRALIAN GEOLOGY. *Geological Survey of South Australia,* Adelaide, 204-23.

FIRMAN, J. B., 1973—Regional stratigraphy of surficial deposits in the Murray Basin and the Gambier Embayment. *Geological Survey of South Australia—Report of Investigation* **39.**

GILL, E. D., 1973—Palaeopedology of the Murray River Region between Mildura and Renmark, Australia. *National Museum of Victoria—Memoir* **34,** 241-51.

GILL, E. D., 1974—Carbon—14 and Uranium/Thorium check on suggested inter-stadial high sea-level around 30,000 BP. *Search,* **5,** 211.

GILL, E. D. & AMIN, B. S., 1975—Interpretation of the 7.5 and 4 metre last interglacial shore platforms in Southeast Australia. *Search,* **6,** 349-96.

HOSSFELD, P. S., 1950—The late Cainozoic history of the southeast of South Australia. *Transactions of the Royal Society of South Australia,* **73,** 232-79.

KAUFMAN, A., 1971—U-series dating on Dead Sea Basin Carbonates. *Geochimica et Cosmochimica Acta,* **35,** 1269-81.

KAUFMAN, A., BROECKER, W. S., KU, T. L. & THURBER, D. L., 1971—The status of U-series methods of mollusc dating. *Geochimica et Cosmochimica Acta,* **35,** 1155-83.

KENLEY, P. R., 1964—Dartmoor 1:63 360 Geological Series, *Gelogical Survey of Victoria.*

KENLEY, P. R., 1971—Cainozoic geology of the eastern part of the Gambier Embayment, southwestern Victoria. *In* WOPFNER, H., & DOUGLAS, J. G. (Editors), The Otway Basin of Southeastern Australia. *Geological Surveys of South Australia and Victoria—Special Bulletin,* 89-153.

KENLEY, P. R., 1976—Southwest Victoria. *In* DOUGLAS, J. G. & FERGUSON, J. A. (Editors), GEOLOGY OF VICTORIA, *Geological Society of Australia—Special Publication* **5,** 290-8.

LAWRENCE, C. R., 1966—Cainozoic stratigraphy and structure of the Mallee region, Victoria. *Proceedings of the Royal Society of Victoria,* **79,** 517-53.

LUDBROOK, N. H., 1961—Stratigraphy of the Murray Basin in South Australia. *Geological Survey of South Australia—Bulletin* **36.**

LUDBROOK, N. H., 1969—Tertiary Period; *in* PARKIN, L. W. (Editor), HANDBOOK OF SOUTH AUSTRALIAN GEOLOGY. *Geological Survey of South Australia, Adelaide,* 172-203.

SINGLETON, O. P. & JOYCE, E. G., 1969—Cainozoic volcanicity in Victoria. *Geological Society of Australia—Special Publication,* **2,** 145-54.

SINGLETON, O. P., MCDOUGALL, I. & MALLETT, C. W., 1976—The Plio-Pleistocene boundary in Southeastern Australia. *Journal of the Geological Society of Australia,* **23,** 299-311.

SMITH, Mrs James, 1880—THE BOOANDIK TRIBE OF SOUTH AUSTRALIAN ABORIGINES. *Government Printer, Adelaide.* Also in facsimile edition, 1965.

SPRIGG, R. C., 1952a—Stranded Pleistocene sea-beaches of the southeast of South Australia and aspects of the theories of Milankovitch and Zeuner. *Report of the 18th International Congress,* **13** (Section M), 226-37.

SPRIGG, R. C., 1952b—The geology of the southeast province, South Australia, with special reference to Quaternary coastline migrations and modern beach development. *Geological Survey of South Australia—Bulletin* **29.**

SPRIGG, R. C., 1958—Stranded sea beaches and associated sand accumulations of the upper southeast. *Transactions of the Royal Society of South Australia,* **82,** 183-93.

SPRIGG, R. C., COCHRANE, G. W. & SOLOMON, M., 1951—Penola map sheet, Geological Atlas of South Australia, 1:250 000 series, *Geological Survey of South Australia.*

TATE, R., 1898—Two deep level deposits of Newer Pleistocene Age (Tintinara and Port Pirie). *Transactions of the Royal Society of South Australia,* **22,** 65-72.

VON DER BORCH, C. C., 1977—Stratigraphy and formation of Holocene dolomitic carbonate deposits of the Coorong area, South Australia. *Journal of Sedimentary Petrology (in press).*

WELLMAN, P., 1974—Potassium-argon ages on the Cainozoic volcanic rocks of eastern Victoria, Australia. *Journal of the Geological Society of Australia,* **21,** 359-368.

Absolute electromagnetic scale modelling and its use in interpretation of TEM response*

B. R. Spies

Scale model studies are often used to determine the distribution of secondary magnetic fields when the numerical approach is unreasonably difficult. Reduction in size (L) is compensated by an increase in conductivity (σ) or frequency (f), or both. In most cases the results are expressed in a way whereby they are independent of the absolute dimensions of the model and the general modelling relation

$$\sigma\mu fL^2 = \text{constant, is valid.}$$

However in some applications such as transient electromagnetic (TEM) modelling it is necessary to determine the power level of the full-scale system. An expression relating the voltage levels of the model and the full-scale system is:

$$V_m/V = L_m T/LT_m$$

where the subscript m represents the model system. This expression must be used in conjunction with the general modelling relation in order to compensate for changes in the modelling parameters.

It is possible to scale time, as well as dimensions and conductivity and, using the above relationships, many geological situations may be simulated with a single model. By varying either one of the parameters conductivity or dimensions while keeping the other constant, the same transient decay curve can be obtained by transposing the individual curves (plotted on a log-log scale) along the time and response axes.

An example illustrates that by modelling field cases absolute quantities such as conductivity can be estimated. Modelling of the Woodlawn orebody gave bulk conductivities of 5 S/m and 20 S/m.

The analysis of TEM data using early and late time responses must be done with care. The response typical of a late time may be similar to an early time response if the electrical or dimensional properties of the conductor are varied. More correctly one should analyse responses in terms of large and small values of the parameter $\sigma\mu L^2/T$.

Introduction

Scale model studies have been used for over 30 years to determine the response of electromagnetic exploration methods to simulated geological conditions and to assist in the design of field systems.

With the advent of computer facilities, numerical modelling methods have become popular; these include the finite element, finite difference, and integral equation methods (Praus, 1975). Numerical modelling methods are too difficult or too expensive in some applications, and scale model studies must be used. This is particularly true in the case of the transient electromagnetic (TEM) method because mathematical solutions are known only for simple models.

The Transient Electromagnetic Method

The transient electromagnetic method, developed in the USSR in the early 1960's, is described by Velikin & Bulgakov (1967). Briefly, the method involves pulsing a square wave of current into an ungrounded loop (see Fig. 1). The changing current in the loop generates a time-dependent magnetic field which causes eddy currents to flow in subsurface conductors. The secondary electromagnetic fields caused by changes in these eddy currents are detected in the same loop, and measured at various sample times ranging from 0.5 to tens of milliseconds. The results are displayed as curves of the voltage decay as a function of time, or transient decay curves, as shown in the bottom of Figure 1. Examples of the use of the TEM method in Australia are given by Spies (1976a).

Electromagnetic scale modelling

The first complete description of the basic theory of electromagnetic scale modelling was given by Sinclair in 1948. A good overall description of scale modelling is given in a paper by Frischknecht (1971). Briefly, scale modelling involves simulating geological conductors by small-scale models of a size that can be handled in a laboratory. The reduction in size is accompanied by an increase in conductivity, or frequency, or both.

Sinclair distinguished between two types of models, geometric and absolute. A geometric model is one in which only the geometric relationships of the electric and magnetic fields are simulated. An absolute model is one in which all scalar and vector components are simulated.

In most electromagnetic systems commonly used in geophysical exploration the parameters measured are

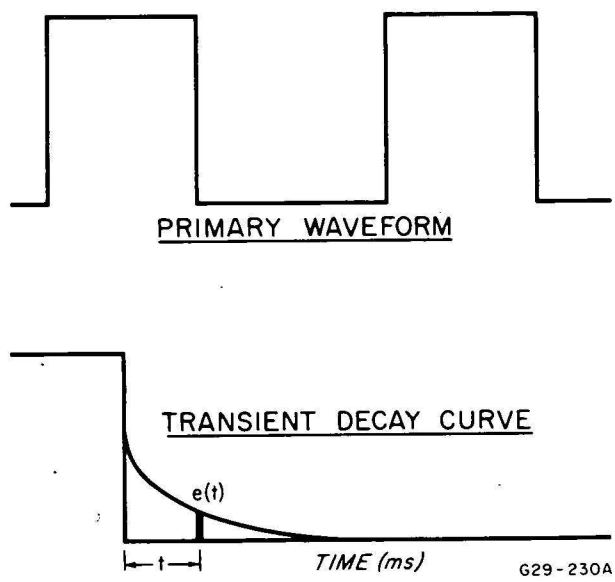

Figure 1. TEM waveforms.

* **Paper presented at 25th International Geological Congress, Sydney, August 1976.**

dimensionless (see Table 1), and model results can be expressed so that they are independent of the absolute dimensions of the model. Since only the geometric configuration of the lines of flux needs to be simulated, models of these systems are geometric models.

In the TEM method (Table 1) the quantity measured is a voltage induced in the loop; this voltage is normalized by dividing by the primary current. The quantity measured is not dimensionless and in fact will change if the conventional scale modelling relation (given in the next section) is used. This would also apply to the magnetotelluric method.

Geometric scale modelling

The relations for geometric scale modelling are:

Frequency domain

$$\sigma_f \mu_f f_f L^2_f = \sigma_m \mu_m f_m L^2_m$$

Time domain

$$\sigma_f \mu_f L^2_f / T_f = \sigma_m \mu_m L^2_m / T_m \quad \ldots . (1)$$

where σ = conductivity,
μ = magnetic permeability, usually assumed to be μ_o.
f = frequency,
L = linear dimension,
T = time.

In these expressions the subscript f refers to the full scale or field system and the subscript m refers to the model. Simply stated, these expressions state that an equivalent geometric response will be obtained if the product of conductivity, permeability, frequency (or 1/time), and linear dimension squared is kept constant.

Absolute scale modelling

The relationship for absolute scale modelling is

$$\frac{V_f}{V_m} = \frac{L_f}{L_m} \frac{T_m}{T_f} \quad \ldots . (2)$$

where V is the measured voltage and the other symbols are as defined earlier (Spies, 1976b). This expression states that the measured voltage will change in a manner proportional to the dimension-scaling factor and inversely proportional to the time-scaling factor.

When modelling systems such as TEM in which the measured quantity is not dimensionless, it is necessary to use the amplitude correction factor (2) in conjunction with the scale modelling relation (1). Sinclair called this type of model an absolute model.

Electromagnetic induction response

The response of induction methods is determined by "induction numbers" or "conductivity parameters" which have the same form as the dimensionless modelling parameter $\sigma\mu f L^2$. For example, the response of a sphere in a uniform alternating field is a function of the parameter $\sigma\mu\omega a^2$, where a is the radius of the sphere (Wait, 1953).

Similarly, the theoretical TEM response of a homogeneous half-space, given by Lee & Lewis (1974) is

$$\frac{e(t)}{I} = \frac{-2L\mu\sqrt{\pi}}{T} \cdot F\left(\frac{\sigma\mu L^2}{T}\right) \quad \ldots . (3)$$

where L is the loop radius.

This expression can be divided into two parts. The dimensionless quantity, $\sigma\mu L^2/T$, is the same parameter as used in the general modelling relation, and the expression $-2L\mu\sqrt{\pi}/T$ is proportional to L/T. If we wish to construct a model of a homogeneous half-space by varying linear dimensions and time, we can see that by keeping $\sigma\mu L^2/T$ constant the magnitude of the response, e(t)/I, will vary as we scale L and T.

Examples of absolute scale modelling

The results in this section were obtained using the scale model facility at Macquarie University, Sydney, which consists of an interactive mini-computer system.

The mini-computer, shown in the centre of Figure 2, is a 32K word Interdata 70, and is used for controlling output waveforms and timing. It is also used for data acquisition and subsequent processing.

The required waveform and sampling details are typed on the teletype shown in the figure, and are transferred by the computer to a small multi-turn loop placed on the model.

The resultant transient decay curve can be studied on a CRO, and then sampled, amplified and digitized, and printed on the teletype. A detailed description of this facility is given by Spies (in prep.).

Half-space model

Figure 3 shows a model of a homogeneous half-space constructed out of typemetal, which is an alloy of lead, antimony and tin. The model is only 8 cm thick, but because of its high conductivity is large enough to simulate a homogeneous half-space over a fairly wide time range. To attempt this with a tank of salt water would require a tank 15 m deep, which would be prohibitively large.

Table 2 shows the modelling parameters for the typemetal model. The model dimensions are 9520 times smaller

SYSTEM	QUANTITY MEASURED	UNITS
HORIZONTAL LOOP SLINGRAM	Ratio of coupling in air to coupling on earth	Dimensionless
TURAM	Amplitude ratio and phase difference of field in two loops	Dimensionless
DIP ANGLE VERTICAL LOOP	Dip of major axis of ellipse of polarization	Dimensionless
AFMAG	Azimuth and dip of major axis of ellipse of polarization	Dimensionless
VLF	Dip and ratio of axes of ellipse of polarization	Dimensionless
TEM	Rate of decay of secondary field normalized by primary current $\frac{V}{I}$	(volt amp^{-1})
MAGNETOTELLURIC	Electric field intensity normalized by magnetic field intensity $\frac{E}{B}$	(volt metre^{-1} tesla^{-1})

Table 1. Parameters measured in common electromagnetic systems.

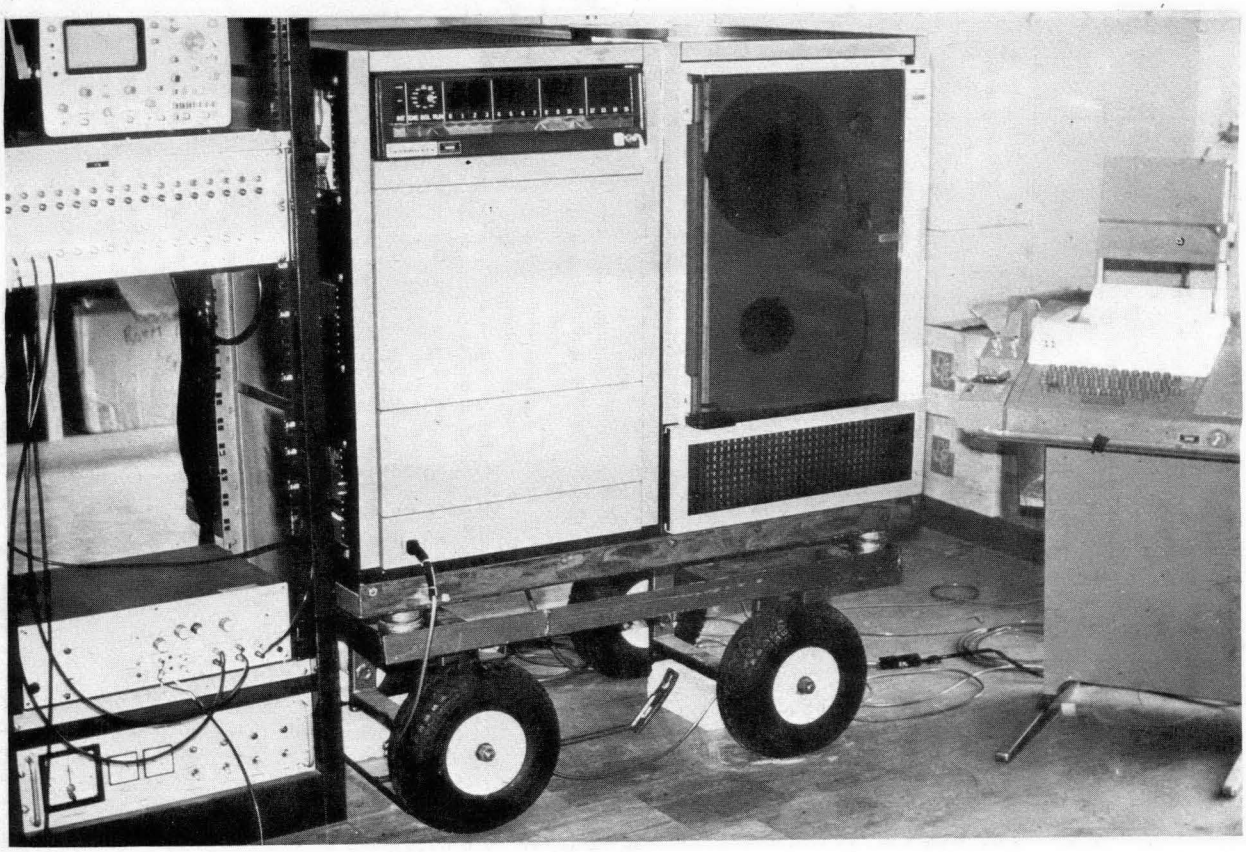

Figure 2. Scale model facility, Macquarie University, Sydney.

than the field dimensions, and the simulated half-space conductivity varies as the time-scaling factor. If we wish to simulate a conductivity of 0.1 S/m for instance, the general modelling relation shows that we must scale the time by a factor of 2.3. The condition relating to amplitude however requires that a correction of 4.1×10^3 be made to the amplitude. The same model can be used to simulate half-spaces of different conductivity simply by varying the time scaling factor.

	FIELD	MODEL
HALF-SPACE CONDUCTIVITY	0.1 S/m	3.9×10^6 S/m
Loop radius	100 m	1.05 cm
Time	1 ms	0.43 ms
$\sigma L^2/T$	10^6	10^6

Amplitude correction $\dfrac{V}{V_m} = \dfrac{L}{L_m} \cdot \dfrac{T_m}{T} = 4.1 \times 10^3$

Table 2. Modelling parameters used to simulate homogeneous half-space.

Figure 4 shows the readings obtained over the model, together with a curve of the theoretical response. The modelled readings have had the appropriate amplitude correction applied to them. The agreement between modelled and theoretical response is a good check on the modelling relations.

Cylinder model

We now go to a more complex example for which numerical results are not available. This example consists of

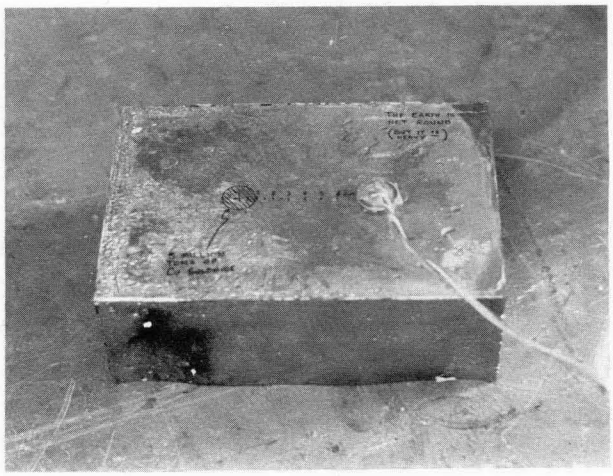

Figure 3. Model of a homogeneous half-space constructed out of typemetal.

cylinders of varying conductivity and size. The cylinders were constructed of copper, aluminium, brass, and typemetal, which gave a conductivity range of 5×10^6 to 5.8×10^7 S/m. The cylinders were either of 2 or 1.4 cm diameter, and the ratios between loop size, cylinder size, and depth in the two models were kept constant. The transient decay curves are shown in Figure 5.

We now show that by using the modelling relation all the models can in fact simulate one case, as long as the parameter $\sigma\mu L^2/T$ is kept constant. If we use different conductivities we scale time directly as conductivity. If we use different values of L (linear dimensions), we scale time as the square root of the dimension-scaling factor. We then obtain the results shown in Figure 6. For the cases in which L is

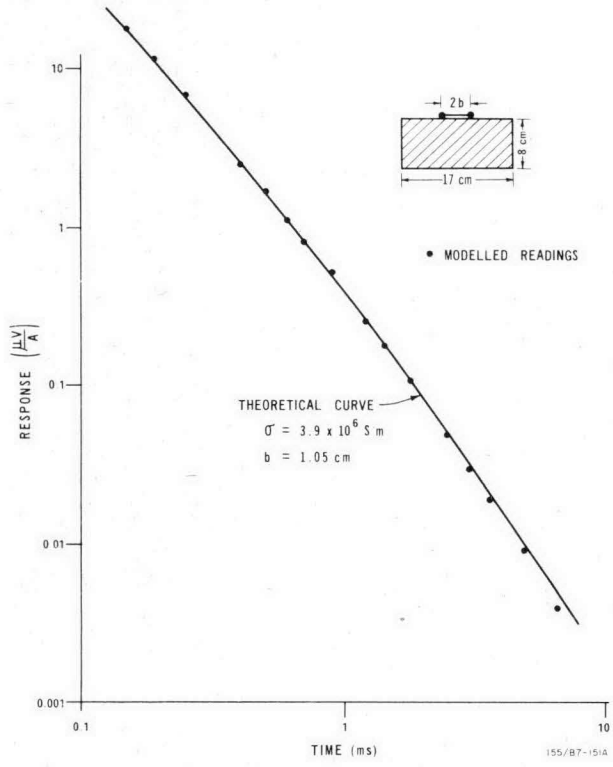

Figure 4. Comparison of modelled and theoretical TEM results from a homogeneous half-space.

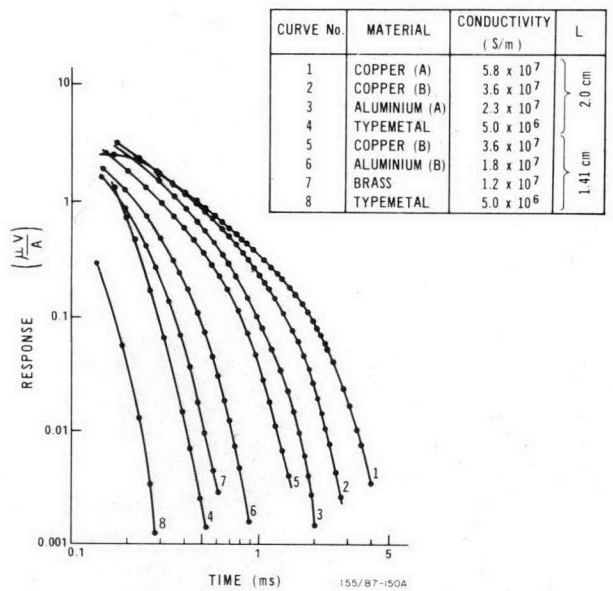

Figure 5. Transient decay curves over cylinders of different size and conductivity.

kept constant while σ is varied, only time is scaled and the amplitude correction factor V/V_m will be proportional to T_m/T. Similarly if σ is kept constant and L varied, T/T_m will be proportional to the square of L/L_m, and V/V_m will be proportional to the square root of T_m/T. If the curves are plotted on a log-log scale, the effect of scaling is a simple transposition of the curves along the time and response axes.

Thus we see that the transient decay curves were not unique. The same curve can come from a whole suite of models simply by varying the conductivity or geometry, provided that the modelling relation is adhered to.

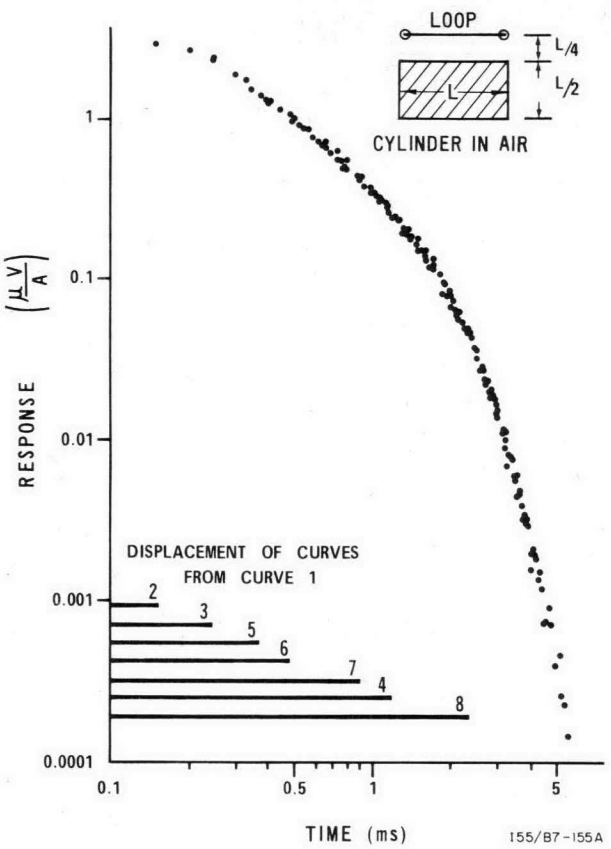

Figure 6. Composite curve obtained by applying the modelling relation.

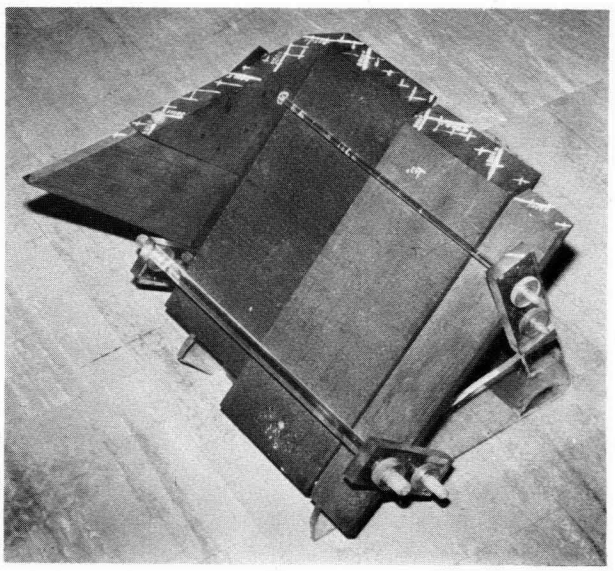

Figure 7. Scale model of Woodlawn orebody.

Woodlawn copper-lead-zinc-deposit model

This example is a model study of a field case, the base metal orebody at Woodlawn, near Tarago, NSW. The orebody is a concordant lens of bedded high grade copper-lead-zinc sulphides, 20 m thick, which dips at about 45°. The near-surface oxidized zone is about 12 m thick, consists mainly of ferruginous clay, and has a sharp contact with the sulphides. The shape of the body is known accurately from more than 100 drill holes. A detailed report of the geology of the orebody is given by Malone *et al.* (1975). Figure 7 shows a scale model of the massive sulphide orebody con-

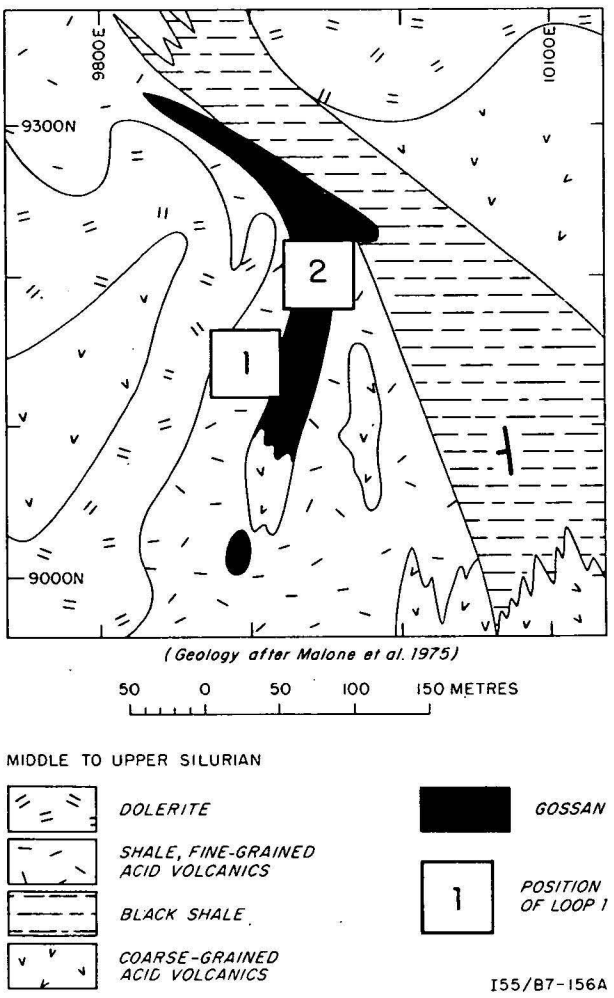

Figure 8. Surface geology and locality plan, Woodlawn orebody.

structed out of graphite. Dimensions are scaled down 670 times, so that the model is 31 cm long. Time can be scaled to allow a good fit between field and model curves, and estimates of conductivity can then be made. Figure 8 shows a plan of the Woodlawn deposit. Both BMR and CSIRO have carried out TEM test surveys at Woodlawn. Field curves shown in Figures 10 and 11 were obtained by CSIRO at positions 1 and 2 of Figure 8, using a sophisticated TEM system (Buselli, 1974).

Initially in modelling the Woodlawn deposit it was assumed the near-surface oxidized zone was resistive, but it was found that the field and model results were dissimilar for the early parts of the decay curves, in which near-surface effects are dominant.

In order to investigate the effect of a conductive near-surface zone, measurements were made with the model buried at various depths. Figure 9 shows transient decay curves at position 2 at depths of burial of 2, 6 and 14 m. The curves have been transposed on the time axis so that they coincide at late times. Because of the scale modelling relations, this also changes the simulated conductivity of the body. The best curve fit is for curve 1 (depth of 2 m and conductivity of 0.23 S/m) and so at Woodlawn the near-surface oxidized zone must be moderately conductive—and not resistive as suggested by earlier work.

Figures 10 and 11 show the model study and field curves from positions 1 and 2 respectively. Curve 1, Figure 10, is the original model study curve, without scaling time. In this loop position, by using the modelling relations, we have a conductivity of 0.23 S/m. However, we can see there is no

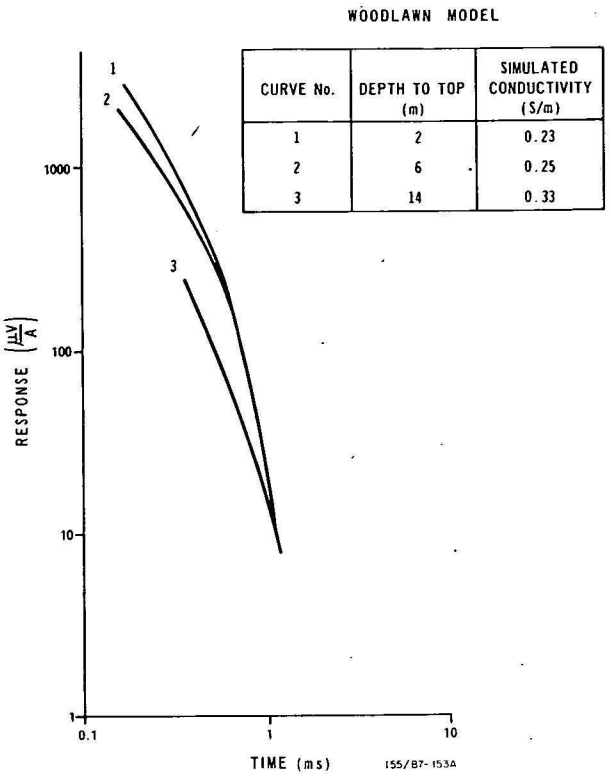

Figure 9. Model results for various depths, Woodlawn orebody.

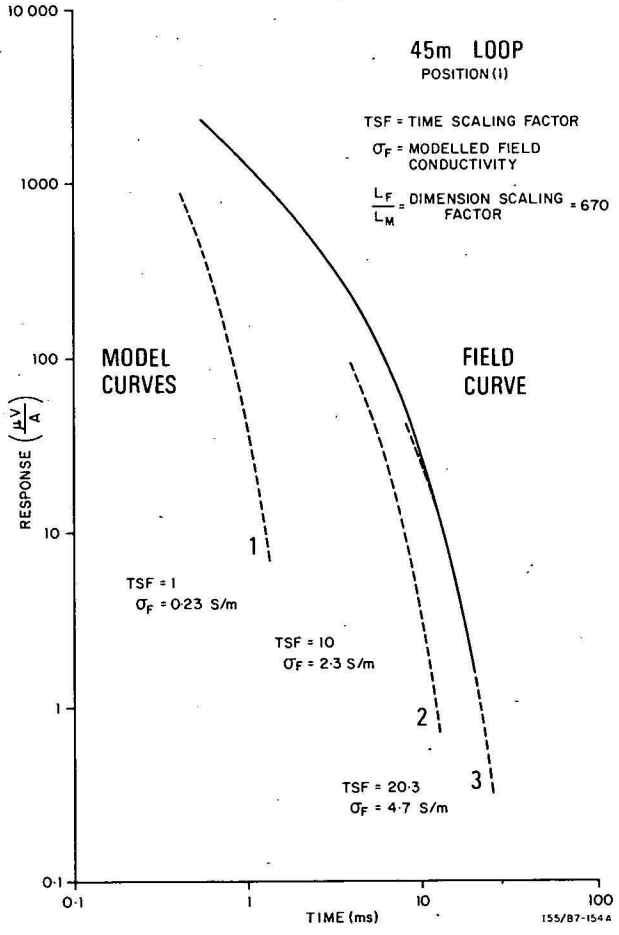

Figure 10. Comparison of model and field results, Woodlawn orebody, position 1.

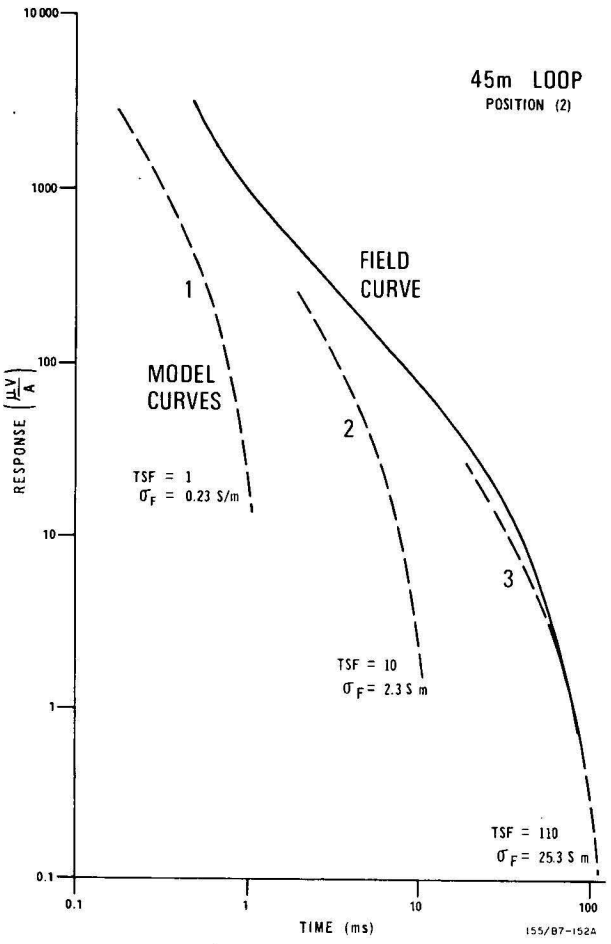

Figure 11. Comparison of model and field results, Woodlawn orebody, position 2.

resemblance between the model and field curves. By using the modelling relations we can scale time and conductivity and, on a log-log graph, the curve can be transposed along the time axis and, also, vertically downwards to account for the amplitude correction. Curve 2 has a time-scaling factor of 10, and the simulated conductivity is 2.3 S/m. Curve 3 has a time-scaling factor of 20.3, and the simulated conductivity is 4.7 S/m. There is a good fit between curve 3 and the field curve, and we can say that for the area under investigation under the loop in position 1 the bulk conductivity of the orebody is about 5 S/m.

Figure 11 shows the results applying the same process in loop position 2. Curve 1 is the model study curve without scaling time. This curve can be moved across as already described to curve 3 which has a reasonable fit to the field curve at late times but not at early times. Since the depth of investigation is related to sample time this means that the model is correct for deeper parts of the orebody, but should have a greater conductivity or be thicker for the more near-surface parts. The overall bulk conductivity of the orebody at loop position 2 must be very high, at least 25 S/m.

Application to rules of interpreting TEM results

For many interpretational procedures rules of thumb are used, and we make use of what are called 'early' and 'late' time asymptotes. For example the response of a sphere at late times is exponential, with a time constant equal to $\pi^2/\sigma\mu b^2$, where σ, μ and b are the conductivity, permeability and radius of the sphere, respectively (Nabighian, 1970). Thus by measuring the slope of the transient decay curve at late

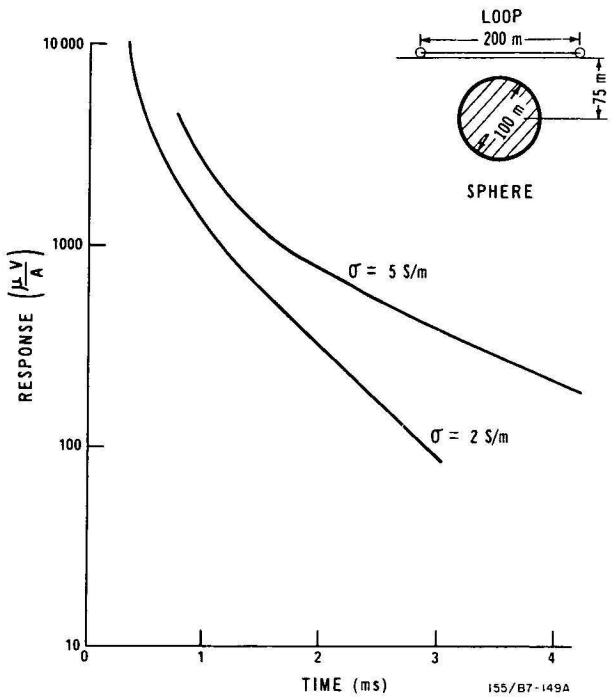

Figure 12. Transient decay curves over spheres of different conductivity.

times we can estimate the conductivity or size of the sphere. But what is a 'late time'?

Figure 12 shows two transient decay curves over identical spheres of different conductivity. The curves are plotted on a log-linear scale so that at late times the asymptotes are straight lines. For the 2 S/m sphere the late time asymptote occurs near 1.5 ms, whereas for the higher conductivity 5 S/m sphere the asymptote does not occur until 3.7 ms. The asymptotes occur at similar values of the parameter $\sigma\mu L^2/T$, and the response typical of a late time for a body may be similar to an earlier time response if the electrical or dimensional properties are varied.

It is obviously important to measure over as wide a time range as possible. When analysing responses from early and late times we must remember that the actual time that we can measure the asymptote will depend on many factors, e.g. the size and conductivity of the body, its depth of burial, and the loop size. More correctly we should analyse responses in terms of large and small values of the parameter $\sigma\mu L^2/T$ rather than in terms of early and late sample times.

Discussion and conclusions

Several results emerge from this study.

The examples with the cylinders and sphere showed that transient decay curves will appear to change in shape as we change either the dimensions of the body or loop, or conductivity of the body. An 'early time' in one situation may be equivalent to a 'late time' in another, so we must measure over a very wide time range in order to get as much information as possible on the subsurface conductivity distribution.

The ability to scale time opens up a new range of possibilities in TEM scale modelling. We have seen that we can estimate bulk parameters such as conductivity or dimensions as long as one is known, a procedure often used with frequency domain methods.

Once the physical and electrical parameters of mineralization in a particular area are specified, it is then possible to

design an electrical or electromagnetic survey which will provide optimum detectability of that style of mineralization. When applied to geophysical exploration, modelling enables one to assign quantitative values to such items as depth of investigation of a method in a particular geological environment. Once a target has been adequately defined, the probability of detecting it is greatly increased.

The Woodlawn results show that such orebodies have a very high bulk electrical conductivity, and therefore electromagnetic methods have a great potential in their detection. The major problem to date is in instrumentation, especially in having a wide enough frequency range to obtain information on the various conductors present (Ward *et al.*, 1974). For similar reasons TEM instruments should also cover a wide range of sample times; 3 or 4 decades of time would be preferable. TEM instruments presently on the market typically have a 1.5 decade time range.

References

BUSELLI, G., 1974—Multichannel transient electromagnetic measurements near Cloncurry. *CSIRO Minerals Research Laboratory Investigations Report* **103.**

FRISCHKNECHT, F.C., 1971—Electromagnetic scale modelling. *In* J. R. WAIT (Editor), ELECTROMAGNETIC PROBING IN GEOPHYSICS 265-320. *Boulder, Golem Press.*

LEE, T., & LEWIS, R., 1974—Transient EM response of a large loop on a layered ground. *Geophysical Prospecting,* **22,** 430-44.

MALONE, E. J., OLGERS, F., CUCCHI, F. G., NICHOLAS, T., & MCKAY, W. J., 1975—Woodlawn copper-lead-zinc deposit. *In* C. L. KNIGHT, (Editor), ECONOMIC GEOLOGY OF AUSTRALIA AND PAPUA NEW GUINEA. *Australasian Institute of Mining and Metallurgy, Melbourne.*

NABIGHIAN, M. N., 1970—Quasi-static transient response of a conducting permeable sphere in a dipolar field. *Geophysics,* **35,** 303-309.

PRAUS, O., 1975—Numerical and analogue modelling of induction effects in laterally non-uniform conductors. *Physics of the Earth and Planetary Interiors,* **10,** 262-70.

SINCLAIR, G., 1948—Theory of models of electromagnetic systems. *Proceedings Institute Radio Engineers,* **36,** 1364-70.

SPIES, B. R., 1976a—The transient electromagnetic method in Australia. *BMR Journal of Australian Geology & Geophysics,* **1,** 23-32.

SPIES, B. R., 1976b—The derivation of absolute units in electromagnetic scale modelling. *Geophysics,* **41,** 1042-47.

SPIES, B. R.—An application of a mini-computer in scale model studies of a transient electromagnetic prospecting system (in prep.).

VELIKIN, A. B., & BULGAKOV, Yu I., 1967—Transient method of electrical prospecting (one-loop version). *UNO International Seminar of geophysical methods of prospecting for ore minerals. Ministry of Geology of the USSR, Moscow.*

WAIT, J. R., 1953—A conducting permeable sphere in the presence of a coil carrying an oscillating current. *Canadian Journal of Physics,* **31,** 670-78.

WARD, S. H., PRIDMORE, D. F., RIJO, L., & GLENN, W. E., 1974—Multispectral electromagnetic exploration for sulphides. *Geophysics,* **39,** 666-82.

Environment of deposition of the Carlo Sandstone, Georgina Basin, Queensland and Northern Territory

J. J. Draper

The Carlo Sandstone is part of the Toko Group of the Georgina Basin. This basin, which straddles the Northern Territory-Queensland border, comprises carbonate and clastic rocks of Cambrian and Early Ordovician age; the Toko Group forms the uppermost and dominantly clastic part of the sequence. The Carlo Sandstone, which is of possible Early Ordovician age (? latest Arenig), consists of very fine to fine quartzose sandstone containing siltstone and mudstone pellets. Minor siltstone and mudstone interbeds are present. The unit is conformable with the underlying Nora and overlying Mithaka Formations. Sedimentary structures present include: flute marks, current crescents, various other current lineations, ripple-marks, cross stratification, lamination and various biogenic sedimentary structures. The palaeocurrent measurements indicate uni-directional currents. Fossils are rare except in the uppermost part of the unit where gastropods, pelecypods, nautiloids, trilobites, brachiopods and fish are present. A study of geometry, lithology, sedimentary structures, palaeocurrents and fossils indicate subtidal to intertidal depositional conditions. Of various depositional models, a barrier model is favoured. The Nora Formation represents the offshore, below wave base sediments; the Carlo Sandstone the barrier, either dunes or bars; and the Mithaka Formation the lagoon-bay sediments. The sediments were deposited in an elongate epicontinental sea that also covered the Amadeus, Wiso and Canning Basins.

Introduction

The Georgina Basin, covering an area of 325 000 km² straddling the Queensland-Northern Territory border (Fig. 1), comprises Cambrian and Ordovician marine rocks (Smith, 1972), together with non-marine and marine Devonian rocks (Smith, 1972; Draper, in prep.). The Toko Group (Casey *in* Smith, 1965) which includes, in stratigraphic sequence, the Coolibah Formation, Nora Formation, Carlo Sandstone and Mithaka Formation is restricted to the Toko Syncline, the Tarlton Range and Dulcie Syncline (Fig. 1). Whereas earlier Ordovician sediments are predominantly carbonate, the Toko Group, of Arenig to Llanvirn age, is predominantly siliciclastic. The Toko Syncline, which contains the thickest (over 3500 m) and most complete sequence in the basin, plunges to the south-east beneath the Mesozoic rocks of the Eromanga Basin.

The Carlo Sandstone (Casey *in* Smith, 1963) crops out in the Tarlton and Toko Ranges (Fig. 2), where it forms the capping on the scarps and part of the plateaus, and also in the Toomba Range, where it is steeply dipping. In Ethabuka No. 1 (Alliance Oil N.L., 1975), the Carlo Sandstone, or its equivalent, was intersected between 1329 m and 1518 m (Fig. 2). The type area for the unit is 3 km south of Carlo Homestead, but no type section has been designated.

The Carlo Sandstone consists of a series of thinly to very thickly bedded, very fine to medium-grained quartzose sandstones, with minor siltstone and mudstone interbeds near the base. The sandstones contain abundant siltstone and mudstone clasts. Inorganic and biogenic sedimentary structures are common.

In the type area the unit is about 60 m thick; just north of Gaphole Creek, 50 m; Eurithethera Soak, 70 m; and on most of the plateau of the Toko Range a thickness of 50-60 metres is inferred. In the Tarlton Range about 20-30 metres is present. Netting Fence No. 1 (Papuan Apinaipi Petroleum, 1965) penetrated 120+ m attributed to the Carlo Sandstone with conglomerate at the top, but examination of the site showed that the well was spudded in ?Cretaceous fluvial sediments which overlap part of the upthrown block of Carlo Sandstone on which the well is located; the actual thickness of Carlo Sandstone is about 110 m. Ethabuka No. 1 (Alliance Oil N.L., 1975) penetrated approximately 190 m of sandstone of similar age to the Carlo Sandstone.

The unit has a gradational conformable contact with both the underlying Nora Formation (Fig. 9b) and the overlying Mithaka Formation. Both these units are predominantly mudstone and siltstone, with thin very fine-grained sandstone interbeds.

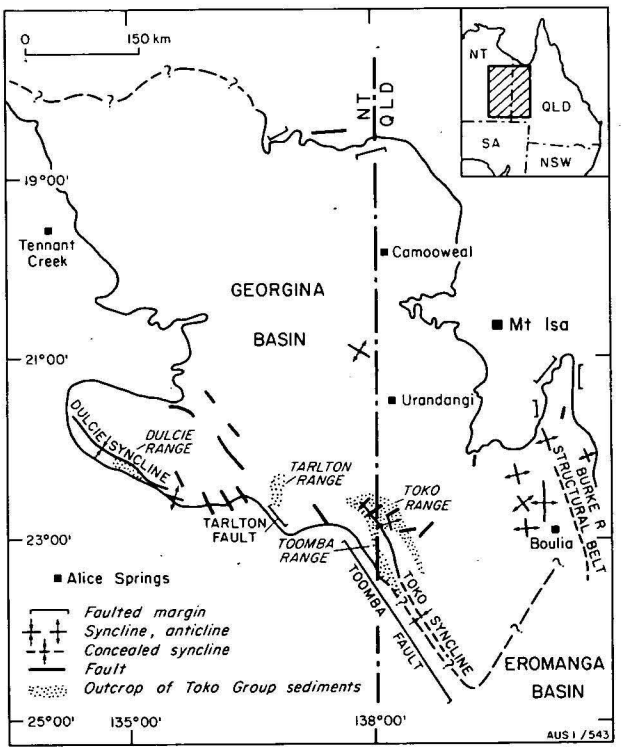

Figure 1. Locality, general geography and general structure of Georgina Basin; and distribution of the Toko Group.

A middle Ordovician age was originally proposed for the Carlo Sandstone (Smith, 1965). However, the few fossils are of little value except that, in the underlying Nora Formation, the conodonts suggest late (but not latest) Arenig (E. C. Druce, pers. comm., 1976). Therefore the Carlo Sandstone may be as old as latest Arenig.

A number of geologists have examined the unit during regional mapping and petroleum exploration (see Smith, 1972 for details). One study of the measurement of current direction data in the Tarlton Range (Vine *in* Smith, Vine & Milligan, 1961) has been published. Measurement of

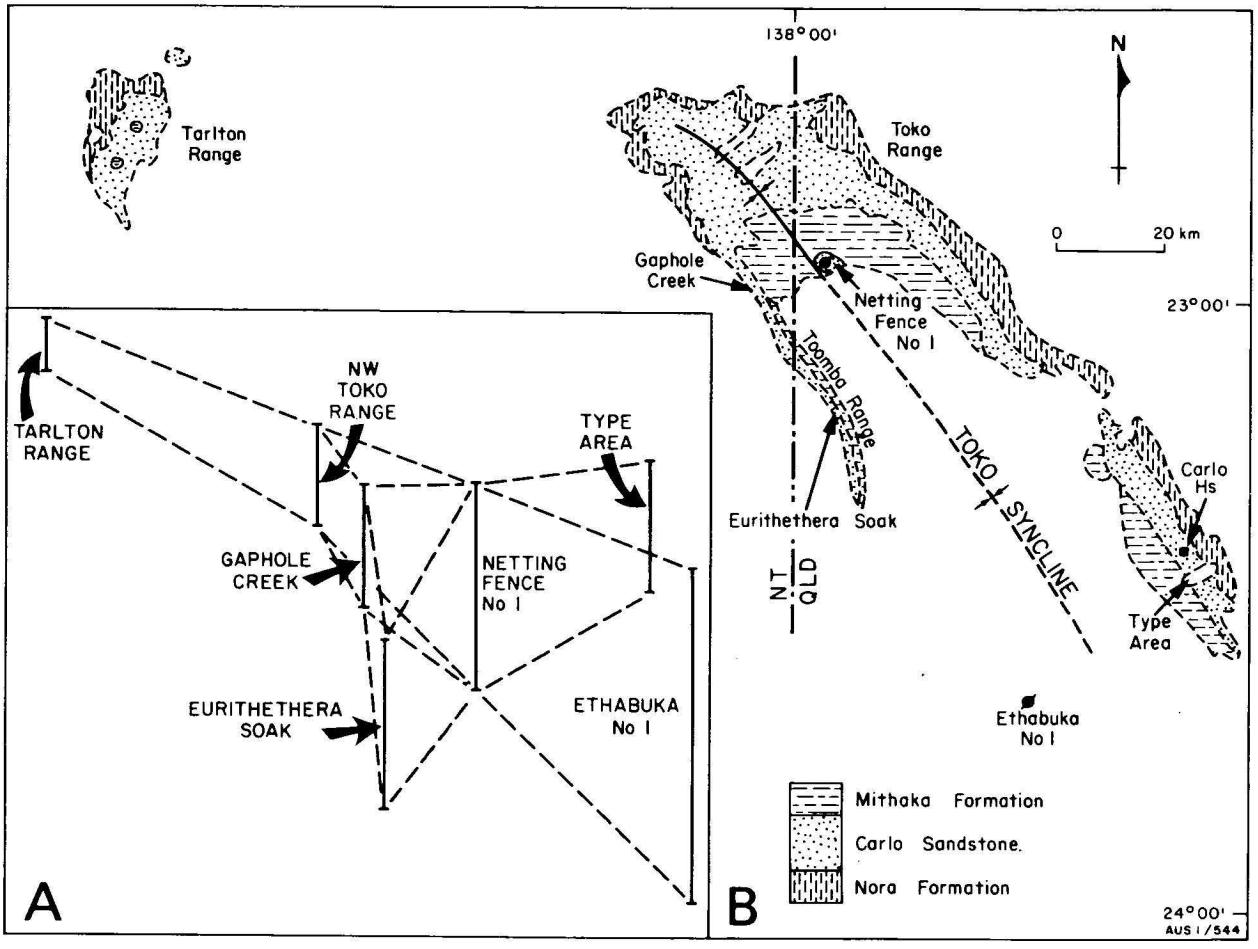

Figure 2 **A. Diagrammatic representation of relative thickness of Carlo Sandstone.**
B. Outcrop distribution map of Nora Formation, Carlo Sandstone, and Mithaka Formation.

current direction from cross strata, ripplemarks and flute casts indicated a principle current direction towards the northwest.

This study is part of a multidisciplinary study of the Georgina Basin (Druce, 1974). The study is based on measured stratigraphic sections, spot observations, and the field and laboratory studies of inorganic and biogenic sedimentary structures. Information on the environment of deposition of the Carlo Sandstone will assist in the analysis of the events which formed the Georgina Basin.

Acknowledgements

Drs E. C. Druce and J. H. Shergold provided useful discussion on stratigraphy, palaeontology and palaeogeography. Dr A. R. Jensen assisted in the sedimentological aspects of the study. Valuable criticism of the draft was received from Drs E. C. Druce, J. H. Shergold and R. V. Burne. The figures were drawn by Mrs S. Davidson, Geological Drawing Office, BMR.

Subunits

Because of the nature of outcrop and reliance on scree for many observations, detailed sequences cannot be erected for the Carlo Sandstone. However, three distinct subunits (A, B, C) are recognized over most of the area of outcrop; each subunit may contain several subfacies, but these cannot be accurately defined at present. Representative sections of the subunits are shown in Figure 3 and the distribution of sedimentary structures in the subunits and in the upper part of the Nora and lower part of the Mithaka Formations is summarized in Figure 4. Measurements of current direction and sense are given in Figure 5. Only two readings (230°, 270°) were obtained from the poorly exposed Subunit C.

In attempting to define ancient sedimentary environments five characteristics of the rock body are critical (Selley, 1970): geometry, lithology, sedimentary structures, palaeocurrents, and fossils. These parameters, together with comparative studies of Recent sedimentary environments, form the basis for any environmental reconstruction. In this paper these parameters will be examined for each subunit and then a model for deposition will be developed. Finally, the palaeogeography will be examined.

Subunit A

Subunit A conformably and transitionally overlies the Nora Formation, is up to 10 m thick, and passes gradationally into Subunit B. The subunit is laterally persistent.

The subunit consists of minor siltstone and mudstone interbeds between thin to thickly bedded, very fine to fine sandstone. Mudstone and siltstone clasts are common and are either distributed throughout beds, confined to upper and lower surfaces, or lie along cross strata. A distinctive, very thickly bedded sandstone containing slumps and possible water-escape structures is present in the upper part at some localities. Beds are generally lensoid and range from several metres to several hundred metres in length.

Quartz constitutes 90 percent or more of the sandstone grains, with slightly undulose monocrystalline quartz grains

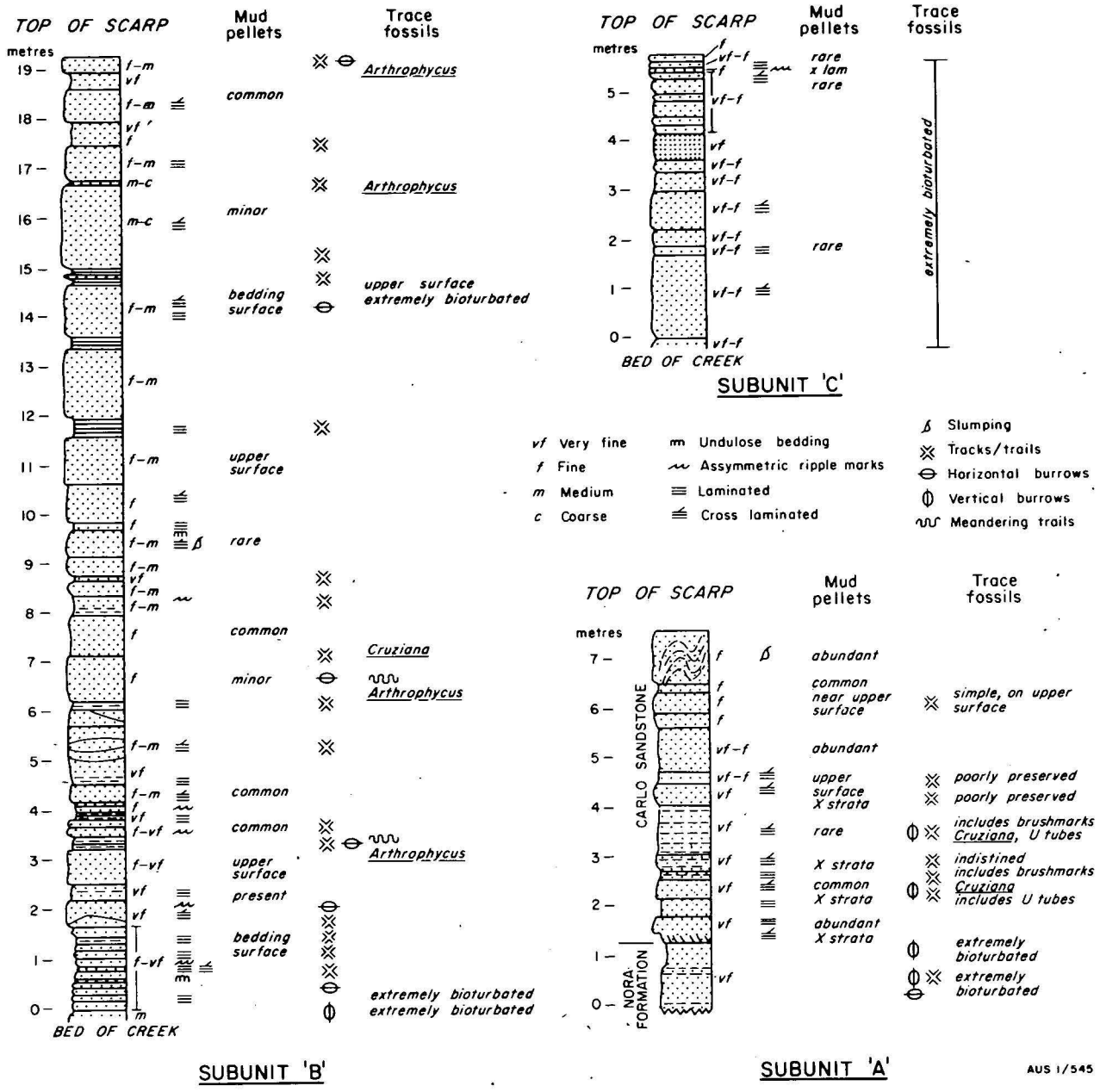

Figure 3. Representative sections—subunits of Carlo Sandstone.

predominant although polycrystalline quartz is common. Quartz overgrowths (some of which are relict) are abundant. These overgrowths obscure the shape of the grains, but the grains appear to be subangular to subrounded. The sediment is generally well sorted. Detrital chert is present in minor amounts. Siltstone and mudstone clasts and matrix make up the remainder of the rock. Accessory minerals include well rounded tourmaline, zircon and rare rutile; minor, possibly reworked, glauconite is present.

Asymmetric ripple marks are common in the subunit but symmetric ripplemarks are rare. Of the asymmetric ripplemarks, linguoid ripplemarks (Fig. 10a) are the most common. Bevelled or flat top ripplemarks (Fig. 10b) with or without grazing trails, tracks, and small runnels are present. Grazing trails and tracks are also present on many of the linguoid ripple-marks. Cross-stratification observed consists of low angle (<12°) simple and planar cross-lamination, and small to medium-scale (5-40 cm) sets, moderate angle (18-28°) planar (and minor trough) cross stratification, which is generally of the individual rather than the coset type.

The most common sedimentary structures in the lower part of the subunit are scour structures, which can be divided into erosional (i.e. fluid-induced) and impact structures. The erosion structures include flute marks, current crescents, and shadows and some grooves, and impact structures include brush, skip and prod marks, and some grooves. Flute marks (Fig. 9, c, d), current crescents (Fig. 9e) and grooves occur as sole markings on sandstone beds. Owing to differential erosion, the beds underlying the sole markings are rarely preserved. Most of the structures were observed in rubble on the scree slope.

Three basic types of lineation occur. Parting lineation (Fig. 9d) is common on upper surfaces or internal laminae surfaces of sandstone. The third type of lineation, indistinct but very common, is preserved as a sole marking on sandstone and appears to result from the movement of sand grains along the surface of the underlying mudstone.

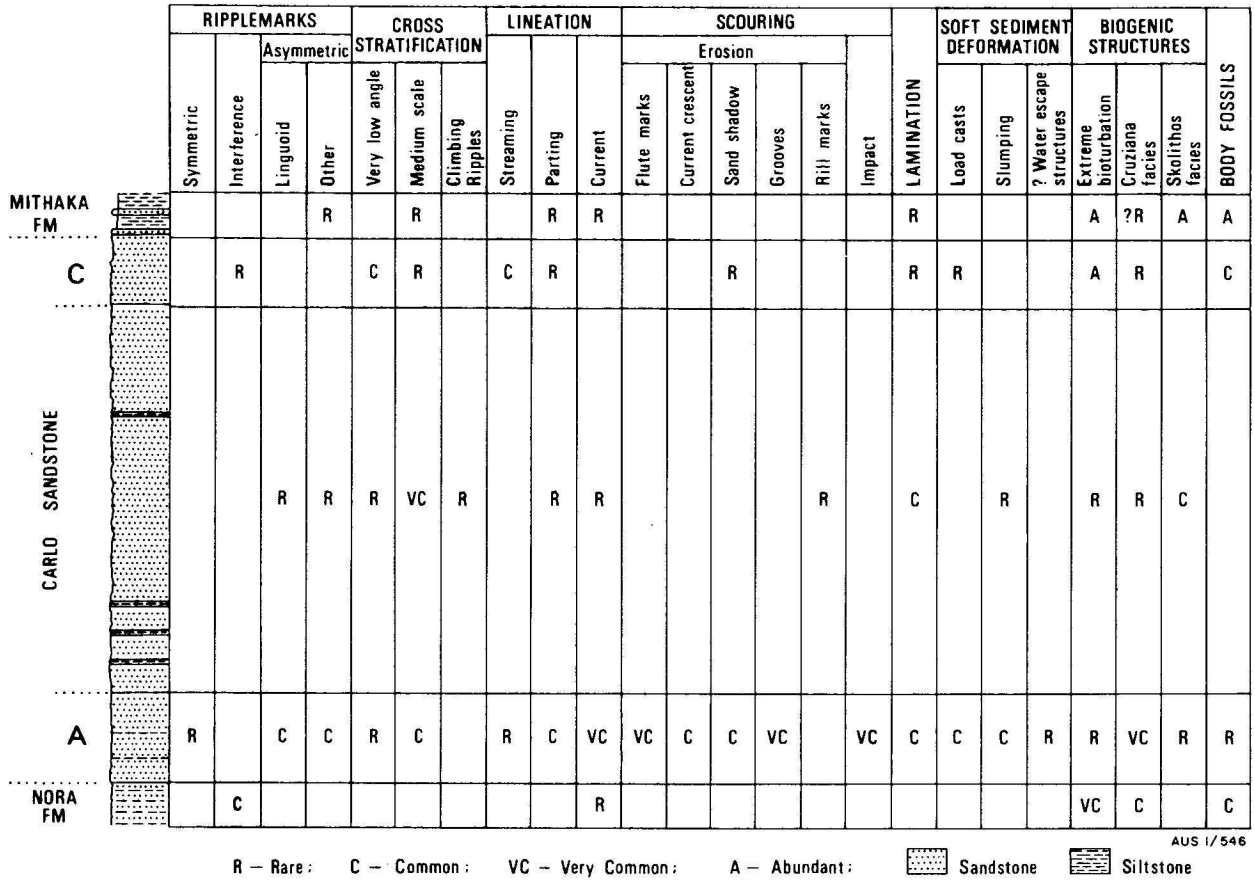

Figure 4. Composite section and summary of sedimentary structures.

Streaming lineation (Conybeare & Crook, 1968) is present, but not common.

Laminations are present in the sandstone and the mudstone. The lamination in the mudstone results from slight colour differences and grainsize variations. Slight changes in grainsize and, in some cases, concentration of silt in discrete layers cause the lamination in the sandstone. Laminated sandstone often shows parting lineations on the upper, lower, and internal surfaces. Biogenic structures are rare and generally consist of isolated *Arenicolites*. Sometimes the sole-marked sandstones are laminated, generally as alternating light and dark layers.

Load casting is present, mainly as oversteepening of flute marks and associated sole markings. However, it is not common, probably because the underlying mudstone and siltstone have a high degree of cohesion. Slumping (Fig. 10d) is seen only on the very thick sandstone bed in which there are possible water-escape structures.

The dominant biogenic structures in this subunit are sole markings on sandstone, and consist of trilobite and arthropod traces (*Cruziana* (Fig. 11a), *Rusophycus* (Fig. 10b), *Diplichnites*, *Dimorphicnus*, and *Merostromichnites* (Fig. 11b)), simple curved and meandering trails, and indeterminate markings and scratchings. Many are associated with flute marks etc, an association previously noted by Crimes (1970) for sublittoral sandstones of Arenig age in North Wales. *Cruziana* and *Rusophycus* are normally attributed to trilobites (Bergstrom, 1973) but many of the associated tracks, trackways and trails can only be classified as possible arthropod traces.

Extreme bioturbation is not common but, where present, it destroys inorganic sedimentary structures.

A number of burrow types are present, in particular *Diplocraterion* (Fig. 6h, 11f), *Arenicolites* (Fig. 6d, 11e), and *Skolithos* (Fig. 6f, 11d). Many of the burrows shown in Figure 6 are present but not common. Only one specimen of *Rhizocorallium* (type (j)) was observed. *Arthrophycus* (Fig. 11c) occurs on both upper and lower surfaces of beds and is a wandering, horizontal burrow which may occur at one or a number of levels in the rock. Many of the burrows, particularly *Arenicolites* and *Diplocraterion*, can be attributed to wormlike animals (Hakes, 1976).

Where possible, current direction measurements were made using cross-stratification, flute marks, current crescents and ripplemarks. Measurements of current sense were made on parting lineation. Previous measurements from the Tarlton Range (Vine *in* Smith et al., 1961) are compared with those from the Toko Range (Fig. 5). Only bulk groupings are examined since poor outcrop and difficulties in obtaining an adequate sampling pattern precluded a detailed study. A predominant direction towards the northwest is indicated for both the Toko and Tarlton Ranges.

Although ichnofossils are very common in the subunit, there is a paucity of body fossils. This paucity may be a result of three interrelated factors: a lack of suitable preserving medium, a predominance of soft-bodied forms, and high porosity, and hence high dissolution potential. The generally undescribed fauna includes pelecypods, nautiloids, brachiopods and gastropods. No trilobite or arthropod has been found in spite of the large number of traces. Pelecypods occur as mounds and casts, either collectively or as isolated individuals. The four species of pelecypods from the Carlo Sandstone described by Pojeta & Gilbert-Tomlinson (in press) probably came from this subunit. Most specimens are disarticulated, fragmented, or are found along cross strata indicating that they have been subjected to extensive current activity.

Discussion

Some idea of the physical processes involved in deposition of the rocks can be obtained from the sedimentary structures. This and the other features of the rock enable the development of a general depositional model for the subunit.

Within the lower sandstone, the scour marks are the most dominant feature. The formation of erosion scour marks is characterized by the following:

(a) the flow must be capable of eroding the sediment;
(b) the marks may form around irregularities on the surface of the sediment (some current crescents, sand shadows), or as the result of variable layer boundary processes (Allen, 1968a);
(c) the rate of scour is a function of sediment movement in and out of the scour;
(d) the material removed from the scour may be deposited adjacent to the scour (current crescents, sand shadows) or completely removed from the general vicinity (flute marks, grooves).

Flutes are formed by flow separation of a trapped eddy rotating around a horizontal axis (Allen, 1968a). The most important parameters are the velocity of the eroding current, and the grainsize and cohesiveness of the eroded material (Blatt, Middleton & Murray, 1972). Many workers had considered that the currents which formed flute marks were sand-laden, mainly because of the common association of these features with turbidity currents, although Rucklin (1938) created similar marks in the laboratory using clear water. There is no theoretical reason why sand-laden currents are required, although Allen (1968a) suggests the presence of grains may modify the intensity of the erosion. In the Carlo Sandstone biogenic overprints suggest a time lag between formation of the flute marks and deposition of the overlying sand.

Some idea of the velocity required can be obtained from Hjulstrom's diagram (modified by Sundborg, 1956). The velocity required to erode cohesive silt and mud is of the order of 1m/sec or greater. At these velocities any sand-sized grains present would be in suspension. This velocity is similar to that shown by Allen (1968a) for the continuation of growth of flutes with a very fine sand in suspension. The flute marks in the Carlo Sandstone are small (2-3 cm long, <1 cm wide) and thus the eroding current was short-lived. The mud and silt removed by the currents is deposited as matrix and clasts in sandstone.

Although flute marks are commonly reported from turbidite deposits (Allen, 1968a), they may form in other environments (Glaessner, 1958; Prentice 1961; Potter & Pettijohn, 1963; Kuenen, 1964; Michaelis & Dixon, 1969). They occur in subtidal and intertidal environments (Klein, 1963; Crimes, 1970). They can form in any environment with a suitable substrate and where current velocities are in excess of 1 m/sec. Klein (1970) reported bottom-current velocities in excess of 1 m/sec in the Minas Basin of the Bay of Fundy.

Impact marks are caused by various objects bouncing, rolling or gouging their way along the sea floor. In this case many are apparently caused by mud and silt pellets and flakes, and also by animals swept along by the current.

Grooves are formed by several different processes. Dzulynski & Walton (1965) consider them continuous tool markings, but it is apparent from the way that grooves in this subunit pass laterally into flute marks that, in some cases at least, current activities alone are responsible for their formation.

The various trilobite and arthropod traces belong to the *Cruziana* Facies of Seilacher (1964). Seilacher's facies concept, based on the assemblage of trace fossils, is still accepted by most workers as a valuable though not unequivocal guide to the environment and a general indication of bathymetry (see for example various authors *in* Frey, 1975). Seilacher suggested a subtidal environment above wave base for the *Cruziana* Facies. In this subunit the fauna is dominated by epifaunal deposit feeders, which prefer relative quiet conditions—although *Rusophycus* and many of the brush marks could indicate higher energy (Banks, 1970).

Conybeare & Crook (1968) attribute linguoid ripplemarks to areas of strong current activity such as tidal channels, and Allen (1968b) to fluvial and intertidal areas. Sinuous and straight asymmetric ripplemarks may represent slightly deeper water (Allen, 1968b). Regularly repeated symmetric ripplemarks are generally formed by wave action, although current activity can form symmetric ripplemarks. Bevelled ripplemarks form in water less than 3 cm deep and are related to falling water levels (Tanner, 1960).

Low-angle simple and planar cross-stratification is most common in beach and offshore bar deposits (McKee, 1964); it forms by an accretionary type process (Blatt, *et al*, 1972). Planar tabular cross-stratification of moderate angle is most typical of delta foresets, but also occurs in alluvial sand plain deposits and offshore bars (McKee, 1964). Trough cross-stratification reflects scour and fill and occurs in fluvial deposits, channels in tidal flats, backshore beaches, alluvial fans, and locally in dunes (McKee, op. cit). Tabular sets form mainly from migration of straight and sinuous ripples, whereas trough sets result from less regular ripple forms, e.g. linguoid ripples give rise to small sets and sinuous and lunate dunes to larger sets (Blatt, *et al*, 1972).

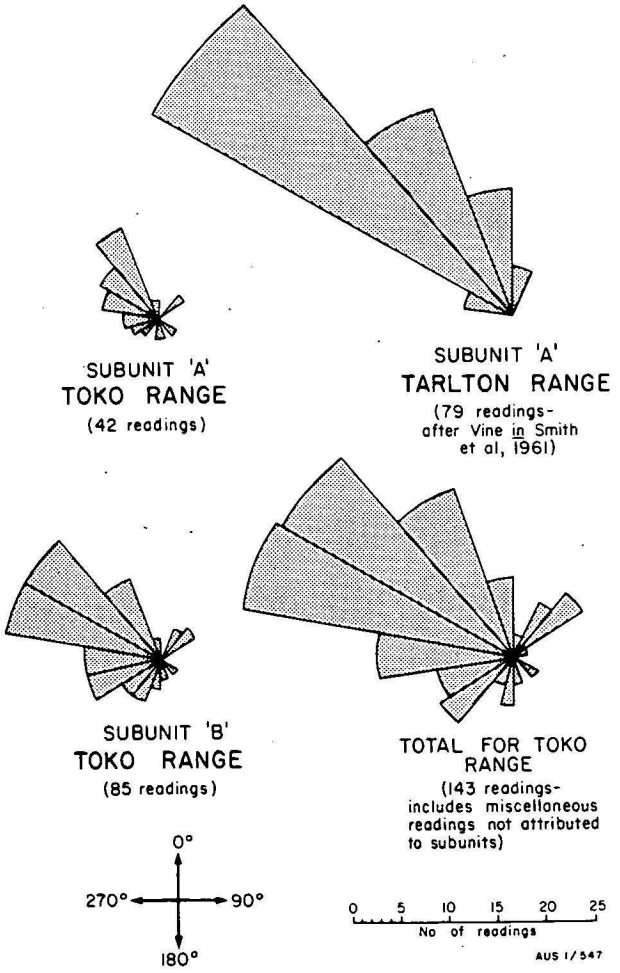

Figure 5. Palaeocurrent direction—Carlo Sandstone.

The types of ripplemarks and cross-stratification recorded would appear to be predominantly those of subtidal and intertidal environments.

Parting lineation forms in the plane-bed stage of the upper flow regime (Allen, 1964), but can also form in the plane-bed stage of the lower flow regime. However, since the parting lineation is laminar a pulsating sediment supply is indicated (Allen, 1964). Streaming lineation is seen on beaches during wave runoff.

Intermittent or periodic deposition, slight changes in velocity of the depositing medium, or changes in provenance can give rise to lamination. For lamination to be preserved, bioturbation, caused by benthonic organisms, must be minimal or non-existent. Suitable environments include stagnant basins or depressions, and areas above normal water level or of rapid deposition. Since laminated mud is not common in the subunit and forms lensoid beds of restricted extent, it was probably deposited in small (100 m^2) depressions in the sandy substrate. The association of much of the laminated sand with parting lineation suggests formation under plane-bed steady flow conditions. Lamination is known to form under upper flow regime bed conditions (Blatt *et al*, 1972) although parting lineation can form under lower flow regime. Other possible causes of lamination are swash and back swash, and tides.

Soft-sediment deformation occurs because of instability in the sediment, caused by surplus pore water which could result from several processes, including rapid deposition which gives the pore water little time to escape. Water from adjacent beds could also be forced into the sediment by compactive forces or by hydraulic head. Load casting results from differential compaction of mudstone and siltstone; and slumping is gravity induced, either spontaneously or triggered off by external stimuli such as earthquakes or wave action. Water-escape structures form under conditions of very high pore-fluid content, and compaction or hydraulic loading. Soft-sediment deformation features, whilst not restricted to particular environments, are generally restricted to areas of rapid sedimentation.

Although many of the observations for this subunit were made on scree, a general vertical sequence can be recognized. Immediately overlying the Nora Formation are flute-marked (included associated structures) sandstones which are individually cross bedded and contain *Cruziana* Facies ichnofossils. The sandstones are interbedded with mudstone and siltstone. Above these sandstones are sandstones containing *Skolithos* Facies ichnofossils, patches of extreme bioturbation, some low-angle cross-strata, lamination, and parting and streaming lineation. The vertical sequence of biogenic structures suggests a change from subtidal to intertidal conditions. There is an overlap between the two ichnofacies: *Cruziana* occurring on the sole and *Diplocraterion* in the upper part of one bed. The subtidal environment is of high energy (flute marks indicate current velocities in excess of 100 cm/sec) and, being of consistent areal extent, is not a channel origin but represents open subtidal conditions. Although the biogenic structures indicate intertidal conditions, the assemblage of sedimentary structures lacks those that are diagnostic of normal tidal-flat deposits (Ginsberg, 1975), such as herringbone, cross-strata, reactivation surfaces, and indications of subaerial exposure. The strong unimodality of the palaeocurrents of the subunit suggests a dominance of longshore over tidal currents. These currents were probably intermittent and variable in velocity as indicated by the alteration of mud and sand, and the apparent time lag between trace formation and infilling. The very thick sandstone bed with slumps and possible water-escape structures must have been deposited rapidly, and may represent the oceanward portion of a washover fan, or be a broad shallow channel.

The environment postulated is a shallowing sequence from subtidal to intertidal, with low intensity tidal currents and tides. Longshore currents were dominant.

Subunit B

Subunit B overlies Subunit A transitionally, and has an inferred thickness of up to 50 m. It consists of thin to very thickly bedded, fine to medium-grained quartzose sandstone, with minor siltstone and mudstone interbeds; the thicker beds tend to occur higher up in the subunit. Siltstone and mudstone clasts are present in some beds and are generally associated with bedding surfaces. The beds are lensoid in nature and dimensions range from 10 m to 400 m.

Petrographically, the sandstones in this subunit are very similar to those in Subunit A. The only difference is a tendency for them to be coarser in grainsize and to coarsen upwards. However, the tendency to coarsen upwards is not seen in all sections.

Rare linguoid and sinuous ripplemarks are present and are similar to those in Subunit A. Cross-stratification consists of common medium-scale planar and trough cross-strata, mainly as cosets, as well as rare very low-angle cross-lamination and climbing ripples. Some of the cross-strata consists of alternating fine and medium sand-size grains. Some large-scale cross-bedding may be present but is obscured by silicification. Parting lineations and rill marks are rare. Lamination is common in all lithologies. Minor slumping is present in some of the thicker beds, while other thick to very thick beds appear to be structureless —although this may be caused by silicification. Current directions are predominantly towards the northwest with a subsidiary direction towards the southwest.

Body fossils have not been found in this subunit, but ichnofossils are present. *Arenicolites, Arthrophycus,* simple vertical burrows and sinuous meandering burrows are common in some localities, but *Cruziana* is rare. Isolated patches of extreme bioturbation are present in the lower part of the subunit.

Discussion

The lower part of this subunit has some features in common with upper part of Subunit A, namely linguoid ripplemarks and *Skolithos* Facies ichnofossils. However, it contains many more thin-bedded sandstones. Rill marks and small channels, as well as a similarity to the upper part of Subunit A, suggest intertidal conditions although once again indications of normal intertidal deposits are absent. The bioturbated sandstone may represent isolated depressions or lagoons.

The upper part of this subunit consists mainly of thick to very thick sandstone, with very minor mudstone and siltstone. Many of the sandstones appear structureless. However, in some, medium-scale trough cross-stratification, slumping and ichnofossils on the upper surfaces of beds indicate deposition in water. Other beds contain possible large-scale cross-bedding masked by silicification. This cross-bedding, if present, allied with the tendency of beds to fracture into large wedges is suggestive of aeolian deposition (Blatt, *et al*, 1972). These thicker bedded rocks overlie possible intertidal rocks, and may represent dunes and barrier flats. The beds containing slumping may represent washover fans deposited rapidly.

Subunit B represents a sequence from upper intertidal conditions into supratidal and washover conditions.

Subunit C

Subunit C overlies Subunit B, is generally less than 10 metres thick, and consists predominantly of medium to

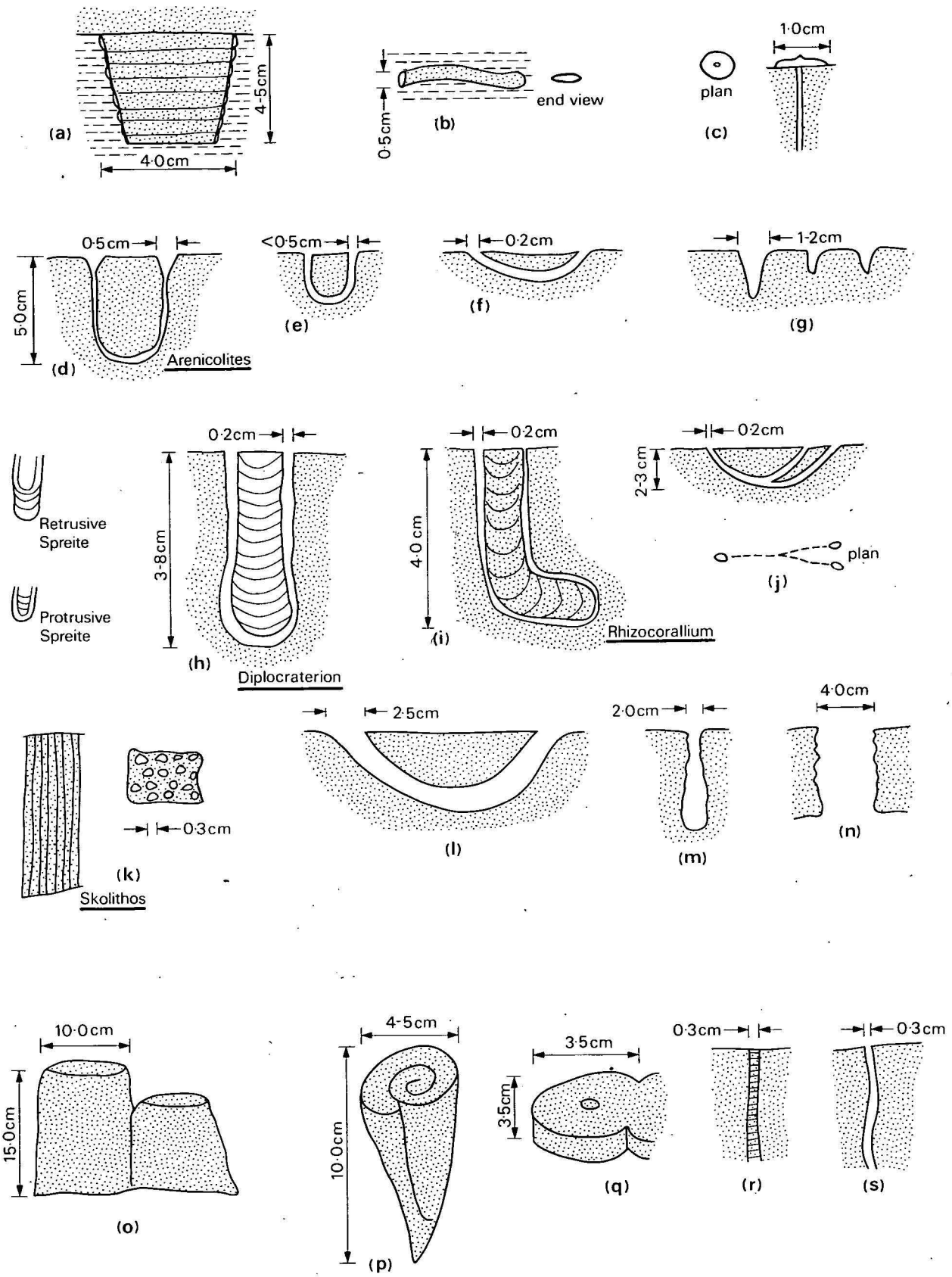

Figure 6. Types of burrows in the Carlo Sandstone.

thick beds of very fine quartzose sandstone, with minor thin and very thick beds. It is overlain conformably by the Mithaka Formation. The lower 90 percent of the unit is extremely bioturbated and mottled, and contains relict lamination and cross-lamination. The lower part is overlain in some areas by well bedded sandstone containing interference ripplemarks, very low-angle cross-lamination, streaming lineation with sand shadows, and rare load casts.

Fossils present, mainly in skeletal hashes, include trilobites, nautiloids, pelecypods, brachiopods, gastropods and fish. At least two species of asaphid trilobite are present (R. A. Fortey, pers. comm, 1976); both are larger (up to 20 cm in length) than the trace-forming types in Subunit A. One species has been referred to *Asaphus thorntoni*? Etheridge (Gilbert-Tomlinson *in* Pojeta & Gilbert-Tomlinson, in press), which is also found in the Stairway Sandstone of the Amadeus Basin (Gilbert-Tomlinson, op. cit.).

Only two current direction measurements were obtained for the subunit but their values (230°, 270°) are consistent with those of the other subunits. The aerial extent of the subunit is difficult to determine as it is generally poorly exposed—although in some areas, where Mithaka Formation is seen to overlie Carlo Sandstone, the subunit is absent.

Discussion

The extremely bioturbated nature of the sandstone probably reflects relatively slow deposition rates in an environment that was protected from major wave and current activity. The absence of body fossils in the bioturbated sandstone suggests low-oxygen environments or hypersaline lagoons (Rhoads, 1975). The sandstone overlying the bioturbated beds contains skeletal hash, interference ripplemarks, low-angle cross-lamination, and streaming lineation with sand shadows: suggestive of shoaling conditions or perhaps a beach. The subunit, therefore, may represent lagoonal areas separated from open marine conditions by shoals and small islands.

Adjacent rocks

Upper part of the Nora Formation

The upper part of the Nora Formation consists of fine-grained yellow, grey and purple sandstone, and white siltstone (Druce *in* Shergold, Druce, Radke & Draper, 1976). The sediments are bioturbated, and contain *Cruziana*, brush marks and various other indeterminate markings (*Cruziana* Facies). Inorganic sedimentary structures are rare and generally consist of small-scale interference ripple marks. Gastropods are common but nautiloids and pelecypods, although present, are not common (Druce, pers. comm.).

Discussion

Druce (in Shergold, *et al*, 1976) suggests shallow inter and subtidal environments for the Nora Formation. The upper part of the unit was probably deposited under subtidal conditions. This is indicated by the fine grain size, presence of *Cruziana* Facies elements, general absence of sedimentary structure and widespread bioturbation. Rhoads (1975) has suggested that the presence of these features indicates a low sedimentation rate in a protected environment. The absence of suspension feeders and presence of deposit feeders indicate either stable sub-strate or non-agitated water (Rhoads, op. cit.).

Lower part of the Mithaka Formation

Although outcrop is poor, there are sufficient exposures to form an overall picture of the lower 10 metres, of medium-bedded, fine to very fine-grained sandstone interbedded with massive siltstone and mudstone. The sandstone beds become thinner, less consistent and less common upwards. A prolific and diverse fauna is present, mainly in the sandstone beds. Large asaphid trilobites (over 30 cm in length), large nautiloids (several metres in length), gastropods, brachiopods, bryozoans, phosphatic brachiopods, sponge spicules, ostracods, *Receptaculites* and fish are present. Pelecypods, often articulated, form shell banks. Conodonts have been recovered from the siltstones and mudstones. A chitinozoan (*Desmochitina complanta*) has been identified from Bedourie Scout Hole (French Petroleum Company, 1974).

A varied and rich ichnofauna is present. The thicker sandstone beds contain a high density of *Diplocraterion* and numerous large variable burrows possibly caused by pelecypods or crustaceans. *Monocraterion* and *Arenicolites* are present. Scratch and brush marks are preserved as sole markings. The thinner sandstones contain numerous surface markings and trails as well as burrows, including *Chondrites*-like burrows. Large *Rusophycus* are present (up to 30 cm in length) and are associated with the asaphid trilobites. The ichnofauna in general suggests *Skolithos* and *Glossifungites* Facies.

Inorganic sedimentary structures are rare, and probably were destroyed by biogenic activity. Asymmetric ripplemarks, parting lineation, current lineation, lamination and cross-lamination are present.

Discussion

Draper (*in* Shergold *et al*, 1976) suggested that the Mithaka Formation was deposited under coastal lagoonal or tidal flat conditions. However, the characteristics of normal tidal deposits (Ginsberg, 1975) are absent. The large number of *Skolithos* and *Glossifungites* Facies elements, and the similarity to the suite of burrows present in intertidal zones of the Wash (Evans, 1965), does suggest that some sort of intertidal conditions existed. It is likely that the tidal range and currents were very small in magnitude. Current-generated sedimentary structures are present, but are often obliterated by bioturbation—indicating that the currents were impersistent and of little strength; this is also suggested by the presence of *Rusophycus*. The size of nautiloids and the presence of fish also indicates subtidal conditions. The articulated nature of the pelecypods suggests little current or wave activity.

Thin discontinuous beds of sandy pelletal phosphorite are present. Phosphorite generally forms under warm conditions, between palaeolatitudes 40°N and 40°S (Sheldon, 1964), and from water with pH range of 7.0 to 7.8 (Cook, 1972). Ironstone ooids, now altered to goethite, are also present and these generally form in shallow water.

The properties of this part of the unit suggest its deposition in a protected yet well oxygenated environment, containing appreciable nutrients, and with limited tidal range and minor current activities. Such conditions could exist in large coastal lagoons or bays protected from the ocean, where there is interchange between the bay or lagoon and the ocean.

Environmental interpretation

From the discussion of the various subunits, a vertical sequence can be erected. At the base is the fine-grained, bioturbated Nora Formation, deposited under subtidal conditions. The Nora Formation passes upwards into the flute-marked sandstone, deposited under subtidal conditions. Above this are intertidal sediments, although the tidal range and currents were minimal. Above this are possible dunes, washover fans or barrier flat sediments. In turn these are overlain by restricted lagoonal, bioturbated sands which are protected by beaches and shoals from the possible lagoonal-bay rocks of the Mithaka Formation.

The model which fills the data best is a barrier-lagoon model. The model discussed in this paper is a combination of Visher's (1965) general regressive marine model and the

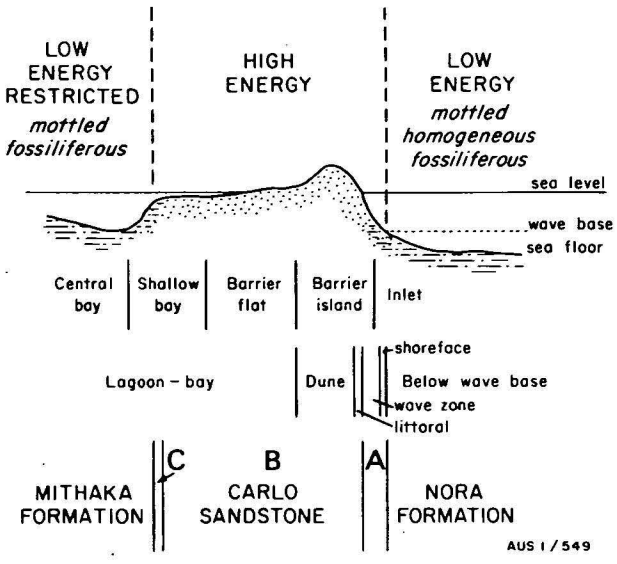

Figure 7. Depositional model proposed for the Carlo Sandstone.

more specific model of Laguna Madre, Texas (Rusnak, 1960). The terminology used from offshore to the dune will be Visher's and the remainder Rusnak's. The main feature of the barrier island model is summarized in Figure 7, and shown diagrammatically in Figure 8. Visher's model is based on general properties of barrier systems and Rusnak's study of Laguna Madre is based mainly on a study of the lagoon and inner edge of the barrier, the outer edge (dune and ocean beach) being ignored.

Visher's first division is the zone below wave base which contains silt and clay, and in which the sediment is bioturbated and contains few sedimentary structures. The Nora Formation represents this zone. The next zone is the shoreface, just above wave base, which contains coarser sediments; sedimentary structures are common and suggest strong currents. This is also the environment in which Seilacher's *Cruziana* Facies would appear. The lower part of Subunit A of the Carlo Sandstone fits this zone—there is evidence of very strong currents, and ichnofossils of the *Cruziana* Facies are present. Above this is the wave zone where ripples start to appear and one would expect a mixing of the *Cruziana* and *Skolithos* Facies ichnofauna. This sequence occurs within Subunit A. In the upper part of Subunit A and the lower part of Subunit B, elements of the *Skolithos* Facies and many of the sedimentary structures would occur on beaches, tidal flats and shoaling bars; this is equivalent to the littoral zone. The next zone is the dune system: apart from occasional possible large-scale cross-bedding and wedge-shaped bedding, there is no evidence for the presence of dunes—many very thick beds lack any sign of organic activity. However, dune systems are not always preserved and can be very difficult to recognize in barrier environments (Dickinson, Berryhill & Holmes, 1972). Alternatively, the barrier may have consisted of shoals and bars. Landward of this zone is the barrier flat. In Laguna Madre the barrier flat consists of tidal flat sediments and washover-fan sediments. The washover-fan sediments are generally the result of bilateral movement of sand through passages between the islands, the main direction of movement being landward. The passages migrate with time. Rapid deposition can occur in these passages. The main source of the sand in barrier flats can be dunes. In Moreton Bay, Queensland, the sand in the large flats and the large washover fan is derived from the dunes on Moreton Island (Maxwell, 1970). Much of Subunit B of the Carlo Sandstone could fit into this zone. Many of the very thick beds, some of which contain slumping, could correspond to washover fans or passage deposits—the very thick beds at the top of Subunit A may represent the seaward expression of such deposits. Many of the thinner laminated beds could correspond to tidal flat sediments.

The next zone is the shallow bay zone and it is here that the transition from Carlo Sandstone to Mithaka Formation occurs. Sandy sediments pass into finer sediments and fossils and bioturbation become common. Furthermore, a shoreface zone is present within the lagoon-bay. This region would correspond to the upper part of Subunit C containing skeletal hash and interference ripple marks. The bioturbated sands in Subunit C may have been deposited in lagoonal depressions separated from the shoreface deposits by shoals—indicated by streaming and parting lineation and sand shadows.

The Mithaka Formation would correspond to part of the shallow bay and the central bay. The formation contains littoral or sublittoral deposits, becoming progressively deeper upwards, and a prolific molluscan fauna, as in Laguna Madre, and in Holocene barrier bay deposits in Gippsland, Victoria (Jenkins, 1976). Ooids are present in Laguna Madre and the Mithaka Formation. Although there is ample evidence of low-energy conditions, there is also some indication of high-energy conditions (skeletal hash, cross-stratification); occasional storm activity may account for the high energy.

In general, the sequence described here has many features in common with a barrier island model. The width and thickness is greater than that described for most ancient barriers. However, this would be a function of sand supply, rate of subsidence, bathymetric slope and relative position of sea level. The thickness and areal extent suggests that the barrier was wide and hence the bathymetric slope relatively slight.

However, in term of thickness, the Carlo Sandstone does not even approach the maximum thickness of 532 metres for the Lower Ordovician Monkman Quartzite of British Columbia, Canada. Jansa (1975) postulated a barrier origin for the Monkman Quartzite, which is underlain by a partly intertidal limestone—calcareous shale—dolomite sequence, and overlain by lagoonal shelf dolomites.

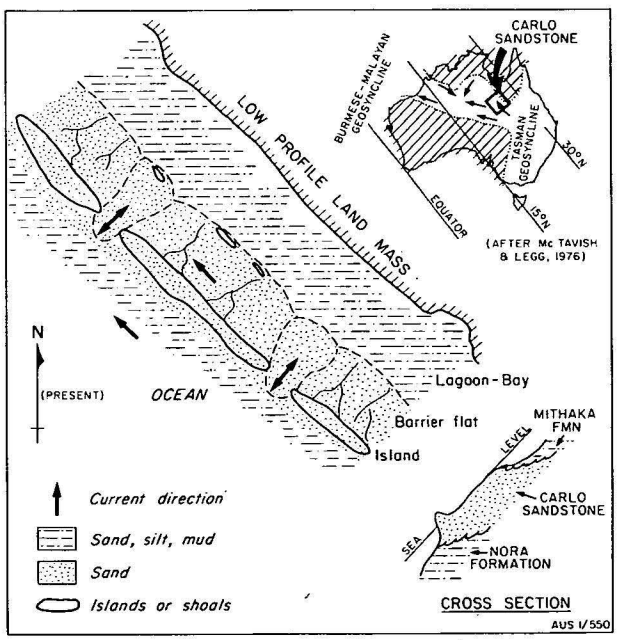

Figure 8. Palaeoenvironmental reconstruction, Carlo Sandstone.

Palaeogeography

A number of authors, most recently McTavish & Legg (1976), have postulated the existence of a narrow shallow epicontinental sea during the Ordovician (Arenig-Llanvirn), linking the Tasman Geosyncline in the east with the Burmese-Malayan Geosyncline through the Georgina, Amadeus, Wiso and Canning Basins (Fig. 8). Palaeomagnetic data indicates that this sea was in the northern hemisphere between 15°N and 30°N (Cook, 1972; McTavish & Legg 1976). The Carlo Sandstone was deposited in the northeastern region of this sea.

The Stairway Sandstone of the Amadeus Basin (Cook, 1972) is similar to the Carlo Sandstone: the Carlo Sandstone has similar features to Unit 1 of the Stairway Sandstone, the Mithaka Formation to Unit 2. The environment of deposition favoured by Cook (1972) for the Stairway Sandstone is a barrier island system similar to that proposed for the Carlo Sandstone. Recent faunal evidence suggests similar ages for the two units (J. H. Shergold, E. C. Druce, pers. comm., 1976).

The Ordovician of Australia is thought to have had a uniformly warm climate (Brown, Campbell & Crook, 1968). The geographic position from palaeomagnetic data supports this postulate. Other authors favour the presence of a warm humid climate becoming more arid towards the end of the Middle Ordovician (Wells, Forman, Ranford & Cook, 1970; McTavish & Legg, 1976). The evidence for warm humid climate cited by these authors is the presence of phosphate and the considerable amount of argillaceous material; while the appearance of anhydrite and halite indicates increasing aridity. The presence of phosphate in the Mithaka Formation supports the presence of a warm climate and the palaeolatitude suggested.

One possible source area for the sediment in the Carlo Sandstone is the Mount Isa Block which contains a mixture of sedimentary, igneous and metamorphic rocks. The types of quartz, the presence of relict over-growths and the maturity of heavy minerals suggest that some of the sediment was certainly derived from sedimentary rocks. The final quartzitic nature of the sand could result from removal of non-quartz minerals during weathering under a warm climate and quiescent tectonic conditions (Folk, 1965) or their degradation during the reworking processes involved in building a barrier. Alternatively, the quartz could have been derived from Adelaidean to Upper Cambrian sedimentary rocks within the Georgina Basin. However, from the information available no definite conclusions can be reached on the provenance of the quartz.

References

ALLEN, J. R. L., 1964—Primary current lineation in the Lower Old Red Sandstone (Devonian), Anglo-Welsh Basin. *Sedimentology*, **3**, 98-108.

ALLEN, J. R. L., 1968a—On criteria for the continuance of flute marks and their implications. *Geologie en Mijnbouw*, **47**, 3-16.

ALLEN, J. R. L., 1968b—CURRENT RIPPLES. *North-Holland Publishing Company, Amsterdam.*

ALLIANCE OIL DEVELOPMENT AUSTRALIA N.L., 1975—Well completion report. *Ethabuka No. 1* (unpublished company report).

BANKS, N. L., 1970—Trace fossils from the late Precambrian and Lower Cambrian of Tinsmark, Norway. *In* CRIMES, T. P. & HARPER, J. C. (Editors), TRACE FOSSILS, *Geological Journal Special Issue* **3**, 19-34.

BERGSTROM, J., 1973—Organization, life, and systematics of trilobites. *Fossils and Strata*, **2**. *Universitetsforlaget, Oslo.*

BLATT, H., MIDDLETON, G., & MURRAY, R., 1972—ORIGIN OF SEDIMENTARY ROCKS. *Prentice-Hall, Englewood Cliffs, New Jersey.*

BROWN, D. A., CAMPBELL, K. S. W., & CROOK, K. A. W., 1968—THE GEOLOGICAL EVOLUTION OF AUSTRALIA AND NEW ZEALAND. *Pergamon, London.*

CONYBEARE, C. E. B., & CROOK, K. A. W., 1968—Manual of sedimentary structures. *Bureau of Mineral Resources Australia—Bulletin* **102.**

COOK, P. J., 1972—Sedimentological studies of the Stairway Sandstone of Central Australia. *Bureau of Mineral Resources Australia—Bulletin* **95.**

CRIMES, T. P., 1970—A facies analysis of the Arenig of Western Lleyn, North Wales. *Proceedings of the Geologists' Association*, **81**, 221-40.

CRIMES, T. P., 1975—The production and preservation of trilobite resting and furrowing traces. *Lethaia*, **8**, 35-48.

DICKINSON, K. A., BERRYHILL, H. L., & HOLMES, C. W., 1972—Recognizing ancient barrier coastlines. *In* RIGBY, J. K. & HAMBLIN, W. K. (Editors), RECOGNITION OF ANCIENT SEDIMENTARY ENVIRONMENTS. *Society of Economic Palaeontologists and Mineralogists Special Bulletin* **16.** 146-59.

DRAPER, J. J., in prep.—The Devonian rocks of the Toko Syncline, Western Queensland. *Bureau of Mineral Resources Australia—Record* **1976/29.**

DRUCE, E. C., 1974—Georgina Basin project 1974-1980: a proposal. *Bureau of Mineral Resources Australia—Record* **1974/44** (unpublished).

DZULYNSKI, S., & WALTON, E. K., 1965—SEDIMENTARY FEATURES OF FLYSCH AND GREYWACKES. *Developments in Sedimentology*, **7**, *Elsevier, Amsterdam.*

EVANS, G., 1965—Intertidal flat sediments and their environment of deposition in the Wash. *Quarterly Journal of the Geological Society of London*, **121**, 209-45.

FOLK, R. L., 1965—PETROLOGY OF SEDIMENTARY ROCKS. *Hemphills, Austin, Texas.*

FRENCH PETROLEUM COMPANY (AUSTRALIA) PTY LTD, 1964—*Etude geologique de la Partie sud du Bassin de Georgina*, R. G. 304 (unpublished company report).

FREY, R. W. (Editor), 1975—THE STUDY OF TRACE FOSSILS. *Springer-Verlag, Berlin.*

GINSBURG, R. N. (Editor) 1975—TIDAL DEPOSITS. *Springer-Verlag, Berlin.*

GLAESSNER, M. F., 1958—Sedimentary flow structures on bedding planes. *Journal of Geology*, **66**, 1-7.

HAKES, W. G., 1976—Trace fossils and depositional environment of four clastic units, Upper Pennsylvanian megacyclothems, Northeast Kansas. *The University of Kansas Palaeontological Contributions*, **63.**

HECKEL, P. H., 1972—Recognition of ancient shallow marine environment. *In* RIGBY, J. K., & HAMBLIN, W. K. (Editors). RECOGNITION OF ANCIENT SEDIMENTARY ENVIRONMENTS. *Society of Economic Palaeontologists and Mineralogists, Special Publication*, **16**, 226-86.

IRWIN, M. L., 1965—General theory of epeiric clear water sedimentation, *Bulletin of the American Association of Petroleum Geologists*, **49**, 445-59.

JANSA, L. F., 1975—Tidal deposits in the Monkman Quartzite (Lower Ordovician) Northeastern British Columbia, Canada. *In* GINSBURG, R. N. (Editor). TIDAL DEPOSITS. *Springer-Verlag, Berlin*, 153-161.

JENKINS, J. J., 1976—Western Port and Southern Gippsland. *In* DOUGLAS, J. G. & FERGUSON, J. A. (Editors), GEOLOGY OF VICTORIA *Geological Society of Australia—Special Publication* **5**, 315-25.

KLEIN, G. de V., 1963—Bay of Funday intertidal zone sediments. *Journal of Sedimentary Petrology*, **33**, 844-54.

KLEIN, G. de V., 1970—Depositional and dispersal dynamics of intertidal sandbars. *Journal of Sedimentary Petrology*, **40**, 1095-1127.

KUENEN, Ph.H., 1964—Deep sea sands and ancient turbidites. *In* BOUMA, A. H. & BROUWER, A. (Editors), TURBIDITES. *Developments in Sedimentology*. **3**, *Elsevier, Amsterdam*, 3-33.

MCKEE, E. D., 1964—Inorganic sedimentary structures. *In* IMBRIE, J., & NEWELL, N. D. (Editors), APPROACHES TO PALAEOECOLOGY. *John Wiley, New York*. 275-92.

MCTAVISH, R. A., & LEGG, D. P., 1976—The Ordovician of the Canning Basin, Western Australia. *In* BASSETT, M. G. (Editor). THE ORDOVICIAN SYSTEM. *Proceedings of a Palaeontological Association Symposium, Birmingham, September 1974, University of Wales Press and National Museum of Wales, Cardiff.*

MAXWELL, W. G. H., 1970—The sedimentary framework of Moreton Bay, Queensland, *Australian Journal of Marine and Freshwater Research*, **21**, 71-88.

MICHAELIS, E. R., & DIXON, G., 1969—Interpretation of depositional processes from sedimentary structures in the Cardium Sand. *Bulletin of Canadian Petroleum Geology*, **17**, 410-43.

PAPUAN APINAIPI PETROLEUM COMPANY LTD, 1965—*P.A.P. Netting Fence No. 1 well, Queensland. Well completion report* (unpublished company report).

POJETA, J. (Jr.) & GILBERT-TOMLINSON, Joyce, in press—Australian Ordovician pelecypod molluscs. *Bureau of Mineral Resources Australia—Bulletin* **174.**

POTTER, P. E., & PETTIJOHN, F. J., 1963—PALAEOCURRENTS AND BASIN ANALYSES. *Academic Press, New York.*

PRENTICE, J. E., 1962—Some sedimentary structures from a Weald clay sandstone at Warnham Buckworks Horsham, Sussex. *Proceedings of the Geologists' Association*, **73**, 171-85.

RHOADS, D. C., 1975—The palaeoecological and environmental significance of trace fossils. *In* FREY, R. W. (Editor), THE STUDY OF TRACE FOSSILS. *Springer Verlag, Berlin*, 147-60.

RUCKLIN, H., 1938—Stromungsmarken in uteren. Muschelbalk des Saarlands, *Senchenbeigiana*, **20**, 94-114.

RUSNAK, G. A., 1960—Sediments of Laguna Madre, Texas. *In* SHEPARD, F. P., PHLEGER, F. B., & van ANDEL, T. H., (Editors). RECENT SEDIMENTS, NORTHWEST GULF OF MEXICO. *American Association of Petroleum Geologists Special Publication*, 153-96.

SEILACHER, A., 1964—Biogenic sedimentary structures. *In* IMBRIE, J. & NEWELL, N. D. (Editors). APPROACHES TO PALAEOECOLOGY. *John Wiley, New York*, 296-316.

SELLEY, R. C., 1970—ANCIENT SEDIMENTARY ENVIRONMENTS. *Chapman Hall, London.*

SHAW, A. B., 1964—TIME IN STRATIGRAPHY. *International Series in the Earth Sciences, McGraw Hill, New York.*

SHELDON, R. P., 1964—Palaeolatitudinal and palaeogeographic distribution of phosphorite. *United States Geological Survey Professional Paper* **501-C**. 106-13.

SHERGOLD, J. H., DRUCE, E. C., RADKE, B. M. & DRAPER, J. J., 1976—Cambrian and Ordovician Stratigraphy of the eastern portion of the Georgina Basin, Queensland and eastern Northern Territory, *25th International Geological Congress, Excursion Guide* **4C.**

SMITH, K. G., 1963—Hay River, N.T.—1:250 000 Geological Series. *Bureau of Mineral Resources Australia—Explanatory Notes* **SF53/16.**

SMITH, K. G., 1965—Tobermory, N.T., 1:250 000 Geological Series. *Bureau of Mineral Resources Australia—Explanatory Notes* **SF 53/12.**

SMITH, K. G., 1972—Stratigraphy of the Georgina Basin. *Bureau of Mineral Resources Australia—Bulletin* **111.**

SMITH, K. G., VINE, R. R., & MILLIGAN, E. N., 1961—Revisions to stratigraphy of Hay River, Huckitta, and Tobermory 4-mile sheets, Northern Territory. *Bureau of Mineral Resources Australia—Record* **1961/65** (unpublished).

SUNDBORG, A., 1956—The River Klaralven, a study in fluvial processes. *Geografiska Annaler*, **38**, 125-316.

TANNER, W. F., 1960—Shallow water ripple mark varieties. *Journal of Sedimentary Petrology*, **30**, 481-85.

VISHER, G. S., 1965—Use of vertical profile in environmental reconstruction. *Bulletin of the American Association of Petroleum Geologists*, **49**, 41-61.

WELLS, A. T., FORMAN, D. T., RANFORD, L. C., & COOK, P. J., 1970—Geology of the Amadeus Basin, Central Australia. *Bureau of Mineral Resources Australia—Bulletin* **100.**

(A) **Cross stratification, channelling and nature of bedding. Carlo Sandstone—Subunit B, Toko Range (Scale shown by hammer).**

(B) **Contact between Nora Formation and Carlo Sandstone, Oodatra Point, Toko Range.**

(C)* **Flute marks, Carlo Sandstone—Subunit A, Toko Range.**

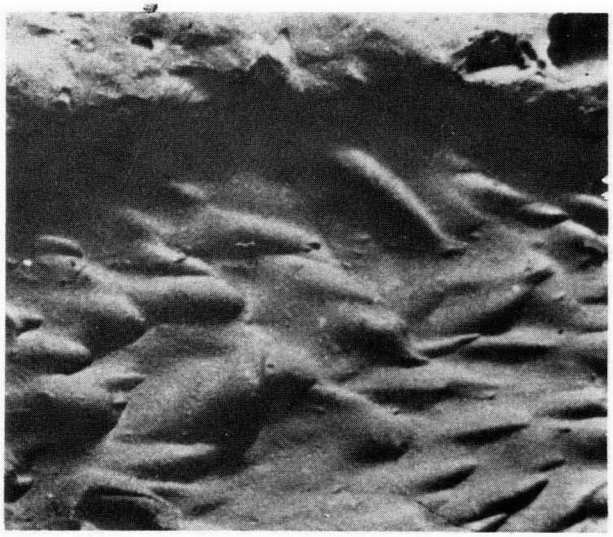

(D)* **Flute marks, Carlo Sandstone—Subunit A, Tarlton Range.**

(E)* **Current crescents. Carlo Sandstone—Subunit A, Toko Range. (Bottom straight edge of tape is 5 cm long).**

(F) **Parting lineation. Carlo Sandstone—Subunit A, Tarlton Range.**

Figure 9.

* sole markings.

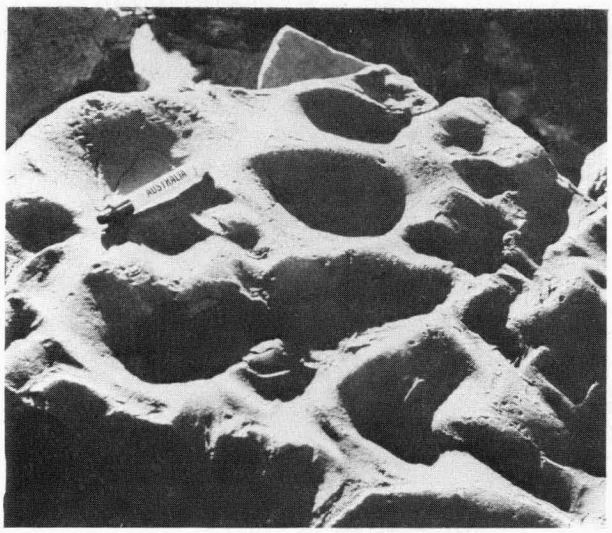

(A) **Linguoid ripplemarks with trails and tracks. Carlo Sandstone—Subunit A, Toko Range (Pen is 12.5 cm long).**

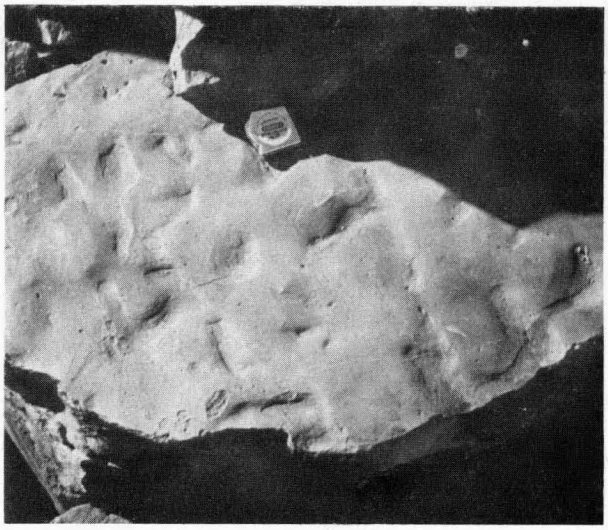

(B) **Bevelled ripplemarks with tracks. Carlo Sandstone —Subunit B, Toko Range.**

(C) **Sinuous asymmetrical ripplemarks. Carlo Sandstone —Subunit A, Toko Range.**

(D) **Slumping Carlo Sandstone—Subunit A, Toko Range.**

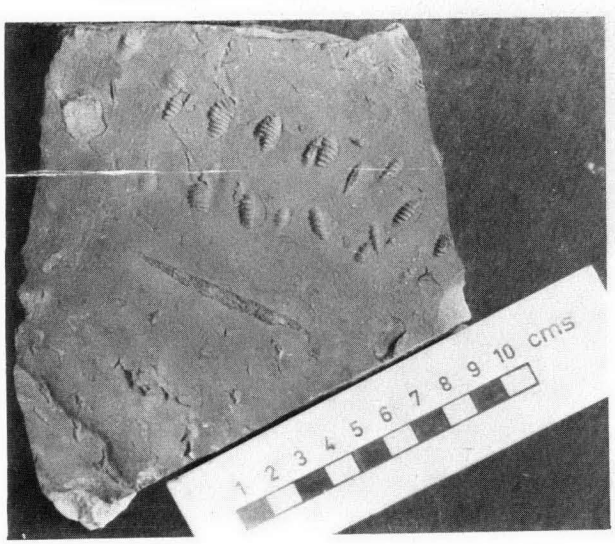

(E)* **Arthrophod (?trilobite) markings. Carlo Sandstone —Subunit A, Toko Range.**

(F)* *Rusophycus* **sp. and indeterminate markings. Carlo Sandstone—Subunit A, Toko Range.**

Figure 10. * sole markings.

(A)* *Cruziana* **sp. Carlo Sandstone—Subunit A, Tarlton Range.**

(B)* **Arthropod (?trilobite) markings which show some similarities to** *Merostromichnites.* **Carlo Sandstone —Subunit A, Toko Range.**

(C) *Arthrophycus* **sp. Carlo Sandstone—Subunit B, Toko Range.**

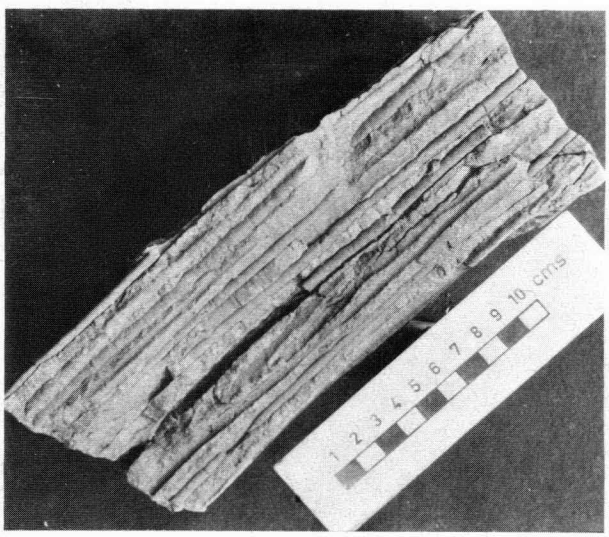

(D) *Skolithos.* **Carlo Sandstone—Subunit A, Toko Range.**

(E) *Areniculites.* **Carlo Sandstone—Subunit B, Toko Range.**

(F) *Diplocraterion.* **Carlo Sandstone—Subunit A, Toko Range.**

Figure 11. * sole markings.

A Rb-Sr geochronological study in the Proterozoic Tennant Creek Block, central Australia

L. P. Black

Rb-Sr isotopic data from total rock and mineral samples provide a broader geochronological framework than has hitherto been available for the Proterozoic rocks of the Tennant Creek Block. The oldest documented event is the amphibolite-facies metamorphism at 1920 ± 60 m.y. of possible basement rocks from the BMR 3 area, to the west-southwest of Tennant Creek township. The lower grade metamorphic rocks of the Warramunga Group were deposited before the major deformation eposide which is inferred to have occurred at about 1810 m.y. Certain of the units within the Warramunga Group, of which the Bernborough Volcanics are an example, underwent isotopic resetting of total-rock systems during subsequent deformation. Granite ages range from 1797 m.y. for a phase of the Tennant Creek Granite to less than 1500 m.y. for the Cabbage Gum and Gosse River East Granites. Dated lamprophyre and porphyry samples yield ages of about 1660 m.y. and 1760 m.y., respectively. Muscovite separates from the Juno, Warrego, Golden Forty, and Nobles Nob mines suggest a common origin for the ore deposits about 1810 m.y. ago.

Introduction

The Proterozoic Warramunga Group, which consists of interbedded sedimentary and volcanic rocks of eugeosynclinal origin, forms the major part of the Tennant Creek Block of central Australia. It is overlain unconformably by sediments of shallower water facies, the Hatches Creek Group in the south and the Tomkinson Creek Group to the north. Regional metamorphism within the Warramunga Group is generally of very low grade. Isolated occurrences of amphibolite-facies rocks have been interpreted as basement, possibly of Archaean age. The Warramunga Group is extensively intruded by igneous rocks which mostly crop out in a northwesterly striking zone centred on Tennant Creek. Granite and porphyry predominate, though diorite, dolerite, and lamprophyre are also present. The Proterozoic rocks are overlain by flat-lying Cambrian rocks and Mesozoic sediments.

There has been very little geochronological investigation of the Tennant Creek area even though it constitutes an important gold and copper mineral field. Only three K-Ar ages, which are reported in Hurley *et al.* (1961), were available for the entire Tennant Creek Block. These granite ages of 1400, 1510, and 1630 m.y. define minimum ages for the sediments within the Warramunga Geosyncline. This paper constitutes the first Rb-Sr study of the Tennant Creek Block. Although it represents a manifold increase in isotopic data, it should not be taken as a definitive study. Considerable future work, which must include the analysis of zircon concentrates, will be required to assess fully the chronology of all rock types.

Analytical techniques

Samples were collected almost exclusively from diamond drill cores to offset the widespread effects of generally deep weathering in the area. Analytical procedures for Rb and Sr were based on the techniques outlined in Page *et al.* (1976), and Williams *et al.* (1976). The 7-8 ng blank levels for both Rb and Sr were not large enough to warrant the application of blank corrections. Regression of the pooled analytical data is based on the work of McIntyre *et al.* (1966). Relative deviations of 0.5 per cent for Rb^{87}/Sr^{86}, and a standard deviation of 10×10^{-5} for Sr^{87}/Sr^{86}, have been used for all regressions, most of which involve samples analysed in 1974. All uncertainty limits are expressed at the 95 percent confidence level. The value $1.42 \times 10^{-11} y^{-1}$ (Neumann & Huster, 1972), as provisionally recommended by the August 1976 meeting of the IUGS International Commission on Stratigraphy (Subcommission on Geochronology), has been used for the decay constant of Rb^{87}. The isotopic data for all samples are presented in Table 1.

A summary of isotopic ages appears in Figure 2.

'Basement' rocks

Diamond drilling has revealed high-grade gneiss below superficial cover about 30 km WSW of Tennant Creek. Whittle (1966) reports that the gneiss belongs to the sillimanite-almandine-muscovite subfacies (Turner & Verhoogen, 1960) of the almandine-amphibolite facies. Typical rock types are garnet-mica gneiss, grunerite-garnet gneiss, plagioclase gneiss, and hornblende-tremolite-garnet gneiss; interlayers of graphically intergrown quartz and feldspar are common. Mendum & Tonkin (in prep.) state that, because of their higher metamorphic grade, the rocks are probably older than those of the Warramunga Group. They do not, however, exclude the possibility that they represent merely higher grade equivalents of Warramunga Group rocks. Mendum and Tonkin (in prep.) are also undecided whether to suggest an Archaean age or to correlate the high-grade gneisses with the Lower Proterozoic Arunta Complex to the south. The metamorphics are intruded by adamellite, alkali microgranite, microdiorite dykes and sulphide-bearing quartz dolerite and gabbro (Whittle, 1966).

Samples used in this study comprise amphibolite collected from DDH 169 in the BMR 3 area. The rock is composed of hornblende, minor quartz, and opaque minerals; chlorite, reddish-brown biotite, and possibly muscovite and sphene appear to be of later origin.

Nine separate total-rock samples were prepared from core. Samples nearest the 192.6-metre level are designated 73063284 A to F; those from the 192.6-metre level, 73063283 A to C. Regression through the analytical points (Fig. 3) generates a model 3 (see McIntyre *et al.*, 1966 for a discussion of regression models) isochron with mean square of weighted deviate (MSWD) of 8.9. The indicated age is 1920 ± 60 m.y. Various workers, for example Lanphere *et al.* (1964), Pidgeon & Compston (1965), Nunes and Steiger (1974), and Marjoribanks & Black (1974), have demonstrated the migration of Sr over distances of at least a metre during amphibolite-grade metamorphism. The relatively high grade of these basic rocks, which are separated in DDH 169 by only 0.3 m, would thus strongly suggest that it is the amphibolite-facies metamorphism which is being documented by the total-rock system. The model 3 interpretation, however, would suggest that perfect Sr-isotope

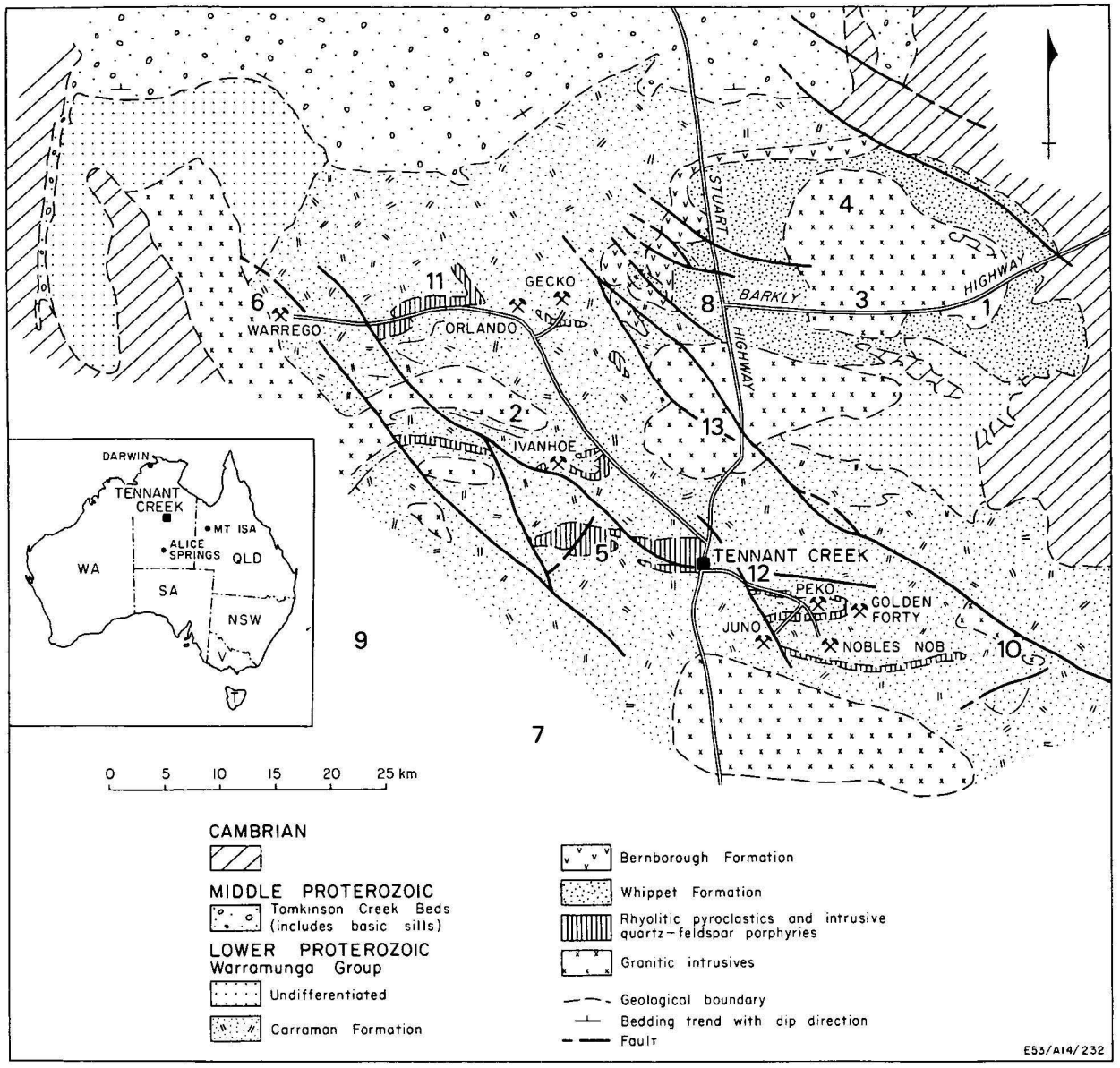

Figure 1. Geological locality map (after Large, 1975). Numbers represent sample locations:
1. Tennant Creek Granite, BMR-NTGS geochemical DDH 1, 2. Red Bluff Granite, BMR-NTGS geochemical DDH 2 & 6, 3. Tennant Creek Granite, BMR-NTGS geochemical DDH 3, 4. Tennant Creek Granite, BMR-NTGS geochemical DDH 4, 5. Porphyry, BMR-NTGS geochemical DDH 5, 6. Warrego Granite, BMR-NTGS geochemical DDH 7, 7. Cabbage Gum Granite, BMR-NTGS geochemical DDH 8, 8. Bernborough Volcanics, BMR-NTGS geochemical DDH 10 & 11, 9. 'Basement' metamorphics, BMR 3 area DDH's 1, 2, 6 & 169, 10. Lamprophyre, East New Hope area NTGS DDH's 1 & 2, 11. Intermediate to basic rocks, area 3 NTGS H7A, 12. Shale, anomaly 6 area NTGS H1, 13. Surface sample of Tennant Creek Granite at Station Hill. The North Seismic Ademellite and Gosse River East Granite sites are located south of the mapped area at latitude 19°46′30″, longitude 134°20′15″, and latitude 19°57′30″, longitude 134°45′21″, respectively.

equilibration has not occurred, even on this restricted scale. A biotite separate moderately enriched in Rb^{87}/Sr^{86} yields a significantly younger age of 1674 m.y., which must reflect a subsequent tectonic event of currently unknown significance.

Warramunga Group

The geology of the Warramunga Group is described at length in Crohn & Oldershaw (1965), Whittle (1966), Dunnet & Harding (1967), and Mendum & Tonkin (in prep.). The Group occupies much of the central part of the Tennant Creek 1:250 000 Sheet area. It is composed of dominantly eugeosynclinal deposits separated by angular unconformity from the overlying shallow-water marine deposits of the Tomkinson Creek and Hatches Creek Groups. Total thickness is difficult to estimate but probably does not exceed 3000 metres (Mendum & Tonkin, in prep.). The Warramunga Group consists of shale, siltstone, greywacke, and interbedded volcanics. Mendum and Tonkin (in prep.) have divided the Group into 10 units. Other recent workers (Large, 1975; Le Messurier, 1976) have incorporated the units of Crohn & Oldershaw (1965), and Dunnet & Harding (1967) into three main formations.

Volcanics from the Bernborough Formation and shale have been used in two independent attempts to date the Warramunga Group directly. The shale comes from Mendum & Tonkin's Bw_6 unit, from near the top of the Warramunga Group. It is equivalent to unit Bw_2 of Crohn & Oldershaw (1965), and Whittle (1966). The unit is uncon-

Sample No.	*D.D.H.*	*Depth in metres*	*Rb (ug/g)*	*Sr (ug/g)*	Sr^{87}/Sr^{86}	Rb^{87}/Sr^{86}
		'Basement'				
73063283 A T.R.	BMR 3, H169	192.9	40.53	211.5	0.72266	0.5542
73063283 B T.R.	"	192.9	36.14	236.6	0.71973	0.4416
73063283 C T.R.	"	192.9	41.78	244.2	0.72053	0.4946
73063284 A T.R.	"	192.6	46.80	146.4	0.73306	0.9251
73063284 A biotite	"	192.6	345.8	14.60	2.6728	81.55
73063284 B T.R.	"	192.6	37.40	197.3	0.72305	0.5483
73063284 C T.R.	"	192.6	79.84	128.4	0.75751	1.805
73063284 D T.R.	"	192.6	33.58	158.7	0.72437	0.6120
73063284 E T.R.	"	192.6	38.11	171.0	0.72578	0.6445
73063284 F T.R.	"	192.6	61.95	157.3	0.73843	1.1404
		Warramunga Group Shale				
73063285 A T.R.	Anomaly 6, H1	252	291.2	32.05	1.4330	28.10
73063285 B T.R.	"	252	278.9	33.48	1.3643	25.60
73063285 C T.R.	"	252	269.3	33.44	1.3460	24.71
73063285 E T.R.	"	252	298.9	30.68	1.4870	30.28
73063285 F T.R.	"	252	271.0	32.54	1.3640	25.59
73063285 G T.R.	"	252	303.8	30.06	1.5168	31.50
73063285 I T.R.	"	252	269.7	32.16	1.3701	25.79
73063285 K T.R.	"	252	261.6	29.76	1.4074	27.12
73063285 L T.R.	"	252	305.4	29.52	1.5326	32.29
		Bernborough Volcanics				
75063306 T.R.	BMR-NTGS 11	46.2	147.2	4.724	3.6736	116.1
75063307 T.R.	"	46.4	149.3	4.774	3.6643	116.4
75063308 T.R.	"	50.9	141.5	4.759	3.4791	109.1
75063310 T.R.	"	42.6	161.1	5.052	3.7383	119.4
75063311 T.R.	"	42.6	157.1	4.616	4.0452	130.4
75063312 T.R.	BMR-NTGS 10	57.6	42.38	31.34	0.81674	3.947
75063313 T.R.	"	47.8	111.3	10.67	1.51001	32.47
75063314 T.R.	"	43.2	178.3	8.638	2.3770	69.35
75063315 T.R.	"	50.8	189.9	11.18	2.0678	55.55
75063316 T.R.	"	63.0	69.04	22.88	0.93401	8.908
		Porphyry				
73063211 A T.R.	BMR-NTGS 5	13.7	320.7	44.46	1.2673	21.97
73063211 C T.R.	"	13.7	268.3	42.03	1.2010	19.32
73063211 J T.R.	"	13.7	299.5	38.57	1.3125	23.75
73063220 T.R.	"	10.7	252.7	43.96	1.1501	17.32
73063221 T.R.	"	11.0	260.5	42.97	1.1752	18.30
73063223 T.R.	"	21.2	262.1	39.25	1.2233	20.25
73063224 T.R.	"	27.3	259.8	44.42	1.1585	17.63
73063225 T.R.	"	25.3	272.3	42.58	1.2021	19.36
73063226 T.R.	"	52.1	266.2	44.11	1.1721	18.22
73063227 T.R.	"	43.3	278.6	62.85	1.0446	13.22
73063227 K-feldspar	"	43.3	432.2	99.55	1.0409	12.94
73063228 T.R.	"	51.8	234.3	47.84	1.0830	14.66
73063229 T.R.	"	64.6	255.6	52.92	1.0763	14.45
73063230 T.R.	"	75.6	260.7	43.64	1.1647	17.97
73063231 T.R.	"	78.0	258.8	40.62	1.1975	19.28
73063233 T.R.	"	88.2	363.9	57.85	1.1853	19.01
		Intermediate to basic rocks				
73063272 T.R.	Area 3, H7A	108.5	29.49	128.7	0.72670	0.6629
73063273 T.R.	"	109.4	39.05	133.1	0.73184	0.8490
73063274 T.R.	"	121.6	33.33	26.64	0.79690	3.644
73063275 T.R.	"	133.2	34.89	141.0	0.72469	0.7155
73063276 T.R.	"	146.2	48.47	151.5	0.73126	0.9259
73063277 T.R.	"	159.4	35.51	147.0	0.72269	0.6985
73063278 T.R.	"	175.6	45.70	122.2	0.73125	1.082
73063280 T.R.	"	216.4	49.31	134.3	0.73178	1.063
73063281 T.R.	"	236.2	67.29	144.7	0.74006	1.347
73063282 T.R.	"	247.8	42.66	123.6	0.73014	0.9984
		Lamprophyre				
73063265 T.R.	East New Hope, H 2	220.1	261.9	58.34	1.0208	13.36
73063266 T.R.	"	220.5	241.4	50.64	1.0406	14.21
73063266 chlorite	"	220.5	9.548	6.424	0.80703	4.333
73063266 K-feldspar	"	220.5	512.0	92.04	1.0856	16.05
73063267 T.R.	"	221.1	173.1	33.25	1.0692	15.56
73063268 T.R.	"	220.8	212.4	39.66	1.0320	16.03
73063269 T.R.	East New Hope, H 1	222.8	389.7	58.44	1.1847	20.15
73063270 T.R.	"	223.3	256.5	51.10	1.0634	15.00
72063493 T.R.	Ivanhoe Mine		104.0	62.51	0.81704	4.854
72063493 biotite	"		1015	40.78	2.7742	86.42

Table 1. Rb-Sr isotopic composition of Tennant Creek samples.

Sample No.	D.D.H.	Depth in metres	Rb (ug/g)	Sr (ug/g)	Sr^{87}/Sr^{86}	Rb^{87}/Sr^{86}
		Tennant Creek Granite				
71860059 biotite	surface sample		714.3	10.60	9.9797	371.0
73063234 T.R.	BMR-NTGS 1	105.5	204.8	82.75	0.89738	7.278
73063234 biotite	"	105.5	736.8	7.133	32.085	1214
73063241 T.R.	BMR-NTGS 3	66.8	168.3	84.65	0.85394	5.821
73063241 chlorite	"	66.8	212.1	101.9	0.86902	6.103
73063251 T.R.	BMR-NTGS 4	63.6	200.9	97.29	0.86099	6.051
73063251 biotite	"	63.6	573.3	18.83	3.621	113.0
		North Seismic Adamellite				
71860061 biotite	surface sample		683.9	8.427	14.295	545.8
		Red Bluff Granite				
73063235 T.R.	BMR-NTGS 2	81.8	88.30	72.87	0.79091	3.527
73063236 T.R.	"	105.8	32.26	105.8	0.72843	0.8825
73063237 T.R.	"	107.6	13.53	115.6	0.71600	0.3383
73063238 T.R.	"	118.3	11.01	117.0	0.71388	0.2719
73063239 T.R.	"	115.7	26.62	112.9	0.72352	0.6815
73063252 T.R.	BMR-NTGS 6	72.2	206.3	50.28	0.99926	12.19
73063253 T.R.	"	19.2	240.6	42.21	1.1357	17.15
73063254 T.R.	"	23.1	209.0	46.18	1.0310	13.48
73063254 K-feldspar	"	23.1	386.4	72.25	1.0913	16.02
73063254 chlorite	"	23.1	22.91	9.066	0.84746	7.396
73063255 T.R.	"	25.3	220.7	55.86	0.99565	11.73
73063256 T.R.	"	32.9	200.9	41.23	1.0554	14.25
73063257 T.R.	"	34.6	199.0	42.12	1.04555	14.09
73063258 T.R.	"	53.6	43.64	42.36	0.78740	2.998
		Warrego Granite				
73063259 T.R.	BMR-NTGS 7	76.5	501.9	39.61	1.6535	39.97
73063260 T.R.	"	77.7	449.3	38.92	1.5653	36.13
73063261 T.R.	"	80.2	367.3	28.30	1.6838	41.05
73063261 chlorite	"	80.2	42.32	8.489	1.0574	14.89
73063261 muscovite	"	80.2	1869	15.26	54.930	2229
73063262 T.R.	"	83.4	310.0	28.92	1.4879	33.31
73063262 chlorite	"	83.4	163.9	9.143	1.9775	58.20
73063262 muscovite	"	83.4	1802	14.53	55.456	2276
73063263 T.R.	"	85.6	520.5	46.53	1.5414	34.93
73063263 chlorite	"	85.6	163.2	11.84	1.6510	43.45
73063263 muscovite	"	85.6	1879	14.54	90.051	3674
73063264	"	83.5	312.3	22.43	1.7633	44.36
		Cabbage Gum Granite				
73063290 T.R.	BMR-NTGS 8	96.3	237.6	29.52	1.2611	24.50
73063291 T.R.	"	97.5	222.6	38.53	1.1166	17.44
73063291 K-feldspar	"	97.5	400.5	54.96	1.2373	22.13
73063291 plagioclase	"	97.5	231.0	53.62	1.0163	12.82
73063291 biotite-chlorite	"	97.5	115.1	4.858	2.3487	79.40
73063292 T.R.	"	99.1	264.9	35.89	1.2206	22.38
73063293 T.R.	"	100.3	256.1	32.45	1.2544	24.00
73063294 T.R.	"	105.5	245.6	36.97	1.1728	20.06
73063295 T.R.	"	106.4	274.9	23.31	1.5225	36.77
73063296 T.R.	"	109.1	237.9	28.35	1.2806	25.59
75063309 T.R.	BMR 3, DDH 1	195.2	222.9	97.15	0.87588	6.734
		Gosse River East Granite				
73063287 A T.R.	DDH 404	151	429.0	730.8	0.74546	1.701
73063287 B T.R.	"	151	425.6	788.7	0.74299	1.564
73063287 C T.R.	"	151	436.5	742.5	0.74585	1.704
73063287 D T.R.	"	151	433.5	767.8	0.74463	1.636
73063287 E T.R.	"	151	437.2	715.4	0.74670	1.771
73063287 F T.R.	"	151	419.0	692.5	0.74652	1.754
73063287 G T.R.	"	151	417.6	758.5	0.74362	1.595
73063287 H T.R.	"	151	421.5	760.0	0.74372	1.607
73063287 I T.R.	"	151	408.4	665.4	0.74742	1.779
73063287 J T.R.	"	151	426.2	736.2	0.74541	1.678
73063287 K T.R.	"	151	428.6	647.2	0.74956	1.920
73063287 K K-feldspar	"	151	547.7	915.8	0.74686	1.733
		Mineralised samples				
75063297 sericite	Warrego Mine		728.7	27.89	3.1556	100.4
75063297 muscovite	"		548.5	15.65	4.1238	135.0
75063298 muscovite	"		405.0	26.88	1.9871	48.95
75063299 muscovite	"		498.7	49.65	1.5222	31.32
75063300 biotite	"		514.7	20.15	2.8472	89.17
75063302 muscovite	Juno Mine		658.5	12.68	7.037	242.8
75063303 muscovite	Aquitaine, DDH 19, TC 8		596.6	14.41	5.1986	172.1
75063304 muscovite	Nobles Nob Mine		430.0	19.34	2.7244	76.87
75063305 muscovite	Golden Forty Mine		571.7	35.39	2.0708	52.87
75063305 muscovite	"		578.9	35.14	2.1419	54.25

Table 1 (continued). Rb-Sr isotopic composition of Tennant Creek samples.

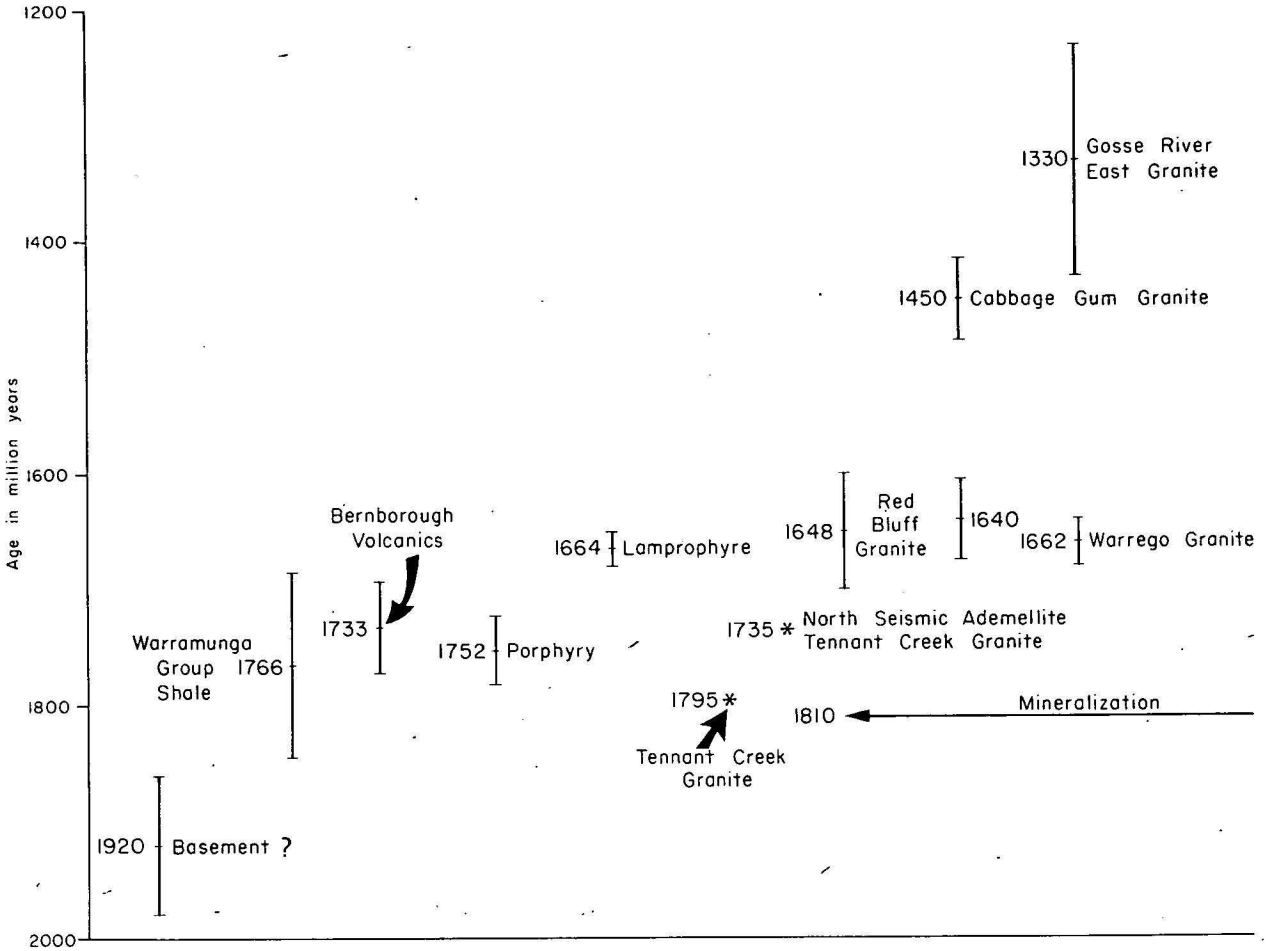

Figure 2. Summary of isotopic ages for the Tennant Creek Block. Many of these ages do not define crystallization (see text).

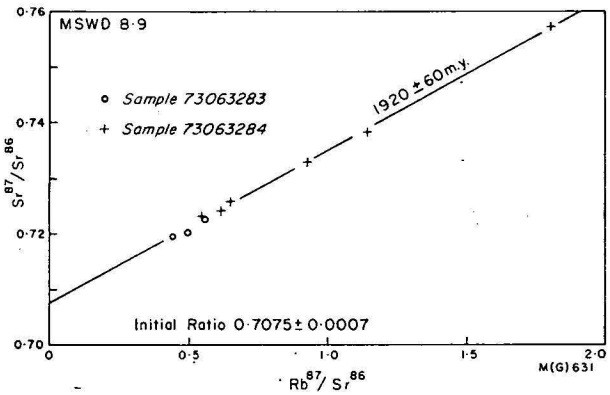

Figure 3. Rb-Sr isochron diagram for the 'basement' rocks.

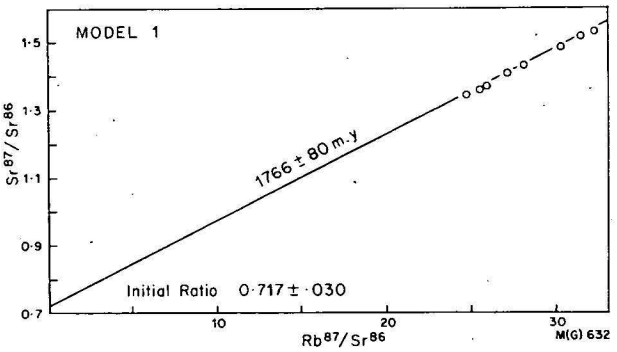

Figure 4. Rb-Sr isochron diagram for shale from the Warramunga Group.

formably overlain by the possibly Adelaidean Rising Sun Conglomerate and the Lower Cambrian .Helen Springs Volcanics. Fresh and unoxidised greywacke, shale, siltstone and rare jasper bands from this unit occur in the Peko and Juno mines (Mendum & Tonkin, in prep.).

The newly dated shale sample comes from the 252-metre level of NTGS DDH 1 in the Anomaly 6 area. It consists of very fine-grained phyllosilicates and subsidiary opaque minerals. Nine total-rock samples were prepared from about one foot of continuous core. These samples define a model 1 isochron (i.e., all scatter can be attributed to experimental error alone) with age of 1766 ± 80 m.y. and initial ratio equal to 0.717 ± .030 (Fig. 4). The relatively large uncertainties relate entirely to the rather small spread (25 to 32) of Rb^{87}/Sr^{86} ratios. In their classic study of the Montagne Noire region of Southern France, Gebauer & Grunenfelder (1974) documented the behaviour of Sr in fine-grained sediments during incipient to low-grade metamorphism. The authors concluded that total-rock isochrons from stratigraphically uncontrolled sediments of this type should generally be interpreted in terms of metamorphic rather than sedimentary ages. Hence, the indicated age of 1766 ± 80 m.y. for the Warramunga Group shale probably reflects a metamorphic resetting; it is thus no more than a minimum age estimate for sedimentation. Further evidence on this matter, which is provided by micas from the ore bodies, and granites intruding the Warramunga Group, will be presented in the Discussion.

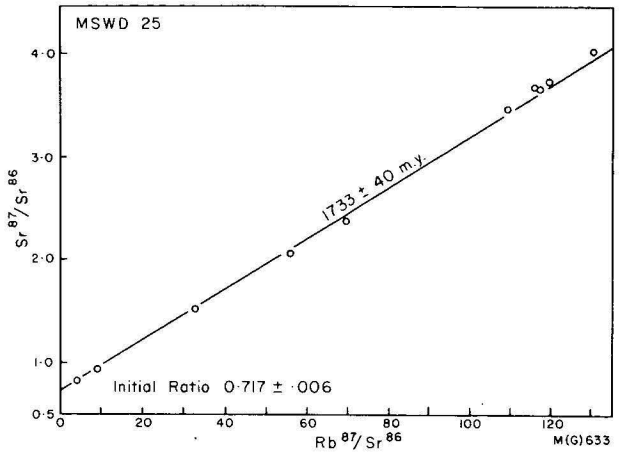

Figure 5. Rb-Sr isochron diagram for the Bernborough Volcanics.

The **Bernborough Formation**, which is comprehensively described by Dunnet and Harding (1967), is designated by Large (1975) and Le Messurier (1976) as the intermediate-level formation within the Warramunga Group. It consists of acid lava, tuff, interbedded tuffaceous greywacke and shale, siltstone, and minor ashstone, and reaches a maximum thickness of 800 metres in the type area.

The analysed samples were taken from two drillholes, DDH 10 (lat. 19°24′40″, long. 134°09′) and DDH 11 (lat. 19°26′, long. 134°8′2″), during the BMR-NTGS geochemical sampling program. Five samples were taken from between 43.2 and 63.0 metres in DDH 10, and five from between 42.6 and 46.4 metres of DDH 11. The rocks show marked signs of post-emplacement alteration. They consist of rounded quartz, variably altered feldspar, and opaque-mineral phenocrysts, set in a groundmass of quartz, fine white mica, and rare chlorite.

Regression through the entire 10 analyses (Fig. 5) yields an age of 1733 ± 40 m.y. from the assumption of a model 3 isochron; MSWD is 25. As was the case with the shale sample, this can be regarded only as a minimum age estimate for the Bernborough Formation. Page (in prep.) has shown that acid igneous rocks which have suffered low-grade metamorphism often yield anomalously young total-rock Rb-Sr ages. This observation has also been made in a study of submarine volcanics on the west coast of Tasmania (Black, unpublished analyses). The moderately large MSWD of 25 indicates non-ideal geological conditions for the generation of the Bernborough Volcanics isochron.

To summarize, then, the ages of 1766 ± 80 m.y. and 1733 ± 40 m.y. determined for the Warramunga Group do not represent crystallization or sedimentation, but appear to indicate a time of subsequent isotopic redistribution. Further evidence on this subject is presented in the Discussion.

Porphyry

The porphyries of the Tennant Creek area have been described by Crohn & Oldershaw (1965), and Mendum & Tonkin (in prep.). The latter have divided them into two lithological varieties, quartz porphyries and quartz-feldspar porphyries. Both types can occur as concordant bodies which are cleaved, and show no apparent contact effects. They can also occur as uncleaved cross-cutting bodies which have silicified adjacent sediments. Elliston (1963, 1968) postulated that the quartz-feldspar porphyry formed authigenically from a colloidal suspension of fine sediment. However, Spry (1963) and Large (1975, quoting his earlier work) have shown that chemical, mineralogical, and textural features relate to a felsic volcanic origin. Quartz-feldspar porphyry is particularly abundant in a northwest-trending granite-rich zone between the Gosse River and the Warrego mine.

The quartz-feldspar porphyry analysed in this study was sampled between the 10.8 and 89.1 metre levels of BMR-NTGS DDH 5, 11 km west-northwest of Tennant Creek. Microscopic examination reveals a high (30-40 percent) phenocryst content. Large, rounded, relatively unaltered alkali feldspar, which commonly displays microcline-twinning, and rounded, often deeply-embayed relict quartz grains dominate. Oligoclase-andesine and opaque minerals are also present. Relict ferromagnesian minerals are pseudomorphed by chlorite-muscovite-opaque mineral aggregates. Green biotite is locally present. Quartz, feldspar and fine-grained phyllosilicates dominate the groundmass.

Regression through the 15 isotopically analysed total-rock samples yields an age of 1760 ± 32 m.y. and an initial ratio of 0.711 ± .008. The relatively large uncertainty of the initial ratio is entirely due to a lack of analyses with Rb^{87}/Sr^{86} ratios less than 13; the analytical points themselves reveal no geological component of scatter about the isochron. Inclusion of an alkali-feldspar separate from sample 73063227 maintains model 1 conditions and produces indistinguishable parameters of 1752 ± 30 m.y. and 0.713 ± .0007 (Fig. 6). It is unlikely that perfect post-crystallization homogenization of Sr could have occurred over the 80 m by which these samples are separated. Hence the indicated age probably denotes the time of intrusion of this porphyritic body. A reset metamorphic interpretation cannot, however, be completely excluded.

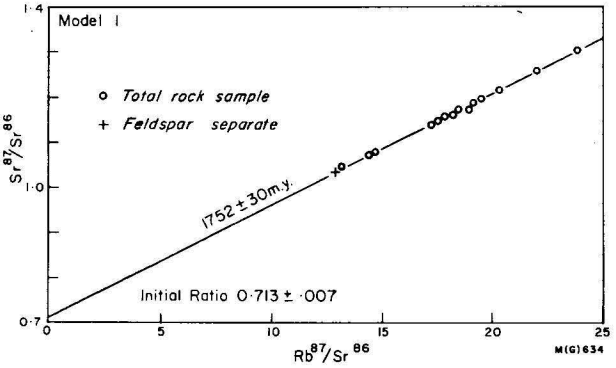

Figure 6. Rb-Sr isochron diagram for the porphyry.

Intermediate to basic rocks

Sills, dykes, and stocks of diorite and dolerite intrude the upper parts of the Warramunga Group and the lower levels of the overlying Tomkinson Creek Group (Mendum & Tonkin, in prep.). Specimens for isotopic analysis were sampled between 106.8 and 247.8 metres in the NTGS's DDH 7A in area 3, 16 km east-northeast of the Warrego mine. In this area an essentially quartz diorite body grades from monzonite towards a gabbroic composition with depth (M. R. Daly, written comm., 1975). Unfortunately, the small spread in Rb/Sr and considerable dispersion of points about the regression (Fig. 7) do not allow the deduction of a meaningful age. The dispersion may arise from primary influences—for example, composite intrusion, isotopically unequilibrated magma, or heterogenous isotopic contamination. Alternatively, it could derive from post-crystallization migration of Sr. Most samples are highly altered; chlorite and epidote commonly replace hornblende and pyroxene, and plagioclase is generally markedly

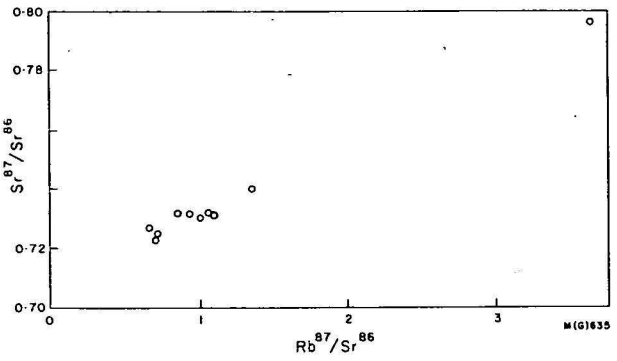

Figure 7. Rb-Sr isochron diagram for the intermediate to basic rocks.

sericitised. There is no correlation, however, between degree of alteration and isotopic composition.

Lamprophyre

Small sills, and dykes of lamprophyre which have been emplaced along faults and shear zones, occur in a NW-striking zone within the Warramunga Group. The lamprophyre is spatially associated with the Warrego, Tennant Creek, and Channingum Granites with which it is thought to relate (Mendum & Tonkin, in prep.). The samples used in this study were collected between 220.1 and 223.3 metres in NTGS's DDH 1 and 2 (350 m apart), near the Channingum Granite, in the East New Hope area. A further specimen, 72063493, was collected from the Ivanhoe mine. Mendum & Tonkin (in prep.) record that lamprophyre near the Channingum Granite consists of large books of biotite in a limonite, hematite, and feldspar groundmass containing minor quantities of quartz. Biotite has been completely replaced by chlorite in the analysed samples. Crohn & Oldershaw (1965) report the presence of amphibole and pyroxene-bearing lamprophyre elsewhere in the Sheet area.

Regression through all six total-rock analyses from DDH's 1 and 2 yields an age of 1673 ± 80 m.y. and initial ratio of 0.699 ± .017 from a model 1 isochron. The large error limits results from a small spread (13 to 20) in Rb^{87}/Sr^{86} ratios. Inclusion of the Ivanhoe mine lamprophyre, with Rb^{87}/Sr^{86} of 5, produces a further, more precisely defined model 1 isochron with age and intial ratio of 1664 ± 16 and 0.701 ± .002, respectively (Fig. 8). The low indicated initial ratio and ideal nature of both isochrons indicates that they define the original age of crystallization for the lamprophyres. Regression through feldspar, chlorite, and total-rock points for sample 73063266 produces values of 1650 ± 113 m.y. and 0.704 ± .011. The uncertainty limits reflect only the small number of analyses, for once more they define a model 1 isochron. A moderately enriched biotite separate from the Ivanhoe mine lamprophyre (72063493) yields an age of 1670 m.y. Comparison of the mean ages of the total-rock isochron, mineral isochron, and the biotite age, indicates 1670 m.y. as the approximate emplacement age. No significant post-crystallization thermal events occurred near either lamprophyre.

Granites

The granites of the Tennant Creek 1:250 000 Sheet area have been discussed by various authors—for example, Crohn & Oldershaw (1965), Dunnet & Harding (1967), and Mendum & Tonkin (in prep.), from whom this resume is derived.

Granites intrude the Warramunga and Hatches Creek Groups but have not been found intruding the Tomkinson Creek Group. They extend from the southeast corner of the Sheet area, northwestwards to beyond the Warrego Mine. Lithological varieties range from minor granodiorite, through fine-grained adamellite, to coarse porphyritic K-rich granite (*sensu stricto*). Foliation is reported to commonly parallel the regional cleavage; locally it appears to be primary. The granites have formed only a low-grade contact aureole. Xenoliths of country rock are not common.

Crohn & Oldershaw (1965) divided the granites of the Tennant Creek One-Mile Sheet area into the Tennant Creek and Cabbage Gum Granite Complexes, both of which were lithologically subdivided. Mendum & Tonkin (in prep.) have subsequently recognised and informally named 20 lithological varieties of granite in the 1:250 000 Sheet area. Their subdivision is followed in this text.

The main outcrops of the **Tennant Creek Granite** occur in the Station Hill, White Hill, and Whippet Trig areas to the north of Tennant Creek township. Le Messurier (1976), and Mendum & Tonkin (in prep.), assume a subsurface connection between these lithologically similar granites.

Sample 73063234 comes from BMR-NTGS DDH 1, situated immediately south of the Barkly Highway 35 km to the northeast of Tennant Creek. The analysed sample represents medium, even-grained, pinkish granite from the 105.5-metre level. It is composed of quartz, perthitic potash-feldspar, heavily sericitized and weakly zoned sodic plagioclase, and interleaved biotite and chlorite with associated opaque minerals. Aggregates of muscovite occur locally. Strain features are not pronounced. Some feldspar grains have iron-stained boundaries.

A small spread in Rb^{87}/Sr^{86} ratios (determined by X-ray fluorescence analysis) does not allow the derivation of a whole-rock age for granite from this drillhole. The only age estimate is provided by a biotite-total rock pair from sample 73063234, which yields a fairly precise value of 1798 m.y. Lithologically similar Tennant Creek Granite from BMR-NTGS DDH 4, 3 km south of Whippet Trig, yields a similar, though less precise, biotite-total rock age of 1794 m.y. Biotite from BMR-NTGS DDH 3, 8 km to the south of DDH 4 has completely altered to chlorite, from which it was not possible to derive a precise age.

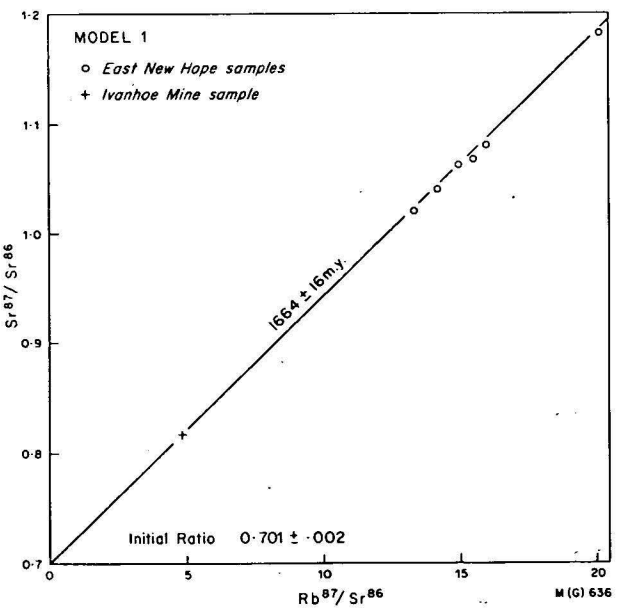

Figure 8. Rb-Sr isochron diagram for the lamprophyre.

A biotite separate from a sample (71860059) collected by Mendum, 12 km north of Tennant Creek produces an age of 1738 m.y. This granite is lithologically quite distinct from the other analysed granite samples. It displays a pronounced metamorphic fabric, and consists of large, rounded, perthitic orthoclase phenocrysts set in a groundmass of altered plagioclase, biotite, and blue opalescent quartz.

All values represent no more than minimum age estimates for the Tennant Creek Granite. The similar ages of the medium-grained granite from DDH's 1 and 4, which are 20 km apart, suggests, however, that a real geological event occurred at about 1796 m.y. This could correspond to the time of granite emplacement.

The **North Seismic Adamellite** crops out to the southeast of Nobles Nob. It has been subdivided by Mendum & Tonkin (in prep.) into two units. A biotite separate (71860061) from one of these, the black and white, mottled medium-grained adamellite, yields a precise Rb-Sr age of 1731 m.y. from an assumed initial Sr^{87}/Sr^{86} ratio of 0.71. The close similarity of this value to that of the porphyritic phase of the Tennant Creek Granite (1738 m.y.) may indicate a real event at this time, which may correspond to granite emplacement.

The **Red Bluff Granite** outcrops near Red Bluff, 20 km northwest of Tennant Creek. Two phases have been recognized by Mendum & Tonkin (in prep.), and both have been dated. Most of the 'granite' is a red-brown, medium to coarse-grained massive adamellite. This phase was collected from DDH 6 of the BMR-NTGS geochemical survey. The medium-grained granite consists of microcline and quartz, which commonly form granophyric intergrowths, heavily sericitized plagioclase, and biotite which has been completely replaced by chlorite. The latter is not sufficiently enriched in Rb with respect to Sr to allow mineral dating. However, seven total-rock samples from 19.2 to 72.2 metres do exhibit sufficient spread (3 to 17) in Sr^{87}/Sr^{86} to generate a well-defined isochron (Fig. 9). This yields an age of 1648 ± 50 m.y. and an initial ratio of 0.716 ± .005. The computer-selected model 2 regression with MSWD of 15 suggests either that there is a small age difference between samples or that the granite has suffered a slight redistribution of Rb and/or Sr since emplacement.

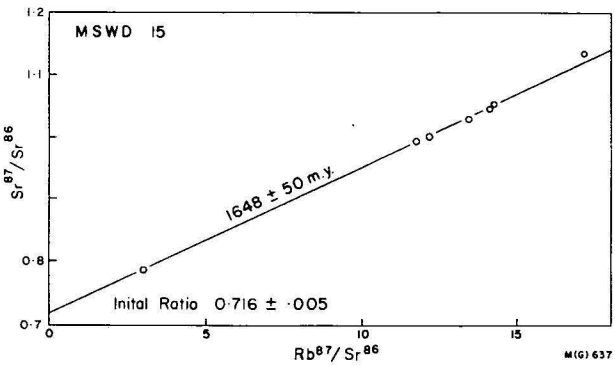

Figure 9. Rb-Sr isochron diagram for the Red Bluff Granite from DDH6 of the BMR-NTGS geochemical survey.

The northwestern part of the Red Bluff Granite was sampled in DDH 2 of the BMR-NTGS geochemical sampling program. Here the somewhat coarser-grained granite contains slightly porphyritic pink K-feldspar. Microscopic examination shows large microcline grains which frequently form granophyric intergrowths with quartz. Plagioclase is heavily sericitized. Biotite is absent, chlorite is rare. Patches of epidote and sphene occur locally. The five samples which generate the total-rock isochron

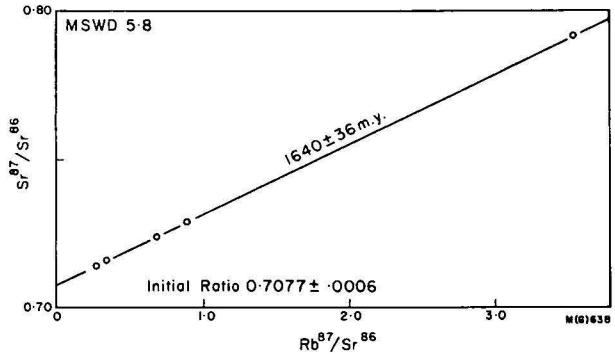

Figure 10. Rb-Sr isochron diagram for the Red Bluff Granite from DDH2 of the BMR-NTGS geochemical survey.

(Fig. 10) were taken from between 81.8 and 115.7 metres below surface. The resultant age is 1640 ± 36 m.y.; the initial Sr^{87}/Sr^{86} ratio is 0.7077 ± .0006. The model 3 isochron with MSWD of 6 implies the correlation of samples with slightly differing initial ratios. The agreement of these relatively precise ages for both phases of the Red Bluff Granite probably indicates a common emplacement age of about 1645 m.y. The significantly different initial ratios, however, show that, even though contemporaneous, the two phases of the granite were not generated from an isotopically common source region.

The **Warrego Granite** crops out in the vicinity of the Warrego mine, 50 km northwest of Tennant Creek. Mendum & Tonkin (in prep.) have divided it into three major lithological varieties. The analysed samples were collected 3 km west of the Warrego mine between 76.5 and 83.5 metres in DDH 7 of the BMR-NTGS geochemical project. The granite here is light-coloured, massive, and medium to coarse-grained. It is composed of unaltered microcline, quartz, and plagioclase (andesine?) which is atypically fresh for granites of this region. Biotite, commonly altered to chlorite, differs markedly in abundance. Books of coarse fresh muscovite occur locally.

Regression through the six total-rock analyses produces an age of 1703 ± 100 m.y. The large uncertainty does not relate to scatter about the isochron for the points fulfil model 1 conditions. It derives, in fact, from the small spread (33 to 44) in Rb^{87}/Sr^{86}. The addition of a chlorite analysis (73063261) maintains model 1 conditions (which may justify its inclusion), increases the range of Rb^{87}/Sr^{86} values to 15, and produces the improved figures of 1662 ± 20 m. y. and 0.702 ± .008 (Fig. 11). This is, however, a somewhat subjective procedure for two other chlorite separates are not concordant (see below). Three muscovite separates from samples 73063261, 73063262 and 73063263 yield ages of 1692, 1674 and 1692 m.y., respectively. The concordancy of these with the mean total-rock and total

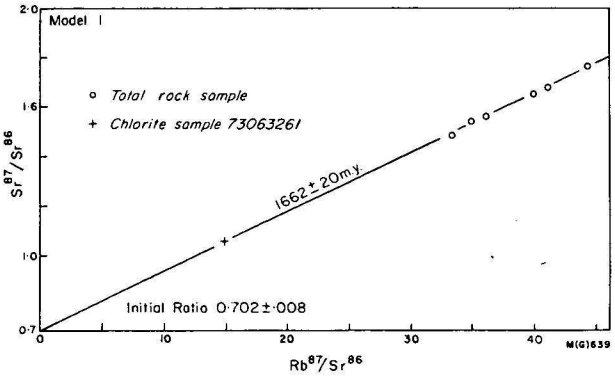

Figure 11. Rb-Sr isochron diagram for the Warrego Granite.

rock-chlorite isochron ages points to a reliable approximate age for the Warrego Granite of 1690 m.y. The low mean initial ratio for the total rock-chlorite isochron of 0.702 militates against a substantially older estimate than the mean age; the muscovite ages against a substantially younger value. The two other chlorite separates (73063262 and 73063263) which are not concordant plot below the total-rock isochron; this is presumably owing at least partly to a post-emplacement thermal event of insufficient magnitude, at this locality, to affect the Rb and Sr systematics of muscovite and chlorite 73063261. Younger granites, which may be the source of this thermal resetting, do exist in the Tennant Creek area, as discussed below.

The **Cabbage Gum Granite Complex** is so poorly exposed that it is known almost entirely from diamond-drill hole intersections. Consequently the relationship between the major phases, which include porphyritic adamellite, augen gneiss and medium-grained gneissic granite, is not known. The analysed samples were taken from pinkish, medium-grained, foliated adamellite in BMR-NTGS DDH 8, 24 km southwest of Tennant Creek. Microscopically the rock consists of slightly phenocrystic microcline, heavily sericitized plagioclase, granular quartz around feldspar and large quartz nuclei, and ragged greenish-brown biotite flakes which are partly altered to chlorite, and often occur with opaque minerals.

Seven total-rock samples were prepared from core taken between 96.3 and 109.1 meteres in DDH 8. These define a model 1 isochron of 1450 ± 36 m.y., and an initial ratio of 0.753 ± .012 (Fig. 12). A further total-rock sample (75063309), taken at 195.2 metres in a different drill hole (DDH 1 in the BMR 3 area), 18 km to the northwest of DDH 8, which does not fit this ideal isochron, indicates a slight but significant difference in age, or initial Sr^{87}/Sr^{86} ratio, or post-emplacement redistribution of isotopes within the Cabbage Gum Complex. This observation may explain the apparent anomaly between the rather precise total-rock Rb-Sr age of 1450 ± 36, and the older K-Ar age of 1630 m.y. reported by Hurley *et al.* (1961) from what Crohn & Oldershaw (1965), and Mendum & Tonkin (in prep.), claim to represent the Cabbage Gum Granite. The localities in question are separated by 27 km. It may be that the Cabbage Gum Complex is composed of granites of distinctly different ages, as might be anticipated from the textural variability shown in hand specimen.

Microcline and a mixed chlorite-biotite separate from specimen 73063291 do not fit the total-rock isochron. It seems quite probable, therefore, that this phase of the granite is not the last thermal manifestation in the Tennant Creek area. The calculated age (1370 m.y.) for the biotite-chlorite mixture should give an older limit for the time of the last event. This argument is supported by data from the Gosse River East Granite (see below). The metamorphic texture of the Cabbage Gum Granite would indicate that the derived age of 1450 ± 36 m.y. could date either post-emplacement tectonism or the time of original emplacement. The ideal nature of the total-rock isochron for DDH 8 samples supports the second alternative. It is, moreover, quite conceivable that the development of metamorphic fabric was approximately synchronous with granite emplacement.

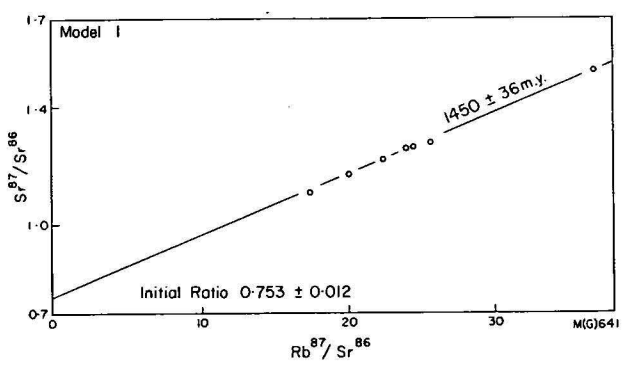

Figure 12. Rb-Sr isochron diagram for the Cabbage Gum Granite.

The **Gosse River East Granite** of Mendum & Tonkin (in prep.) forms sparse outcrops to the east of the Gosse River, 50 km east-southeast of Tennant Creek. It is a pinkish brown, medium and even-grained granite—in the strict sense, and consists of microcline, heavily sericitized plagioclase, quartz, chlorite, and opaque minerals. The analysed samples were taken from depths in DDH 404 (Australian Development Ltd) between 150.7 and 151.3 metres. Regression through 11 total-rock samples from this section yields a model 1 isochron with age and initial ratio of 1300 ± 100 m.y. and 0.714 ± .002. Addition of a microcline analysis yields a further model 1 isochron, with statistically unchanged values of 1330 ± 100 m.y. and 0.713 ± .002 (Fig. 13). The apparent equilibrium between total-rock and feldspar is a consistent, though not necessarily conclusive argument that the Gosse River East Granite represents one of the final thermal events within this area. It must be emphasised that the computer-generated age limits could conceivably be a little optimistic for this suite which has a spread in Rb^{87}/Sr^{86} from only 1.56 to 1.92.

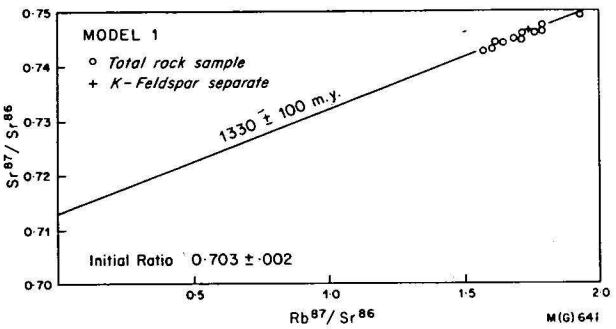

Figure 13. Rb-Sr isochron diagram for the Gosse River East Granite.

Economic geology

The following resume is drawn from the works of Ivanac (1954), Crohn & Oldershaw (1965), Whittle (1966), Dunnet & Harding (1967), Large (1975), Le Messurier (1976), and Mendum & Tonkin (in prep.). The Tennant Creek area is primarily an important gold and copper field, though small concentrations of bismuth, selenium, lead and zinc are also found. All economic mineralization in the Tennant Creek mineral field is associated with hematite and/or magnetite bodies. These range from a few inches to more than 10 metres in width and may be up to several hundred metres long. These 'ironstones', which are both structurally and lithologically localised, occur exclusively within the Carraman Formation (informal name, see Large (1975) and Le Messurier (1976)) of the Warramunga Group, for which a shale age of 1766 ± 80 m.y. was derived. Crohn & Oldershaw (1965) report that shear zones, nearby porphyry intrusions, the shale-greywacke succession, and especially the hematite shale horizon, provide favourable depositional loci. Most ironstone bodies are pipe-like to lenticular, but irregular bodies are also found. Their location is controlled by structures formed during the main folding episode.

Although there is agreement on the association of economic mineralization with the ironstones, there remains considerable controversy over their specific genesis. For example, the granites (Ivanac, 1954), 'sedimentary'

porphyries (Elliston, 1963), igneous prophyries (Crohn & Oldershaw, 1965), and basic rocks (Whittle, 1966; Dunnet & Harding, 1967) have all been suggested as sources for the economic mineralization. The recent study by Large (1975) provides a strong case for the production of the hydrothermal ore-bearing fluids by dewatering of sediment near granitic intrusions. Reactions with host rocks produced a systematic chemical variation within the fluid, and the consequent zonation within the orebodies. New isotopic data have provided further evidence on the origin of the ironstones.

Speciments from various mineralized areas and relevant geological information were made available by local mining companies. Geopeko Ltd supplied samples from the Juno and Warrego Mines. That from Juno (75063302) comes from the footwall side partly below the No. 2 ironstone body, and is associated with a small body of mineralization. It is composed mainly of chlorite and magnetite. Small quantities of variably sized muscovite which are present yield a precise Rb-Sr age of 1810 m.y. P. Le Messurier (written comm., 1976) believes that, as there is no evidence of later thermal events, this sample from the hydrothermally altered zone should reflect the time of mineralization.

Four samples from the Warrego mine were dated. The first (75063297) is from 10 level in the No. 1 orebody. It consists of chlorite, magnetite, muscovite, and aggregates of sericite. Separated sericite and muscovite yield ages of 1693 and 1757 m.y., respectively. Sample 75063298 was collected on level 10 in the No. 3 orebody. It consists of quartz, magnetite, and interleaved muscovite and chlorite. The muscovite gives an age of 1810 m.y. Sample 75063299, which consists of quartz, chlorite, magnetite, and fine-grained muscovite, was collected from level 5 in the No. 1 orebody. This sample produces a relatively imprecise Rb-Sr muscovite age of 1803 m.y. from an assumed initial Sr^{87}/Sr^{86} ratio of 0.71. Quartz-chlorite-magnetite-apatite-biotite rock from level 5 in No. 1 orebody is represented by sample 75063300. Separated biotite indicates an approximate age of 1665 m.y. Samples 75063297, 75063298, and 75063299 represent hydrothermally altered wallrock adjacent to ironstone. Sample 75063300 is one of many chlorite-muscovite-biotite dykes which occur throughout the mine, and are most common within the ironstone. Le Messurier (1975) reports that the micas from both occurrences should have formed during mineralization. The older muscovite values of about 1810 m.y., then, probably define this time, whereas the younger muscovite age of 1757 and the sericite and biotite ages of 1693 and 1664 m.y., may reflect subsequent minor thermal events. Biotite responds more readily than muscovite to heating and the fine-grained sericite would be expected to behave similarly.

Australian Development Limited supplied specimens from their Nobles Nob and Golden Forty mines. The sample from the former consists mainly of chlorite, euhedral magnetite, abundant muscovite, and some quartz. As the muscovite is only moderately enriched in Rb^{87}/Sr^{86} (77), any calculated age is slightly dependent on assumed initial ratio. Variation from 0.71 to 0.73 produces ages between 1820 and 1805 m.y. The Golden Forty sample is rather fine-grained, and consists of a chloritic matrix containing euhedral magnetite, abundant small muscovite flakes, some of which form veins, and locally quartz. An age of 1810 m.y. is obtained from averaging the results of two somewhat mediocre Sr mass-spectrometer runs.

An additional sample was obtained from DDH 19 in the TC8 deposit, 4.5 km west of Tennant Creek, which is jointly owned by Aquitaine Australia Minerals Pty Ltd, Le Nickel (Australia) Exploration Pty Ltd, Gesellschaft mbH and Western Nuclear Australia Limited. This sample consists of chlorite, commonly acicular magnetite, quartz, and some small flakes of muscovite. A fairly precise age of 1816 m.y. obtained from muscovite is in agreement with the bulk of muscovite ages from mineralized samples in the Tennant Creek mineral field. The significance of these results is discussed in the next section.

Discussion

The low-grade metamorphic environment of the Tennant Creek Block does not favour the establishment of unequivocal geochronological ages. Any interpretation of the isotopic data must consequently depend heavily on observed geological relationships.

The key for correlation of isotopic data with the sequence of tectonic events affecting the Warramunga Group is provided by the relationships of economic mineralization to folding. The orebodies, which are dated at about 1810 m.y., are localized by structures formed during the main folding event with its associated, east-west-oriented, slaty cleavage. Furthermore, recent workers (e.g., Large, 1975; Le Messurier, 1976) maintain that the mineralization was contemporaneous with, rather than significantly later than, the main folding, and can consequently be dated at about 1810 m.y.

Error limits for the shale age (1766 ± 80 m.y.) in the Warramunga Group are not precise enough to decide whether the shale is significantly younger than 1810 m.y. However, the apparent age of the Bernborough Volcanics, which Mendum & Tonkin (in prep.) consider to be lower in the stratigraphic sequence than the dated shale, is significantly younger, at 1733 ± 40 m.y. The results of Gebauer and Grunenfelder (1974), reported earlier, indicate that shale ages are particularly susceptible to isotopic resetting. Hence, both total-rock ages could presumably have been reset by a subsequent event corresponding perhaps to the development of the 'phase 3' conjugate shear systems described by Dunnet and Harding (1967), and Mendum & Tonkin (in prep.). Further evidence for this conclusion is provided by the biotite age (1738 m.y.) for the Tennant Creek Granite near Station Hill. The phase 3 folding is more strongly developed at this place than elsewhere in the Tennant Creek area. The sedimentary rocks display strong S3 cleavage; strong deformation features within the granite itself would therefore be expected to be related, at least in part, to this deformation. Consequently, the biotite age of 1733 m.y. may be regarded as a probable minimum estimate for this period of folding. The similarity of this age to that of the North Seismic Adamellite may not be coincidental, and may in fact define the synchronous emplacement of both masses, the former in a region of high stress and the latter in a stress-free environment to the southeast. This value of 1733 m.y., which fits so closely the mean age for the Bernborough Volcanics, would then provide the most precise time estimate available for the phase 3 deformation.

Le Messurier (1976) notes several post-main-episode folding and shearing events. The limits provided by the foliated Cabbage Gum Granite of 1450 ± 36 m.y. may well reflect one of these. Poor outcrop, however, does not encourage detailed structural analysis of the deformation in the vicinity of the Cabbage Gum Granite.

There is currently no evidence for major tectonic activity after the emplacement of the Gosse River East Granite. Moreover, as might be expected from the stratigraphy, the Middle Palaeozoic Alice Springs Orogeny, which was sufficiently intense to reset mineral ages over large areas of the Arunta Block to the south, e.g., Stewart (1971), Marjoribanks and Black (1974), Armstrong and Stewart (1975) and Black (1975), is not expressed at all in the Tennant Creek Block.

The low regional metamorphic grade of the Warramunga Group should be noted here. Le Messurier (1976), and

Mendum & Tonkin (in prep.), ascribe greenschist facies conditions; Wyborn (pers. comm., 1976), however, postulates even lower grades, for detrital plagioclase is not albitized, and chert fragments in sediments have not recrystallized. In the absence of elevated regional temperatures, total-rock resetting, especially for shale, must relate principally to dynamic effects and the accompanying migration of residual water within these essentially unmetamorphosed rocks.

Some authors (e.g. Dunnet & Harding, 1967; Mendum & Tonkin, in prep.) consider the Tomkinson Creek Group to predate the main folding. If this is correct, the isotopic inferences would require a pre-Carpentarian initiation of sedimentation for that group. Recently, however, Australian Development Limited (1976) have suggested that the Hatches Creek and Tomkinson Creek Groups postdate the main folding and associated east-west axial-plane cleavage of the Warramunga Group. It will require detailed structural analysis within the Tomkinson Creek Group before the current isotopic data can be used to define its chronology.

The poorly exposed rocks to the southwest of Tennant Creek, which were metamorphosed to amphibolite grade at 1920 ± 60 m.y., currently yield the oldest isotopic age for the area. Even so, it cannot be stated unequivocally that these rocks predate those of the Warramunga Group which give substantially young mineral and total-rock ages. From previous discussion it is apparent that the Warramunga Group ages reflect only tectonic events subsequent to deposition. No reliable age estimate for the latter is yet available. Indeed, Dunnet & Harding (1967) have inferred a folding episode older than the main deformation. It could be speculated that this 'phase 1' folding was synchronous with the amphibolite-facies metamorphism at about 1920 m.y. The presently exposed parts of the Warramunga Group could have been at a sufficiently high crustal level to escape all but the slightest tectonic effects. The amphibolite-facies rocks, however, would have formed at deeper levels and been subsequently uplifted.

An alternative explanation is that the amphibolite-facies rocks do in fact represent basement to the Warramunga Group as a superficial examination of the isotopic data would suggest. In this case the inferred phase 1 folding of Dunnet & Harding (1967) could either not have taken place, as contended by Mendum & Tonkin (in prep.), or be completely masked by the effects of the subsequent dominant deformation. Current isotopic data are not sufficient to decide whether the amphibolite-facies rocks represent basement or merely higher grade equivalents of the Warramunga Group. U-Pb zircon studies on the Bernborough Volcanics should resolve this problem.

Overall, the data indicate a considerable range of emplacement ages. The Tennant Creek Granite biotite age of about 1800 m.y. can be confidently assumed as a minimum estimate for the initiation of intrusion. The age grouping around 1660 m.y. must be also primary for the following reasons. First, the two different phases of the Red Bluff Granite, from separate drillholes, yield indentical total-rock ages. Second, the low initial ratio of 0.701 ± .002 for lamprophyre, combined with its moderate Rb^{87}/Sr^{86} values (average about 15), precludes post-emplacement isotopic redistribution. Lastly, the combination of muscovite ages and low mean initial Sr^{87}/Sr^{86} ratio for the total-rock isochron representing the Warrego Granite, does not allow significant variation of postulated age from the preferred value of about 1690 m.y.

The present isotopic data apparently indicate subsequent relative quiescence for about 200 m.y. up to the emplacement of the Cabbage Gum and Gosse River East Granites. Evidence for the primary nature of the youngest granite ages is not as conclusive as for the other groups. It is, however, reasonably persuasive. Confidence in the age of the Gosse River East Granite (1300 ± 100 m.y.), for example, is restricted by the small spread in Rb^{87}/Sr^{86}. This is offset, however, by the ideal nature of the total-rock isochron, whether or not the K-feldspar analysis is included. Moreover, mixed biotite-chlorite ages of 1370 and 1390 m.y. for the Cabbage Gum and Warrego Granites (sample 73063262) may support a geological event at this time. The high initial ratio and deformation structures within the Cabbage Gum Granite could be taken as suggestive of a reset isotopic age. As stated earlier, though, the perfect nature of the total-rock isochron, for samples separated by up to 13 metres, should indicate a primary age, perhaps synchronous with the deformation.

Some of the marked initial Sr^{87}/Sr^{86} variability for the igneous rocks of the area—for example the value for the Bernborough Volcanics—relates to post-emplacement isotopic re-equilibration. Most, however, appears to be primary. Even within a single rock type, for example the Red Bluff Granite with values of 0.7077 ± .0006 and 0.716 ± .005, there is evidence of initial Sr^{87}/Sr^{86} variation. The high and somewhat variable values are characteristic of the S-type granite as defined by Chappell & White (1974). Petrographic and chemical evidence also indicates an S-type origin for these rocks (Wyborn, pers. comm., 1976). The low indicated initial ratio for the Warrego Granite is puzzling however, especially as it appears petrologically comparable to the other granites. Further, detailed isotopic work will be required to resolve this apparent anomaly.

The isotopic evidence, then, suggests a range in granite ages of perhaps as much as 500 m.y. The distribution of this age range conflicts with the field observations, for most authors (e.g. Crohn & Oldershaw (1965), Dunnet & Harding (1967), and Large (1975)), at least by inference, consider the granites to predate or be roughly contemporaneous with the main deformation. So far no granites have been found to be as old as the minimum deduced age of the main deformation (1810 m.y.) However, the 1796 m.y. age for biotite from the Tennant Creek Granite is only one percent less. In that this is a minimum age, the difference may not be significant. Further, some of the granites which remain to be dated may prove to be older than those already studied.

Large (1975) has developed a theory of ore formation in the Tennant Creek area from detailed studies of the Juno mine. He envisages a hydrothermal solution derived by release of formation water within argillaceous sediments by heat from adjacent granite and porphyry intrusives. Leaching from the sediments increased the acidity of the solution, which subsequently reacted with favourable host rocks to form the iron-rich ore bodies. Large considers that both ore (Au, Cu, Bi and Se) and gangue components may have originated in the sedimentary rocks. The present isotopic data are clearly incompatible with Large's suggestion that the last phase of igneous activity is related to economic mineralization. They would suggest that only the earliest granites might provide a favourable heat source for the release of water from the sediments to form the ore-bearing fluids.

As deduced earlier, the agreement, with one exception, of muscovite ages from the mineralized rocks indicates 1810 m.y. as the approximate time of ore formation. The lone exception was probably reset by a local thermal event, as was postulated for the biotite and sericite samples from the Warrego Mine. The concordance of muscovite ages is strong evidence for a common age and, by inference, common origin for the ore deposits of at least the Warrego, Juno, Golden Forty and Nobles Nob mines.

Acknowledgements

I wish to thank M. R. Daly for his assistance in sample collection and the continuing interest he has shown during collection and assessment of the data. W. B. Dallwitz, J. Ferguson, A. D. Haldane, R. G. Dodson, R. W. Page, S. E. Smith and D. Wyborn, of the Bureau of Mineral Resources, provided valuable discussion and critically read preliminary drafts of the manuscript. I am grateful to M. W. Mahon, T. K. Zapasnik and J. L. Duggan for technical assistance in sample preparation and processing. Geopeko Ltd., Australian Development Ltd., and Aquitaine Australia—Minerals Pty Ltd supplied samples from mineralized areas for analysis with background information, and gave permission to quote the results.

References

ARMSTRONG, R. L., & STEWART, A. J., 1975—Rubidium-strontium dates and extraneous argon in the Arltunga Nappe Complex, Northern Territory. *Journal of the Geological Society of Australia*, **22**, 103-15.

AUSTRALIAN DEVELOPMENT LTD., 1976—Nobles Nob Mine. General description of geology and operations. *Excursion Guidebook 47C, 49A, 49C. 25th International Geological Congress, Sydney.*

BLACK, L. P., 1975—Present status of geochronological research in the Arunta Block, N.T. *Proterozoic Geology—Geological Society of Australia, First Australian Geological Convention, Adelaide, May 1975, Abstracts.*

CHAPPELL, B. W., & WHITE, A. J. R., 1974—Two contrasting granite types. *Pacific Geology*, **8**, 173-74.

CROHN, P. W., & OLDERSHAW, W., 1965—The geology of the Tennant Creek one mile sheet area, N.T. *Bureau of Mineral Resources, Australia—Report* **83.**

DUNNET, D., & HARDING, R. R., 1967—Geology of the Mount Woodcock 1-mile sheet area, Tennant Creek, N.T. *Bureau of Mineral Resources, Australia—Report* **114.**

ELLISTON, J. N., 1963—Sediments of the Warramunga Geosyncline; *in Syntaphral tectonics and diagenesis: Symposium, Geology Department, University of Tasmania*, L1 to L45.

GEBAUER, D., & GRÜNENFELDER, M., 1974—Rb-Sr whole-rock dating of late diagenetic to anchimetamorphic, Palaeozoic sediments in Southern France (Montagne Noire). *Contributions to Mineralogy and Petrology*, **47**, 113-30.

HURLEY, P. M., FISHER, N. H., PINSON, W. H., & FAIRBAIRN, H. W., 1961—Geochronology of Proterozoic granites in the Northern Territory, Australia. Part 1: K-Ar and Rb-Sr age determinations. *Bulletin of the Geological Society of America*, **72**, 653-62.

IVANAC, J. F., 1954—The geology and mineral deposits of the Tennant Creek Goldfield, N.T. *Bureau of Mineral Resources, Australia—Bulletin* **22.**

LANPHERE, M. A., WASSERBURG, G. J. F., & ALBEE, A. L., 1964—Redistribution of strontium and rubidium isotopes during metamorphism, World Beater Complex, Panamint Range, California; *in* CRAIG, H., MILLER, S. L., & WASSERBURG, G. F. J. (Editors), ISOTOPIC AND COSMOCHEMISTRY *North Holland, Amsterdam.*

LARGE, R. R., 1975—Zonation of hydrothermal minerals at the Juno Mine, Tennant Creek Goldfield, Central Australia. *Economic Geology*, **70**, 1387-1413.

LE MESSURIER, P. L., 1976—Notes on the Tennant Creek Gold-Copper-Bismuth Field; *in* Precambrian Structures and metamorphic rocks of Central Australia and Tennant Creek, N.T., *25th International Geological Congress, Sydney, Excursion Guide* **47C** 15-22.

MCINTYRE, G. A., BROOKS, C., COMPSTON, W., & TUREK, A., 1966—The statistical assessment of Rb-Sr isochrons. *Journal of Geophysical Research*, **71**, 5459-68.

MAJORIBANKS, R. W., & BLACK, L. P., 1974—Geology and geochronology of the Arunta Complex, north of Ormiston Gorge, Central Australia. *Journal of the Geological Society of Australia*, **21**, 291-300.

MENDUM, J. R. & TONKIN, P. C., in prep.—Geology of the Tennant Creek 1:250 000 Sheet area, Northern Territory. *Bureau of Mineral Resources, Australia—Bulletin.*

NEUMANN, W., & HUSTER, E., 1972—Neubestimming der halbwertszeit des ^{87}Rubidiums durch vergleich von messungen an den getrenntent isotopen ^{87}Rb and ^{85}Rb. *Zeitschrift für Naturforschung*, **27a**, 862-63.

NUNES, P. D., & STEIGER, R. H., 1974—U-Pb zircon, and Rb-Sr and U-Th-Pb whole-rock study of a polymetamorphic terrain in the Central Alps, Switzerland. *Contributions to Mineralogy and Petrology*, **47**, 255-80.

PAGE, R. W., in prep.—Response of U-Pb zircon and Rb-Sr total-rock and mineral systems to low-grade regional metamorphism in Proterozoic igneous rocks, Mount Isa, Australia.

PAGE, R. W., BLAKE, D. H., & MAHON, M. W., 1976—Geochronology and related aspects of acid volcanics, associated granites, and other Proterozoic rocks in The Granites-Tanami region, northwestern Australia. *BMR Journal of Australian Geology and Geophysics*, **1**, 1-13.

PIDGEON, R. T., & COMPSTON, W., 1965—The age and origin of the Cooma Granite and its associated metamorphic zones, New South Wales. *Journal of Petrology*, **6**, 193-222.

SPRY, A. H., 1963—The diagenesis of mobile sediments, reply, *in Syntaphral Tectonics and Diagenesis: A Symposium*, (S. W. Carey, Convenor): *Geology Dept., University of Tasmania*, L46-L57.

STEWART, A. J., 1971—Potassium-argon dates from the Arltunga Nappe Complex, Northern Territory. *Journal of the Geological Society of Australia*, **17**, 205-11.

TURNER, F. J., & VERHOOGEN, J., 1960—IGNEOUS AND METAMORPHIC PETROLOGY. *McGraw-Hill*, New York.

WHITTLE, A. W. G., 1966—The paragenesis and origin of the Tennant Creek mineral deposits. *Ph.D. thesis, University of Adelaide* (unpublished).

WILLIAMS, I. S., COMPSTON, W., CHAPPELL, B. W., & SHIRAHASE, T., 1976—Rubidium-strontium age determinations on micas from a geologically controlled, composite batholith. *Journal of the Geological Society of Australia*, **22**, 497-506.

Metasomatic history and origin of uranium mineralization at Mary Kathleen, northwest Queensland

G. M. Derrick

The Mary Kathleen uranium deposit in northwest Queensland is contained in west-dipping middle Proterozoic calcareous, dolomitic and alkali-rich metasediments of the Corella Formation, which are metamorphosed to hornblende hornfels grade by the Burstall Granite, and are also intruded by a swarm of rhyolite and microgranite dykes associated with this granite. An early, higher temperature metasomatic event has formed K feldspar-rich and scapolite-pyroxene bands from the original metasediments; a later lower temperature metasomatic event has resulted in extensive garnetization and skarn replacement of earlier formed rocks, and uraninite-allanite mineralization. Fluids associated with this second event appear to be enriched in Na, Cl, H_2O, O, U and rare earths, and are spatially and probably genetically related to the rhyolite dyke swarm. This is supported by the high uranium content of the dykes (12 ppm average) compared to that in Burstall Granite (7 ppm), metasediments (3.5 ppm), quartzite (1 ppm) and basic rocks (0.7 ppm).

Uranium-rich fluids moved westwards from the dykes, following decreasing temperature gradients. They were impeded in most places by a chemically inert layer of quartzite, but breached this barrier in at least two places and intersected a sequence containing permeable lenses of conglomerate, within which the broadly stratabound orebody was deposited. Similar orebodies could be expected in the vicinity of other permeable zones stratigraphically above quartzite and adjacent to fractures and acid dykes, but such sites appear to have been removed by faulting and erosion. However, fractured areas of the quartzite hanging wall (i.e. the eastern side of the quartzite), in the vicinity of rhyolite dykes, could also be sites of economic uranium mineralization at depth.

Introduction

The Mary Kathleen uranium deposit was discovered in July, 1954 by the Walton-McConachy prospecting syndicate, and is located about 60 km east of Mount Isa, in northwest Queensland. Construction of the open-pit mine, treatment plant and township commenced in 1956, and from 1958 to 1963 4500 tons of U_3O_8 were produced for the United Kingdom Atomic Energy Commission. From 1963 to 1975 the entire operation was placed on a care-and-maintenance basis; rehabilitation commenced in 1975, and production of uranium oxide commenced in 1976, in order to fulfil contracts for 4740 tonnes of uranium oxide to be delivered between 1976 and 1982.

Reserves at Mary Kathleen were formerly 9 483 000 tonnes at 0.131% U_3O_8, of which 6 430 000 tonnes at 0.119% U_3O_8 remain (Hawkins, 1975). These figures are equivalent to about 12 000 tonnes and 7 000 tonnes of U_3O_8 respectively.

Host rocks to the Mary Kathleen uranium deposit are garnet-diopside skarn, thin-bedded calc-silicate granofels, feldspar-rich cobble and boulder conglomerate, impure marble, mica schist, quartzite and amphibolite of the Corella Formation, which together with the Ballara Quartzite form the Mary Kathleen Group (Derrick, Wilson & Hill, 1977), of Carpentarian (or middle Proterozoic) age, about 1670-1700 m.y. old (Page, 1976) (Fig. 1). The term 'granofels' (Goldsmith, 1959) describes a mainly medium to coarse-grained granoblastic metamorphic rock without, or with only indistinct, foliation or lineation. The rock may be uniform in mineral composition, or it may contain layers of differing composition in which non-directional minerals predominate. At Mary Kathleen the calc-silicate granofels were probably a sequence of interbedded dolomitic marl and sodic shale.

The Mary Kathleen Group occupies most of the Eastern geosyncline in the Mount Isa region, and overlies granitic and volcanic basement complex to the west (Carter, Brooks & Walker, 1961). At Mary Kathleen, the Corella Formation metasediments are intruded by the Burstall Granite, and metamorphosed to low-pressure amphibolite facies and hornblende hornfels grade; they are also intruded by a swarm of rhyolitic and microgranitic dykes associated with and younger than the granite (Fig. 2), and by minor dolerite dykes.

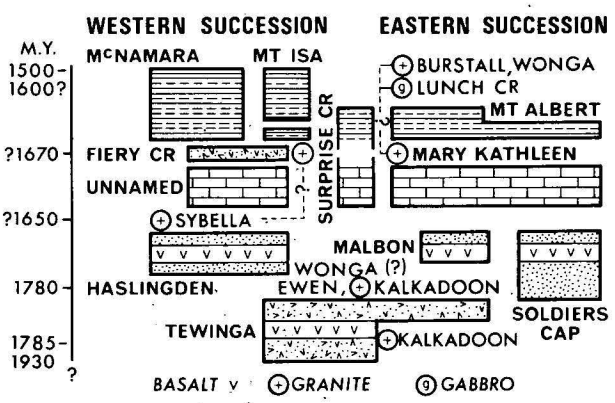

Figure 1. Stratigraphic column, Mount Isa region.

The earliest publication on Mary Kathleen described a new mineral, stillwellite, a lanthonon-bearing borosilicate (McAndrew & Scott, 1955). Matheson & Searl (1956) published the first detailed account of the geology of the deposit, and concluded that the mineralization was epigenetic, and was located in the western limb of an overturned syncline. The position of the synclinal axis relative to the orebody was modified by Hughes & Munro (1965), who considered the ore to be near the axial zone of the syncline, and that the western limb of the syncline was truncated by shearing. They also regarded the mineralization as epigenetic, related to late-phase emanations from the Burstall Granite; garnet was regarded as a prerequisite for the formation of uranium ore, within a favourable host rock and structure.

By contrast, Hawkins (1975) raised the possibility of the uranium in the orebody having been remobilized from within the sedimentary pile during metamorphism, and suggested that narrowing of the ore-zone at depth reflected variation in the original sedimentary environment. The environment was considered to be near-shore, in which silty calcareous sediments were deposited in restricted basins behind sandbars, and algal reefs were developed locally.

Whittle (1960) described in detail the various metamorphic and metasomatic phenomena associated with the orebody, and presented a paragenetic sequence of mineral

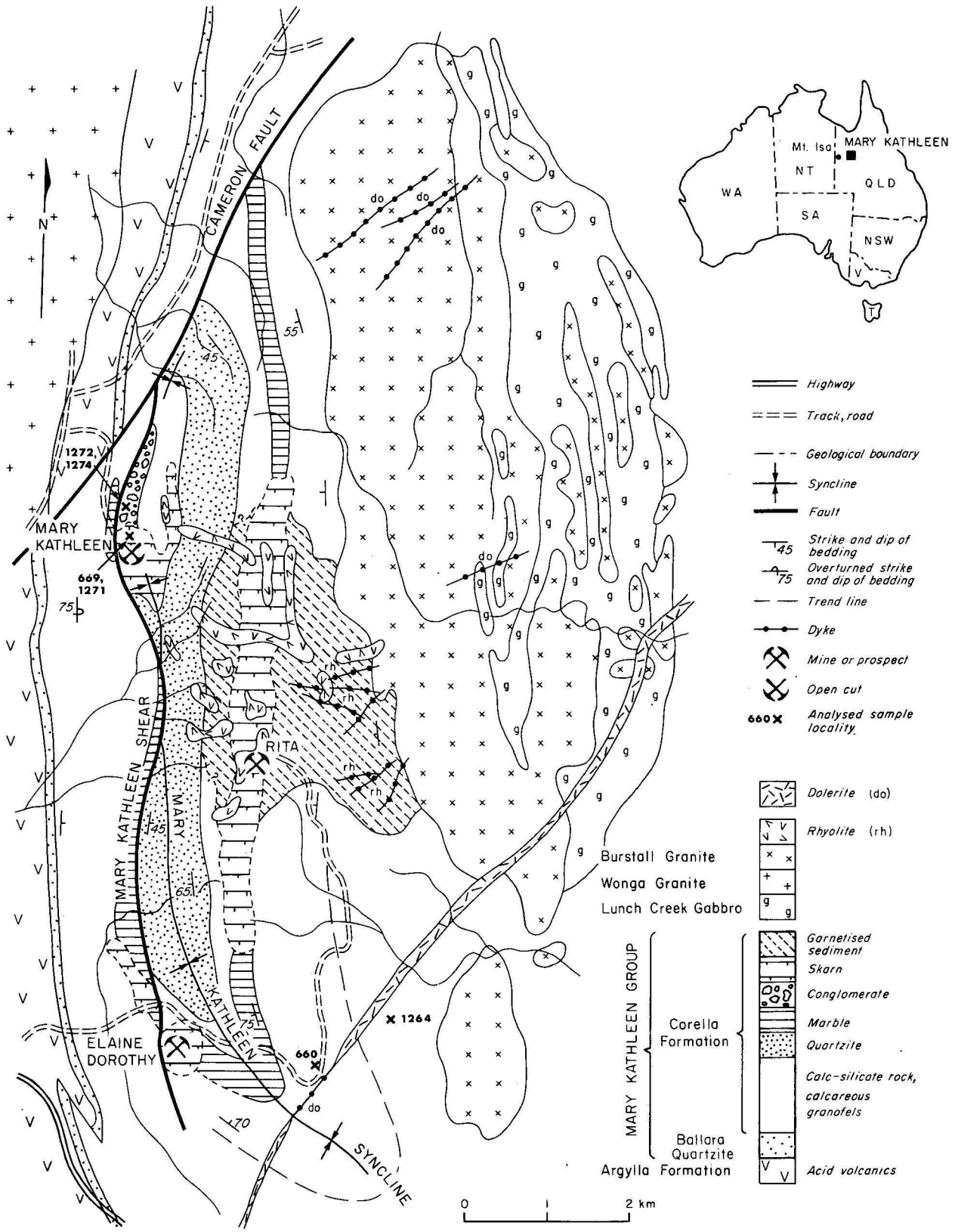

Figure 2. Geological map, Mary Kathleen area.

formation, in which garnet was thought to form first, closely followed by feldspar, scapolite and uraninite-bearing allanite. This sequence is modified in this paper (Fig. 5) to incorporate petrographic data from areas a few kilometres east and southeast of the open cut.

The precise stratigraphic location of the deposit is not yet clear; it may be situated either within the axial zone or on the east limb of the Mary Kathleen syncline (Fig. 2), following the work of Hughes & Munro (1965), and is a vein and replacement-type orebody broadly stratabound within a lenticular unit of garnetized conglomerate and scapolite-diopside granofels. The ore is a fine-grained uraninite-allanite

assemblage which replaces skarn; uraninite is disseminated within the allanite. Other less important uranium-bearing minerals in the ore include stillwellite and apatite.

The purpose of this paper is to make a preliminary assessment of the two contrasting hypotheses of ore formation noted above, in the light of mapping and geochemistry by the author over the period 1970-75. An understanding of the sequence of metamorphic events and the extent and nature of metasomatism, as determined from field and laboratory examination, is critical to the problem, and will be discussed first. These results will then be integrated with data on the uranium content of various rock types, and conclusions drawn as to the source of the uranium, the formation of the orebody, and the exploration potential of other areas in the Mary Kathleen syncline. Some of the conclusions must be regarded as tentative, because of the generally non-systematic nature of the sampling in some areas. A joint project currently in progress in BMR is designed to test some of the conclusions fully, and is based on systematic sampling of marble, skarn and dyke rocks, undertaken in 1976.

Metamorphism and metasomatism

Over wide areas the Corella Formation has undergone metamorphism ranging up to amphibolite facies grade; indicator minerals such as andalusite, sillimanite and cordierite attest to the low pressure nature of this metamorphism. Near Mary Kathleen, wollastonite is common in marble within the east limb of the syncline, and indicates that higher temperature (?650°C) hornblende-hornfels facies conditions were probably attained within 3 to 4 km of the Burstall Granite.

These relatively high-grade calc-silicate granofels and impure marble layers in the east limb of the Mary Kathleen syncline are extensively metasomatized; alteration and replacement phenomena are widespread, and at least two periods of metasomatism are recognized.

First metasomatic event

Evidence for this metasomatism is derived from a sequence of calc-silicate granofels in the southern half of the eastern limb of the syncline. The parental (pre-metasomatic) rocks are dark grey to black bands of very fine-grained chert-like granofels interlayered with coarse-grained impure marble bands; both rock types show alteration to monomineralic or bimineralic metasomatic assemblages, and the various stages of replacement may be observed directly along the strike of the beds, or be inferred from relict textures preserved in the bands (Fig. 3).

The replacement sequence in the **fine-grained bands**, in which black chert-like granofels is transformed to an essentially monomineralic band of pink microcline granofels, is summarized in Figure 3. Four types of replacement bands are recognized, A, B, C_1 and C_2, and their colour and mineral assemblages (in decreasing order or abundance) are as follows:

Type A (parental): grey to black: diopside-oligoclase-sphene-?microcline-opaque oxide pigmentation (?graphite).

Type B: grey to grey-green: diopside-albite/oligoclase-scapolite-K-feldspar.

Type C_1: pale grey-green to pale pink: K-feldspar-diopside-Na feldspar-sphene.

Type C_2: pink: K-feldspar-Na feldspar-sphene.

The change from type A to type B involves the addition of a NaCl-rich scapolite (mainly dipyre, Ma_{80} to Ma_{65}), and the loss of dark pigmentation; from B to C_1 the major change is the addition of clouded K feldspar, and a reduction in the scapolite content. No major source of potassium is evident in types A and B, and it has probably been derived from some external source. The loss of scapolite from B to C_1 also indicates that Na, Cl, and possibly Ca have migrated from the system. From C_1 to C_2 most diopside is removed, concomitant with a further enrichment in K feldspar, which suggests a loss of Ca and Mg, and a further gain of K.

Chemical analyses of types A and C_2 are listed in Table 1. The significant metasomatic changes from these analyses are

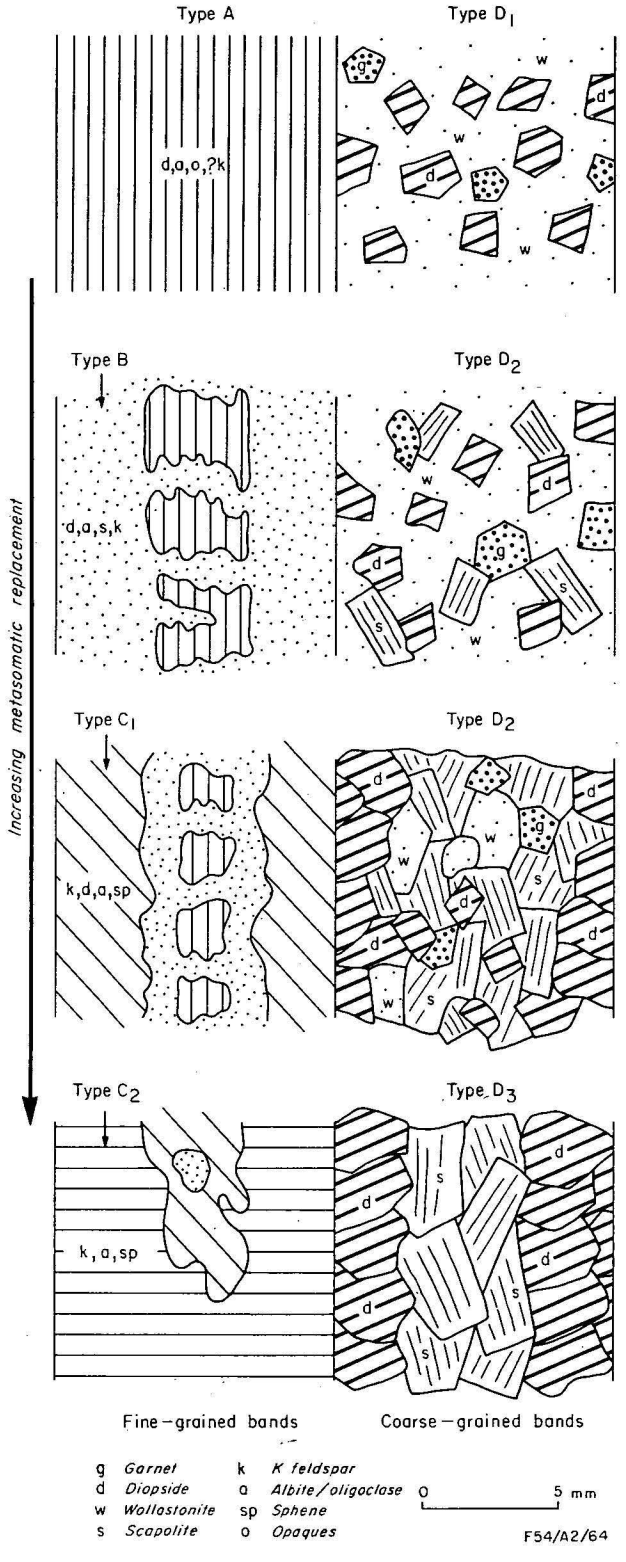

Figure 3. Diagrammatic sketch of mineralogical changes along bands during the first metasomatic event (see text for details).

Sample No.	660D (unaltered)		1264P (altered)		% gain (+)**
Oxide	Wt.%	cations/100(0)*	Wt.%	cations/100(0)	or loss (−)
SiO_2	57.84	33.3	63.25	36.4	+9
TiO_2	0.85	.3	.73	.3	0
Al_2O_3	18.02	12.2	18.22	12.3	+1
Fe_2O_3	0.4	.1	.21	.09	−10
FeO	2.08	1.0	.31	.14	−86
MnO	0.09	.04	.02	.009	−77
MgO	2.05	1.7	0.2	.17	−90
CaO	7.06	4.3	1.79	1.1	−74
Na_2O	4.92	5.5	3.47	3.81	−31
K_2O	4.19	3.0	10.54	7.7	+157
P_2O_5	0.24	.1	.18	.08	−20
H_2O^+	.97		.06		
H_2O^-	.07		.16		
CO_2	.20		.15		
S	.095		0.02		
	99.07		99.31		

* Recalculated on basis of cations pers 100 oxygen anions. ** Comparison of cation proportions.

Table 1. Summary of metasomatic changes in fine-grained calc-silicate rocks, Mary Kathleen.

Sample No.	660L (unaltered)		1264D (altered)		% gain (+) or
Oxide	Wt.%	cations/100(0)*	Wt.%	cations/100(0)	loss (−)**
SiO_2	49.66	29.49	52.23	31.84	+8
TiO_2	0.51	.22	.41	.18	−18
Al_2O_3	11.46	8.02	11.91	8.56	+7
Fe_2O_3	.38	.16	1.94	.89	+456
FeO	3.98	1.97	7.00	3.56	+80
MnO	0.36	.18	.16	.08	−55
CaO	23.15	14.73	14.47	9.45	−36
Na_2O	2.95	3.39	4.85	5.73	+69
K_2O	0.67	0.50	.63	.49	−2
P_2O_5	0.18	.09	.07	.03	−66
H_2O^+	0.74	2.93	.68	2.76	−6
CO_2	3.55	2.87	.4	.33	−88
S	0.02		0.02		
	99.93		98.70		

* Recalculated on basis of cations per 100 oxygen anions. ** Comparison of cation proportions.

Table 2. Summary of metasomatic changes in coarse-grained calc-silicate rocks, Mary Kathleen.

loss of Fe^{2+}, Ca, Mg, and Na; and gain of K. Si and Al proportions have remained relatively constant during the alteration.

In the **coarse-grained bands**, (Type D), the parental impure marble (Type D_1), is transformed to a coarse-grained scapolite-diopside/hedenbergite granofels (Type D_3), as shown in Figure 3. Mineral assemblages are as follows:

Type D_1: pale green diopside-wollastonite-colourless grossular garnet-sphene-calcite-minor opaques.

Type D_2: scapolite-wollastonite-diopside-grossular garnet-sphene-albite-calcite.

Type D_3: scapolite-green diopside/hedenbergite.

In types D_1 and D_2 all minerals are evenly distributed throughout the band, but in type D_3 the scapolite and pyroxene are segregated into a central coarse zone of scapolite, flanked by coarse pyroxene (Fig. 3).

The addition of scapolite in the transition from Type D_1 to D_2 parallels the change from Type A to Type B in the fine-grained bands. Scapolite from Type C_1 bands may have contributed to the considerable amounts of scapolite in Type D_3 bands, but the presence of texturally different types of scapolite in D_3 bands (Fig. 4) suggests that at least two generations of scapolite may be present. Table 2 shows the major chemical changes in the transition from Type D_1 to D_3 bands. The main element lost is Ca, and elements gained include Fe^{3+}, Fe^{2+}, Mg and Na; as in the fine-grained bands Si and Al values remain relatively constant.

Some local metasomatic exchange has taken place between the fine and coarse-grained bands—Ca, Mg, Na and Fe have migrated outwards from the fine-grained

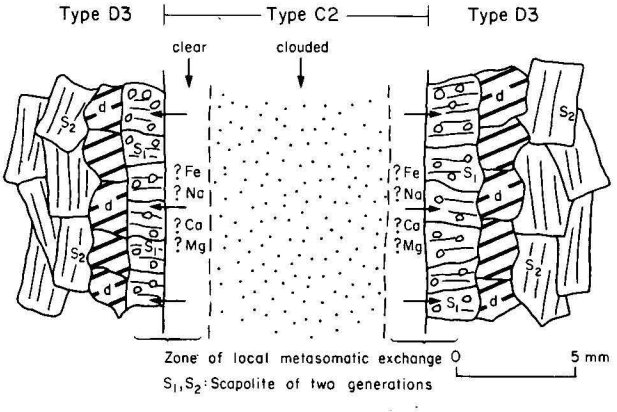

Figure 4. Diagrammatic sketch of metasomatic exchange between bands during first metasomatic event (see text for details).

bands to produce marginal zones of fibrous scapolite studded with pyroxene inclusions. These bands are in turn bounded by Type D_3 coarse granoblastic pyroxene and scapolite (Fig. 4).

The mobility of the alkalis, especially Na and K, and the presence of at least two generations of chlorine-rich scapolite, testify to the likely abundance of Na, Cl, and K in the fluid phase accompanying metamorphism. This phase may represent formation fluids mobilized from a halite-bearing sedimentary pile by the Burstall Granite, but actual addition of chlorine, potassium and possibly other elements from late-stage Burstall Granite fluids cannot be discounted.

Second metasomatic event

This event is marked by the extensive development of garnet and skarn within the Mary Kathleen syncline, especially in a broad aureole adjacent to the rhyolite dyke swarm; as a replacement zone in areas of the marble unit in the syncline; and, most importantly, within the orebody sequence of conglomerate and scapolite-diopside granofels (Fig. 2).

All the products of the first metasomatic event are extensively veined and replaced by garnet, particularly the coarse-grained scapolite-diopside bands; the finer grained bands of K-feldspar are less affected by garnetization. The garnet, an andradite-rich variety, is associated with albite/oligoclase aggregates, uraninite mineralization and abundant hydrothermal alteration. Ferrohastingsite is a common alteration product of diopside and hedenbergite, and with decreasing temperatures the fluid phase during this second stage of metasomatism appears to have favoured the formation of hydrated calcium-aluminium silicates such as chabazite, epidote, tremolite and prehnite, secondary wollastonite in veins, tourmaline, calcite, fluorite, and ubiquitous scapolite. Minor sulphides (pyrrhotite, chalcopyrite, pyrite, galena, molybdenite) post-date garnet formation but antedate most of the prehnite and calcite deposition. The paragenetic sequence of mineral occurrence shown in Figure 5 (modified from Whittle, 1960) is based on field and microscopic observation of veining, cross-cutting and pseudomorphous replacement relationships between the various mineral phases. Their possible relationship to the Burstall Granite and rhyolite dykes is also shown.

Fluids associated with this second metasomatic event appear to have contained high concentrations of Na and Cl

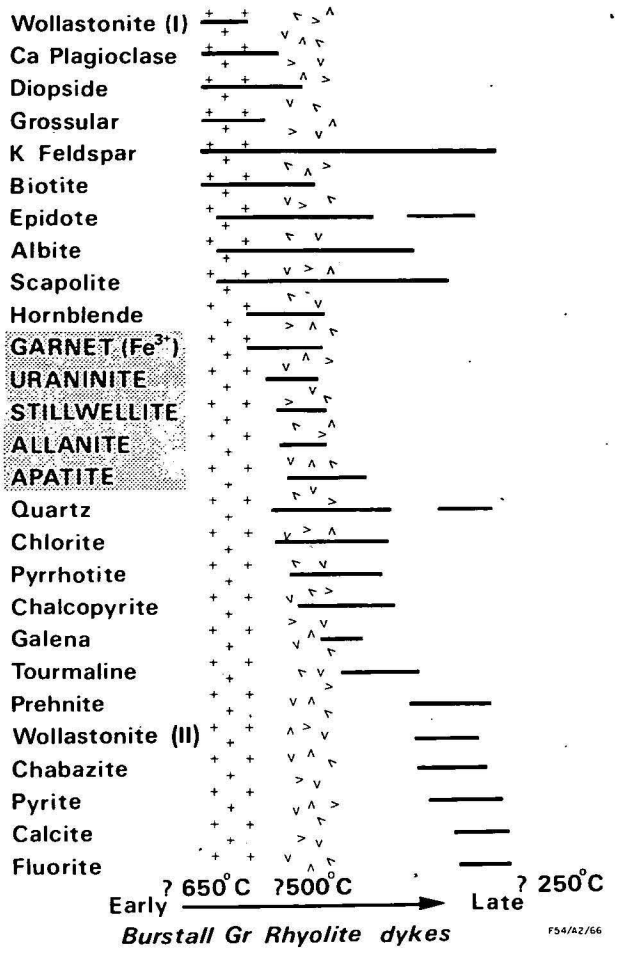

Figure 5. Paragenetic sequence of crystallization of mineral phases.

as in the first phase, but in addition were probably enriched in Fe, (especially Fe^{3+}), Ca, CO_2, H_2O, and uranium and rare-earth elements.

The conglomerate sequence containing the uranium mineralization at Mary Kathleen has not been notably affected by the first metasomatic event, but has been greatly modified by the second event; chemical analyses of the matrix of relatively unaltered conglomerate and heavily

Sample No.	*1272 (unaltered)*		*1274M (altered)*		*% gain (+) or*
Oxide	*Wt.%*	*cations/100(0)**	*Wt.%*	*cations/100(0)*	*loss (−)***
SiO_2	66.45	38.18	57.04	34.22	−10
TiO_2	0.52	0.22	0.68	0.3	+36
Al_2O_3	10.85	7.35	11.1	7.85	+7
Fe_2O_3	8.35	3.61	3.88	1.75	−52
FeO	0.65	0.31	3.57	1.79	+477
MnO	0.1	0.04	0.23	0.11	+175
MgO	0.14	0.11	2.16	1.93	+1654
CaO	0.55	0.30	10.32	6.63	+2110
Na_2O	0.66	0.73	1.83	2.12	+190
K_2O	7.85	5.75	6.7	5.12	−11
P_2O_5	0.2	0.09	0.4	0.20	+122
H_2O^+	1.24		.47		
H_2O^-	.98		.09		
CO_2	.05		.60		
S	.015		.02		
	98.60		99.09		

* Recalculated on basis of cations per 100 oxygen anions. ** Comparison of cation proportions.

Table 3. Summary of metasomatic changes in diopsidic conglomerate matrix, Mary Kathleen

Sample No.	1272 (unaltered)		1271M 669M (altered)			% gain (+) or
Oxide	Wt.%	cations/100(0)*	Wt.%	Wt.%	cations/100(0)Y	loss (−)**
SiO_2	66.45	3.18	37.12	38.03	25.28	−33.7
TiO_2	.52	.22	.49	.52	.25	+1
Al_2O_3	10.85	7.35	7.72	7.93	6.2	−15
Fe_2O_3	8.35	3.61	18.57	18.31	9.33	+157
FeO	.65	.31	1.69	1.31	.84	+170
MnO	.10	.04	.48	.49	.27	+575
MgO	.14	.11	.31	.20	.25	+127
CaO	.55	.30	31.60	30.67	22.45	+7366
Na_2O	.66	.73	.43	.20	.41	−43
K_2O	7.85	5.75	.21	1.24	.62	−89
P_2O_5	.20	.09	.38	.51	.24	+166
H_2O^+	1.24		.19	.15		
H_2O^-	.98		.23	.09		
CO_2	.05		.15	.10		
S	.015		.085	.105		
	98.60		99.65	99.85		

* Recalculated on basis of cations per 100 oxygen anions. ** Comparison of cation proportions. Y Average of recalculated 1271M and 669M analyses.

Table 4. Summary of metasomatic changes in garnetiferous conglomerate matrix, Mary Kathleen.

garnetized and diopside-rich matrix closer to the orebody allow an estimate of metasomatic gains and losses during this episode (Table 3, Table 4).

Table 3 shows that the quartzofeldspathic matrix of diopside-bearing conglomerate is enriched in Ca, Mg, and Fe^{2+}. Alkalis show variable behaviour, but some K depletion and Na enrichment are indicated. The movement of K may have contributed to rims of microcline which surround both quartzite and acid volcanic clasts in the conglomerate. In samples of garnetiferous matrix, Table 4 shows substantial enrichment of Ca, Mg, Mn and Fe^{2+}, as well as Fe^{3+}; a marked depletion in K and Si is also evident.

As noted earlier, the second metasomatic phase, in which garnet and hydrothermal minerals were pervasively developed, and with which uranium mineralization is intimately associated (e.g. Mary Kathleen, Rita), is mainly confined to a broad envelope surrounding the rhyolite dykes (Fig. 2). Although the Elaine Dorothy U prospect is an apparent exception to this generalization, it is located within the marble unit (Fig. 2), which appears to be most receptive to garnetization. Fluids from the eastern areas may have migrated towards the Elaine Dorothy anomaly.

As well as a spatial association, the rhyolite dykes may show some genetic relationship to the garnetizing and mineralizing phase of metasomatism, insofar as the dykes contain mineral phases which are also widespread in the metasomatized country rock. For example, the rhyolite dykes contain accessory amounts of hedenbergite, red-brown garnet, allanite, fluorite, zircon and sphene, as well as marginal albitite phases, and in addition are markedly enriched in uranium. It is likely that fluids related to the rhyolite dyke suite have modified the pre-existing pore fluid system in the country rock simply by the addition of water, volatiles, alkalis and oxygen. No addition of skarn-forming elements such as Ca, Mg, and Fe need be postulated, since they are widespread in the sedimentary pile. Oxygen may be an especially significant addition to the system, because of the increase in Fe^{3+} relative to Fe^{2+} which accompanies the formation of skarn.

Uranium distribution

Various rock types from the Mary Kathleen syncline within 6 km of the Mary Kathleen orebody have been analysed for uranium, using the delayed neutron technique (Green, Mateen & Rose, 1974). The results are listed in Table 5.

Rock Type	Uranium Content (ppm)	No. of Samples	World average abundances* (ppm)	
Marble	2.0	6	limestone	2
Calc-silicate granofels	3.3	50	shale greywacke	4 3
a. feldspathic bands *b. diopsidic bands*	4 3	12 12		
quartzite, quartzite clasts	1.7	6	quartzite	0.5
skarn	4.7	6		
gabbro	0.8	10		
dolerite	0.6	3	basalt	0.6
altered dolerite	3.7	7		
granite	7	13	granite	4.8
rhyolite, microgranite	12	13		

* After Taylor (1966)

Table 5. Uranium content of rocks in the Mary Kathleen syncline, compared to some average abundances.

Uranium content of granofels throughout the Mary Kathleen syncline ranges from 1.3 ppm to 6.6 ppm, and averages 3.3 ppm. There is only a slight correspondence between uranium content and proximity to the Burstall Granite; samples adjacent to the contact average 3.5 ppm, compared with the overall average of 3.3 ppm, and an average of 2.8 ppm for rocks west of the Mary Kathleen shear (Fig. 2). Comparative data listed in Table 5 indicates that uranium in these Mary Kathleen metasediments approximates world average values.

Metasediments from within the zone of pervasive garnetization (which envelopes the rhyolite dykes) average 3.5 ppm U, compared to 4 ppm and 3.1 ppm U for sediments to the north and south of this zone, respectively. No systematic sampling has yet been undertaken of sediments immediately adjacent to the rhyolite dykes to determine whether they are enriched above the average value for sediments in the entire syncline. Five skarn

samples however, show notable enrichment adjacent to the dykes, from 3 ppm to 6.6 ppm, and more sampling has been undertaken to confirm this trend.

The major quartzite unit in the sequence (Fig. 2), and quartzite clasts in the conglomerate, contain low uranium values, from 0.7 to 1.7 ppm. Relatively unaltered conglomeratic and pebbly arkose along strike and north of the orebody contains 2 ppm U, and suggests that the conglomerate zone was not unduly enriched in uranium prior to garnetization and uranium mineralization.

The Lunch Creek Gabbro, to the east of the Burstall Granite, contains 0.8 ppm, and dolerite and orthoamphibolite of various ages in the same area contain from 0.3 to 0.9 ppm—about the world average for basic rocks. However dolerite dykes within the Mary Kathleen syncline which show evidence of hydrothermal alteration, show a three-fold increase in uranium content to about 4 ppm.

The Burstall Granite contains 7 ppm U, well above the world average of about 4 ppm for these rocks, but similar to the uranium content of other large plutons in the Mount Isa region (Table 6). However the rhyolite dykes (12 ppm U average; range 6 to 22 ppm) are markedly enriched in uranium, and the values are comparable to those of other granites in northern Australia known to be associated with uranium mineralization.

Origin of uranium

The uranium at Mary Kathleen may have been derived from the Burstall Granite and the associated rhyolite dykes, or by mobilization from within the sedimentary pile during metamorphism. Regarding the latter hypothesis, in the zone of pervasive garnetization, mobilization of 2 ppm of uranium from a volume of metasediment 3000 m x 1000 m x 600 m would produce a mass of 12 000 tonnes of uranium oxide, which is comparable with the size of the original orebody at Mary Kathleen. Although mobilization and transport of uranium during metasomatism is a feasible process (as illustrated by the U content of altered dolerite dykes), the uniform uranium content throughout sedimentary rocks in the east limb of the Mary Kathleen syncline suggests that large-scale extraction of uranium from the sediments has not occurred, although more systematic sampling is required to verify this point.

Regarding the former hypothesis, it is clearly established that uranium mineralization is allied to skarn formation, which in turn is best developed in dolomitic and other metasediments in a broad aureole surrounding the network of rhyolite dykes. The dykes themselves are highly enriched in uranium, and it is proposed here that a genetic connection exists between the rhyolite dykes, metasomatism, skarn formation and economic uranium mineralization.

Formation of the orebody

Intrusion of the Burstall Granite into the Corella Formation metasediments probably resulted in mobilization of an alkali and chloride-rich pore fluid in the sedimentary pile, and the formation of extensive feldspathic, diopsidic and scapolitic metasomatites grossly parallel to original bedding. At a slightly later stage in the magmatic cycle, rhyolite dykes related to the Burstall Granite were intruded, and hydrothermal fluids associated with the dykes enriched the pre-existing fluid phase in uranium, Ca, CO_2, and H_2O, and facilitated the conversion of Fe^{2+} to Fe^{3+}; extensive garnetization also occurred.

Uranium-rich fluids travelled outwards in a westerly direction, presumably down falling temperature gradients, in a broad envelope adjacent to the dykes. The fluids were restricted in most places by a chemically inert barrier of quartzite, but breached this barrier in at least two places (Fig. 2), just east and southeast of the orebody. Stratigraphically above the quartzite the fluids intersected a calcareous, dolomitic and siliceous sequence containing lenses of conglomerate, and deposition of uranium occurred because of lower temperature conditions, possibly near 500°C (Whittle, 1960), and relatively permeable host rock.

Guides to exploration

Orebodies similar to Mary Kathleen could be expected in the vicinity of other permeable zones stratigraphically above the quartzite unit, and adjacent to fractures and acid dykes, but such sites appear to have been removed by faulting along the Mary Kathleen shear, and subsequent erosion. However, structurally favourable areas of the quartzite hanging wall (i.e. the eastern edge), in the vicinity of rhyolite dykes, could also be sites of economic uranium mineralization where uranium-rich fluids have ponded beneath the quartzite, in the zone of pervasive garnetization.

Summary and conclusions

1. Low concentrations of uranium in unaltered conglomerate, and a relatively uniform distribution of uranium in the calc-silicate rocks, indicate that formation of an

	1	*2*	*3**	*4**	*5**	*6**	*7**	*8**	*9*	*10*	*11*
U	7.1	6.6	7	12	12.8	5	4	11	2.2	4	4.7
Th	21.1	27.2	57	69	48	34	8	46	22	19.5	20
U/Th	.33	.24	.12	.17	.27	.15	.5	.24	.10	.2	.23
Number of samples	4	8	13	13	32	6	10	72	28	42	

Mount Isa
1. Kalkadoon Granite
2. Sybella Granite
3. Burstall Granite
4. Burstall rhyolite

Northern Territory
5. Rum Jungle Complex
6. Nanambu Complex
7. Nimbuwah Complex

Georgetown
8. Elizabeth Creek Granite
9. Newcastle Range Volcanics
10. Forsayth Granite

11. World average

* Units associated with uranium deposits

Sources:
1,2 Farquharson & Richards, 1974; 3, 4 Author; 5 Heier & Rhodes, 1966; 6, 7 S. Needham, BMR, pers. comm. 1976; 8, 9, 10 Sheraton, 1974; 11 Clark *et al.* 1966, Taylor, 1966.

Table 6. Uranium in granites

orebody by in situ metamorphism of syngenetic uranium concentrations, or by large-scale extraction of uranium from metasediments, is unlikely to have occurred. Nevertheless, the quantity of uranium present within the garnetized sedimentary pile would be sufficient to provide the orebody at Mary Kathleen.

2. Uranium enrichment is related to a skarn-forming metasomatic event associated with the intrusion of rhyolite dykes.

3. The rhyolite dykes contain above-average uranium contents, and are postulated as the major source of uranium at Mary Kathleen.

4. Formation of the orebody resulted from a favourable combination of temperature, structure, and permeable host rock.

5. Further exploration is recommended immediately below a quartzite unit in the vicinity of the rhyolite dykes, about 650 m stratigraphically beneath the Mary Kathleen orebody.

Acknowledgements

An earlier version of this paper was read to Section 4 of the International Geological Congress at Sydney in August, 1976. I wish to thank R. M. Hill, Dr J. Ferguson, R. Ryburn and W. Roberts for their comments on the draft manuscript, Dr D. C. Green of the Department of Geology and Mineralogy at the University of Queensland for assistance with the determination of uranium values, and Dr P. Furness, formerly of the same institution, for writing the computer program used in the recasting of chemical analyses into cationic proportions. The diagrams were drawn by R. W. Bates in the BMR Drawing Office.

References

CARTER, E. K., BROOKS, J. H., & WALKER, K. R., 1961—The Precambrian mineral belt of Northwestern Queensland. *Bureau of Mineral Resources Australia—Bulletin* **51.**

CLARK, S. P. Jr., PETERMAN, Z. E., & HEIER, K. S., 1966—Abundances of uranium, thorium and potassium. *Geological Society of America—Memoir* **97,** 522-41.

DERRICK, G. M., WILSON, I. H., & HILL, R. M., 1977—Revision of stratigraphic nomenclature in the Precambrian of northwestern Queensland VI. Mary Kathleen Group. *Queensland Government Mining Journal.* **78,** 15-23.

FARQUHARSON, R. B., & RICHARDS, J. R., 1974—U-Th-Pb isotope systematics related to igneous rocks and ore Pb, Mount Isa, Queensland. *Mineralium Deposita,* **9,** 339-56.

GOLDSMITH, R., 1959—Granofels, a new metamorphic rock name. *Journal of Geology,* **67,** 109-10.

GREEN, D. C., MATEEN, A., & ROSE, A., 1974—Delayed neutron determination of U in Australian rocks—an inexpensive, precise exploration procedure. *Isotope Geology Laboratory Report* **2,** 1971-74, *University of Queensland Geology Department* (abstract).

HAWKINS, B. W., 1975—Mary Kathleen uranium deposit; *in* KNIGHT, C. L. (Editor)—ECONOMIC GEOLOGY OF AUSTRALIA AND PAPUA NEW GUINEA, Volume **1**—Metals, 398-402, *Australasian Institute of Mining and Metallurgy, Melbourne.*

HEIER, K. S., & RHODES, J. M., 1966—Thorium, uranium and potassium concentrations in granites and gneisses of the Rum Jungle Complex, Northern Territory, Australia. *Economic Geology,* **61,** 563-71.

HUGHES, F. E., & MUNRO, D. L., 1965—Uranium ore deposits at Mary Kathleen; *in* MCANDREWS, J. (Editor)—GEOLOGY OF AUSTRALIAN ORE DEPOSITS (2nd edition), *8th Commonwealth Mining and Metallurgical Congress,* **1,** 256-63.

MATHESON, R. S., & SEARL, R. A., 1956—Mary Kathleen uranium deposit, Mount Isa-Cloncurry district, Queensland, Australia. *Economic Geology,* **51,** 528-40.

MCANDREW, J., & SCOTT, T. R., 1955—Stillwellite, a new rare-earth mineral from Queensland. *Nature,* **176,** 509-10.

PAGE, R. W., 1976—Response of U-Pb zircon and Rb-Sr total rock systems to low grade regional metamorphism in Proterozoic igneous rocks, Mount Isa, Australia. *Annual Report of the Geophysical Laboratory, Carnegie Institute of Washington. Year Book* **75.**

SHERATON, J. W., 1974—Chemical analyses of acid igneous rocks from northeast Queensland. *Bureau of Mineral Resources Australia—Record* **1974/162** (unpublished).

TAYLOR, S. R., 1966—The application of trace element data to problems in petrology; *in* PHYSICS AND CHEMISTRY OF THE EARTH, **6,** *Pergamon Press, Oxford.*

WHITTLE, A. W. G., 1960—Contact mineralization phenomena at the Mary Kathleen uranium deposit. *Neues Jahrbuch für Mineralogie—Abhandlungen* **94,** 798-830.

The Lander Trough, southern Wiso Basin, Northern Territory

P. J. Kennewell, S. P. Mathur, and P. G. Wilkes

The Lander Trough forms the east-southeast trending, southern and deeper part of the Wiso Basin, and is flanked on the north by an extensive less deformed area of the Basin. Recent geological mapping, shallow stratigraphic drilling, and a reassessment of geophysical data in the southeastern part of the trough provide additional information on the nature and structure of the rocks it contains.

Beneath the Cainozoic superficial material, three sequences of rocks are distinguished. The upper sequence consists of ?Late Palaeozoic Lake Surprise Sandstone; the middle of Cambrian or Ordovician sediments and volcanics; and the lower of Proterozoic rocks. The ?Late Palaeozoic sequence is flat-lying and thin (100-250 m), whereas the Early Palaeozoic sequence forms a wedge which thins to the north and thickens southwards to about 800 m in the deepest part of the trough. The Proterozoic sequence forms the 'basement' to these Palaeozoic sediments of the Wiso Basin.

The trough is indicated to be a downwarp in the crust, about 300 km long and 100 km wide, bounded by an overthrust fault system against the Arunta Block on the south. The fault system is considered to be contemporaneous with the post-Devonian Alice Springs Orogeny which affected the Ngalia and Amadeus Basins farther to the south.

The presence of a thick (up to 800 m), partly marine sequence of Cambrian and Ordovician sediments upgrades the petroleum potential of the Lander Trough area, as gas has been found in such sediments in the depositionally and structurally similar Amadeus Basin to the south, and the Toko Syncline of the Georgina Basin to the southeast.

Introduction

The Wiso Basin in the Northern Territory comprises the east-southeast trending Lander Trough and an extensive, less deformed area flanking this to the north (Fig. 1). The basin is continuous with the Daly River Basin and the northern part of the Georgina Basin in the north, and with the southern part of the Georgina Basin in the southeast—although these connections are obscured by Cretaceous and Quaternary deposits. The Wiso and Georgina Basins appear to share a similar structural and depositional history. Precambrian rocks underlying the basin include The Granites-Tanami Block on the west, the Arunta Block on the south, and the Tennant Creek Block on the east.

A relatively thick sequence of presumed sedimentary rocks in a trough covering an area approximately 300 km by 100 km was inferred from aeromagnetic and gravity surveys (Aero Service, 1964; Flavelle, 1965); the structure containing them was called the Lander Trough by Milligan *et al.* (1966). The presence of bedded rocks in the subsurface was confirmed by a reflection and refraction seismic survey in the southeastern part of the trough (Ray Geophysics, 1967). An extensive aeromagnetic survey (Adastra Hunting Geophysics, 1967) provided estimates of the depth to magnetic sources (Fig. 5) in the basin area.

Because of sparse outcrops and extensive aeolian sand cover the nature of the rocks filling the trough has been the subject of speculation. On the basis of their seismic work, Ray Geophysics (1967) surmized that the deeper reflections (D and E in Fig. 3) could be from a Cambrian sequence, and that there were possibly up to 2200 m of Palaeozoic rocks in the Lander Trough. Milligan (1976), in reviewing the geology of the Wiso Basin, concluded that a significant part of the section considered by Ray Geophysics (1967) to be Palaeozoic could be Adelaidean sediments. However, no deep drilling has been undertaken in the area and the nature of the rocks at depth remains untested.

In 1974 a program of remapping, shallow stratigraphic drilling, and reviewing existing geophysical data in the basin area was undertaken to obtain more definitive information on the nature and structure of the sediments. This paper presents new interpretations of the geophysics, attempts to relate them to the known geology of the trough and surrounding areas, and suggests a coherent picture of the structure and geology of the Lander Trough. The geology, Bouguer anomaly contours, estimated depths to

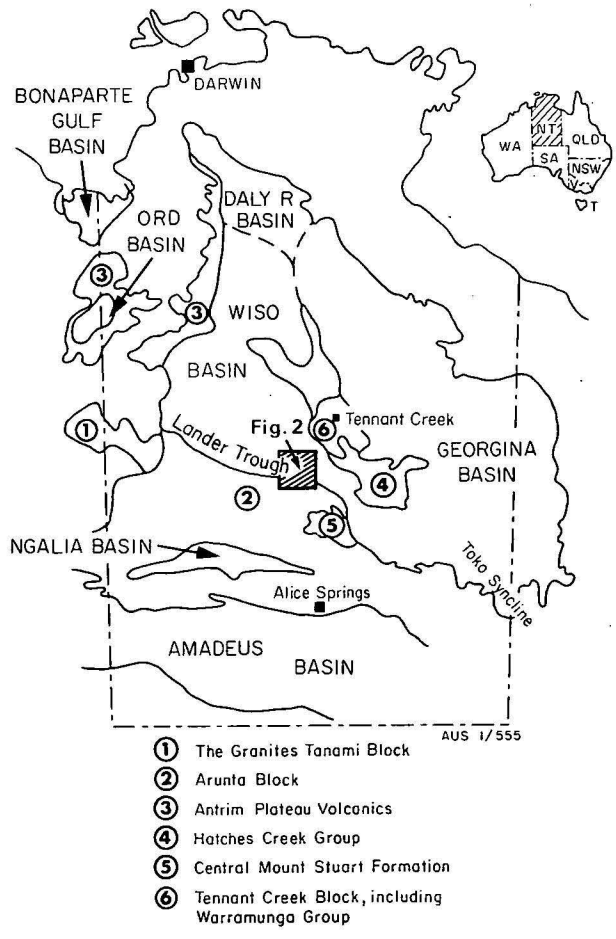

Figure 1. Location map showing approximate extent and regional setting of the Lander Trough.

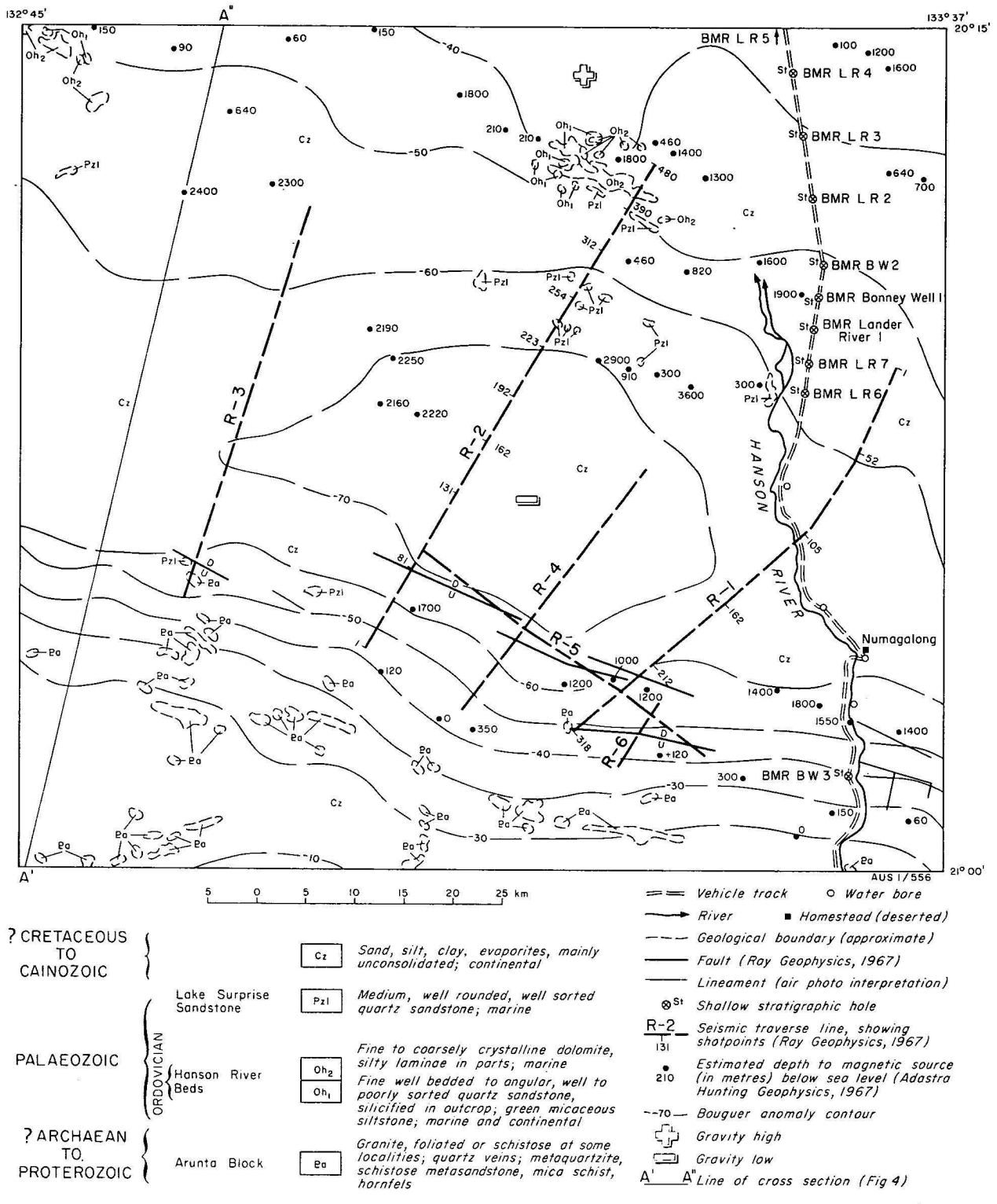

Figure 2. Map of the southeastern part of the Lander Trough area showing the geology, stratigraphic holes, seismic traverses, Bouguer anomaly contours, and estimated depths to magnetic sources.

magnetic sources, and the location of stratigraphic holes and seismic traverses are shown in Figure 2.

Seismic data

The results of the seismic reflection and refraction survey (Ray Geophysics, 1967) were examined in detail and the principal horizons recorded on the better quality traverses, R-1 and R-2, are shown in Figure 3. Two refractors, A and B, and three reflectors, C, D and E have been mapped. Refractor B and reflector D almost certainly represent the same lithological boundary. Similarly, refractor A and reflector C are closely related and in most places seem to represent another boundary. These boundaries separate three sequences:

1. A flat-lying sequence, about 100 to 250 m thick, unaffected by the faulting on the southwest, with velocities in the range 2100 to 2930 m/sec, which is typical of

moderately consolidated sandstone, siltstone and claystone.

II. A wedge-shaped sequence thickening from 350 m in the northeast to 800 m in the southwest, faulted against the Arunta Block on its southwestern margin, with apparent velocities in the range 3260 to 4180 m/sec, which may represent carbonates and harder sandstone, siltstone and claystone.

III. An underlying sequence of south-dipping bedded rocks containing a poor quality but mappable reflector E (see Fig. 3), with apparent velocities in the range 5790 to 6460 m/sec, typical of quartzite, marble, and other metamorphic rocks.

The range of refraction velocities for the three sequences and the depths of the two refractors (A and B) have been computed from the refraction data, and the depths to the reflectors (C, D, and E) computed from the reflection times using a velocity function based on the refraction velocities and normal-move-out corrections. Since reversed refraction

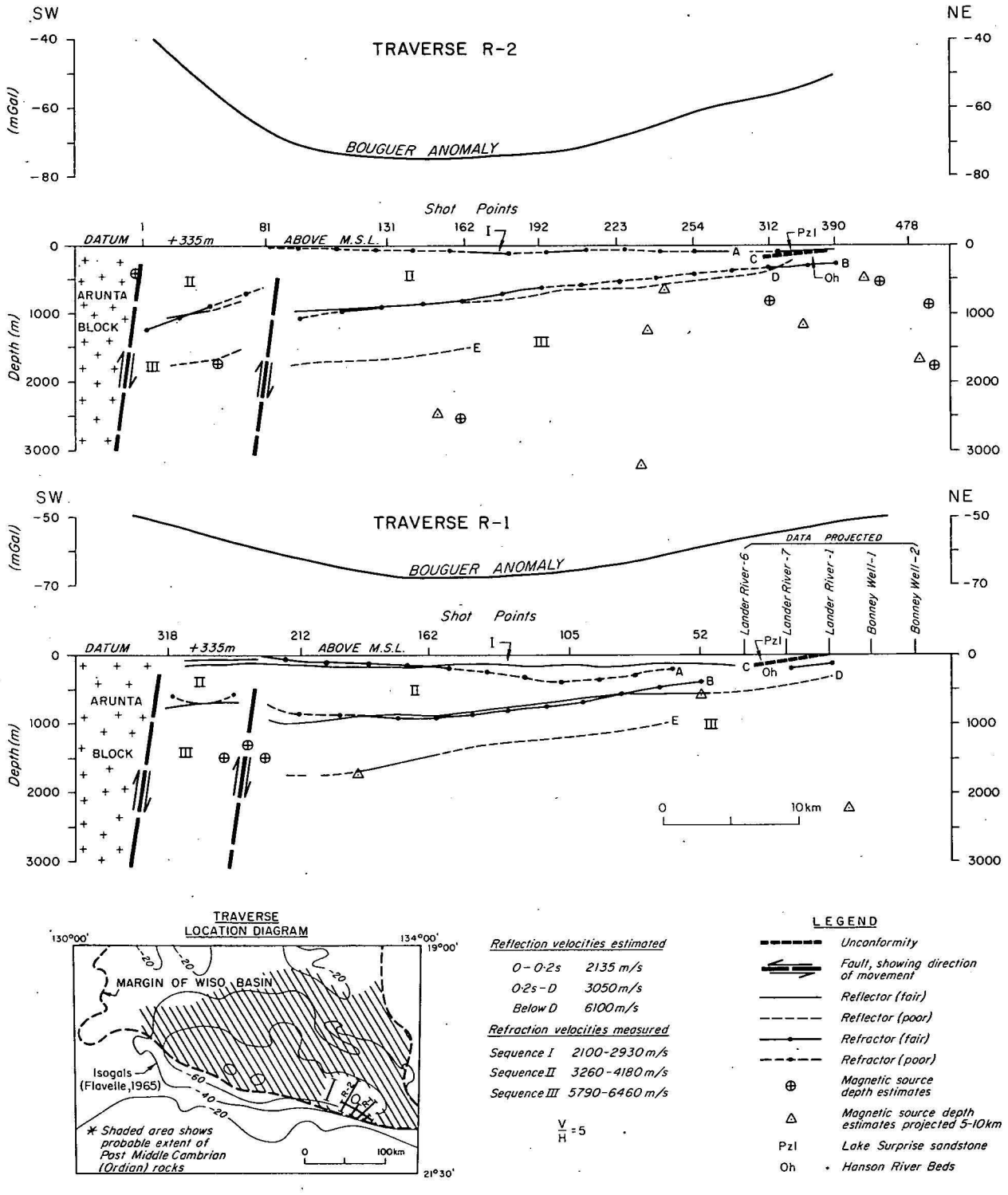

Figure 3. Sections along the seismic traverses R-1 and R-2 (Fig. 1) showing seismic horizons, magnetic source depth estimates, and stratigraphic hole data.

profiles were not recorded, the accuracy of velocity and depth estimates is considered to be only ± 20 percent.

Gravity data

The Bouguer anomaly contours (Fig. 2) show an east-southeasterly trending gravity low larger in extent than the trough suggested by the seismic survey. The 1000 m of unmetamorphosed rocks in the trough (sequences I and II) account for only 6 mGal of the 30 mGal change in the anomaly, assuming a density contrast of 0.15 t/m^3 between these rocks (dominantly sediments) and the underlying Proterozoic rocks. The gravity low in this area is part of the Lander Regional Gravity Low (Fraser *et al.*, in prep.), the northernmost of the series of prominent easterly trending regional gravity lows in central Australia. Sediments in the Ngalia, Amadeus and Officer Basins are associated with larger regional gravity lows to the south and similarly account for only a fraction of the total gravity anomaly. The major parts of these extensive lows and the intervening regional gravity ridges, have been attributed (Mathur, 1976) to deep crustal folding and faulting consistent with the geological structure. The gravity lows have been interpreted as areas of crustal downwarp in which sedimentary rocks are preserved, and the intervening gravity ridges as areas of uplift from which the sediments have been eroded. A similar interpretation for the Lander Regional Gravity Low (Fig. 4) implies that the Lander Trough contains a sequence of bedded rocks preserved in a crustal downwarp bounded on the south by an overthrust fault. The seismic data support this broad interpretation of the structure but insufficient information is available to confirm the thrust nature of the fault.

Aeromagnetic data

Aeromagnetic data for the Lander Trough (Fig. 5) is reproduced from the survey flown for American Overseas Petroleum (Adastra Hunting Geophysics, 1967). The survey was flown at approximately 380 m above ground level with a 3.2 km line spacing. Line direction was approximately northeast-southwest.

Interpretation indicates that there are several different magnetic horizons which produce superimposed anomalies. Estimated depths to magnetic sources are shown on Figures 2 and 5. Figure 5 also shows two major interpreted faults.

In the Wiso Basin and adjacent areas, magnetic anomalies are associated with the Antrim Plateau Volcanics, Hatches Creek Group, Warramunga Group and Arunta Block (see Fig. 1).

Prominent anomalies over the Arunta Block to the south of the trough produce an abrupt change in magnetic character, and indicate the position of the southern margin of the trough.

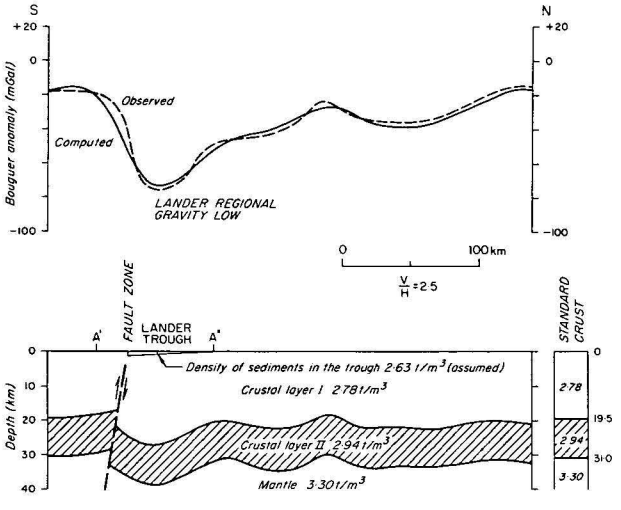

Figure 4. Regional gravity profiles and interpreted crustal structure model across the eastern part of the Lander Trough.

Integrated interpretation

The nature of the rocks forming the three sequences identified from the seismic data is difficult to determine directly, as aeolian sand covers the area. A few low outcrops (Fig. 2), and BMR shallow stratigraphic drilling in 1974 (Kennewell & Huleatt, in prep.) provide the only available information.

The refractor A/reflector C boundary, when projected to the surface on traverse R-2, closely corresponds to the exposed unconformity between the presumed Late Palaeozoic Lake Surprise Sandstone (Kennewell & Huleatt, in prep.) and the underlying Ordovician Hanson River Beds. Similarly, on traverse R-1, the same unconformity dips southwards as indicated by projected borehole data (Fig. 3) and corresponds approximately to the refractor A/reflector C boundary. A close relationship should not be expected, as the drillholes have been projected about 8 km along strike.

The refractor B/reflector D boundary is not exposed in this area, but rises to within 250-330 m of the surface at the northeastern end of traverses R-1 and R-2. Shallow magnetic sources close to the boundary in this part of the area may indicate the presence of lavas stratigraphically equivalent to the Early Cambrian Antrim Plateau Volcanics. The boundary probably represents the contact between slightly metamorphosed Proterozoic rocks and the overlying Palaeozoic sediments of the Wiso Basin.

If these interpretations are correct, sequence I is probably the Lake Surprise Sandstone, a well-rounded, well-sorted, medium-grained sandstone with low-angle cross-bedding and slumping in parts, which is probably of Late Palaeozoic age.

Sequence II most likely consists of Cambrian to Ordovician rocks. The basal rock units are uncertain in this area, but Cambrian dolomite, dolomitic siltstone, and red sandstone was intersected in drillholes to the north (Kennewell & Huleatt, in prep.), and sandstone, siltstone, claystone and dolomite of the overlying Hanson River Beds by BMR Lander River 1, 2 and 3 and BMR Bonney Well 1 and 2. The youngest fossils recorded from this sequence are of late Arenig to Llanvirnian (Ordovician) age, but as the sequence apparently dips southwards, younger rocks may be present, obscured by sequence I. The discrepancy of refractor A dipping beneath reflector C on traverse R-1 (Fig. 3) may indicate refracting horizons within sequence II.

Reflector C on traverse R-2 (Fig. 3) was not recorded in the central and southwest part of the traverse, probably because the seismic recording and processing techniques used obscured near-surface detail. The seismic velocities for sequences I and II are compatible with the interpreted rock types.

Sequence III is considered to consist of Proterozoic rocks. The basis for this is:

(a) high seismic velocities
(b) the interpretation of the refractor B/reflector D boundary as the base of the Palaeozoic rocks
(c) the occurrence of magnetic anomalies associated with sequence III, for which the most likely sources are basic lavas of the Hatches Creek Group which crop out to the east (Fig. 1; Smith, 1961).

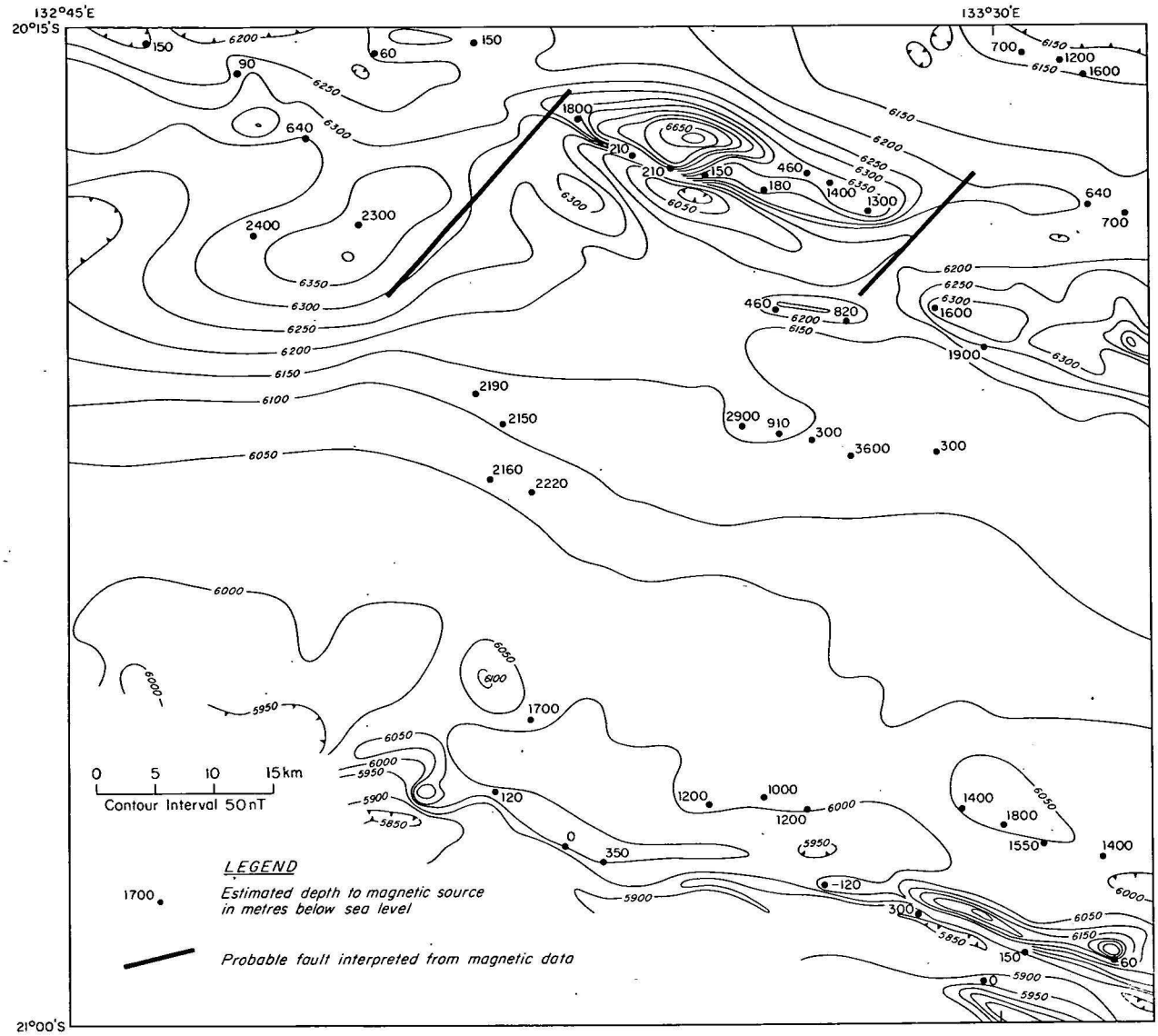

Figure 5. Aeromagnetic intensity contour map with estimated depths to magnetic sources and interpreted faults. The magnetic field shows a west-northwest trend and the abrupt change in its character on the south indicates the position of the southern margin of the trough.

The presence of the poor quality reflector E, and other discontinuous but conformable reflection events above and below it (not shown on Fig. 3) suggests that these rocks are bedded. The reflector E about 800 m below the refractor B/reflector D boundary is probably a boundary between two distinct rock units within sequence III. The upper, more strongly bedded unit is possibly a lateral equivalent of the Adelaidean Central Mount Stuart Formation which crops out as gently folded sandstone, arkose and siltstone overlying the Arunta Block 70 km to the south (Fig. 1). The lower, less distinctly bedded sequence is probably the Proterozoic Hatches Creek Group which crops out as moderately folded sandstone, siltstone, conglomerate and volcanics 60 km to the east, in the Bonney Well 1:250 000 Sheet area (Fig. 1). The occurrence of most magnetic horizons below horizon E, or horizon E extrapolated, supports this interpretation.

Conclusions

The combined interpretation of the results from geological mapping, shallow stratigraphic drilling and reassessment of geophysical data indicates that the Lander Trough is an area of crustal downwarp bounded on the southwest by a fault system against the Arunta Block, and that in the southeastern part three main rock sequences are present beneath the Cainozoic superficial cover. The uppermost sequence I, which is flat-lying and relatively thin, is interpreted as the ?Late Palaeozoic Lake Surprise Sandstone. It shows thinning in the northwest direction, from a maximum thickness of 250 m on traverse R-1 to 100 m on traverse R-2. The sequence II is considered to consist of Cambrian to Ordovician, partly marine, sediments. It forms a wedge and thickens towards the southwest from 350 m at the northeast end of the traverses to a maximum of 800 m in the thickest part of the trough. Sequence I overlies sequence II unconformably. Sequence III forms the basement to the Palaeozoic sediments of the Wiso Basin. It is Proterozoic in age and probably includes the Adelaidean Central Mount Stuart Formation, which is about 800 m thick, and the Early Proterozoic or Carpentarian Hatches Creek Group, which is several thousand metres thick in outcrops to the east.

The fault system which forms the southwestern margin of the trough affects the sequences II and III but not sequence I, and hence is post-Ordovician in age and may be contem-

poraneous with the Alice Springs Orogeny of the Ngalia and Amadeus Basins.

The extent and depth of the trough beyond the area of the seismic survey are uncertain. Geological, gravity and aeromagnetic data suggest however that the trough extends to the west-northwest and east-southeast over most of the stippled area shown on the location diagram in Figure 3, covering an area about 300 km long and 100 km wide.

To test the interpretation of the Lander Trough presented here and better evaluate the petroleum potential of the Palaeozoic sediments, stratigraphic drilling at the northern edge of the trough where the Palaeozoic section is thin (e.g. shotpoint 312, traverse R-2) is required. If the presence of Cambrian and Ordovician sediments in the trough is confirmed, its petroleum potential would be upgraded, for gas has been discovered in sediments of the structurally similar Toko Syncline of the Georgina Basin to the southeast, and the Amadeus Basin to the south.

References

ADASTRA HUNTING GEOPHYSICS PTY LTD, 1967—An airborne magnetometer survey, Wiso Basin, N.T., *for* American Overseas Petroleum Ltd (unpublished).

AERO SERVICE LTD, 1964—Interpretation report of airborne magnetometer survey over Tanami area, Northern Territory, *for* Exoil Oil Co. Pty Ltd (unpublished).

FLAVELLE, A. J., 1965—Helicopter gravity survey by contract, N.T. & Qld, 1965. Part I. *Bureau of Mineral Resources, Australia—Record* **1965/212** (unpublished).

FRASER, A. R., DARBY, F., & VALE, K. R., (in prep.)—A qualitative analysis of the results of the reconnaissance gravity survey of Australia. *Bureau of Mineral Resources, Australia—Report.*

KENNEWELL, P. J., & HULEATT, M. B., (in prep.)—The geology of the Wiso Basin. *Bureau of Mineral Resources, Australia—Bulletin.*

MATHUR, S. P., 1976—Relation of Bouguer anomalies to crustal structure in southwestern and central Australia. *BMR Journal of Australian Geology and Geophysics*, **1**, 277-286.

MILLIGAN, E. N., 1976—Geology of the Wiso Basin; *in* R. B. LESLIE, H. J. EVANS, & C. L. KNIGHT (Editors) Economic Geology of Australia and Papua New Guinea—3. Petroleum. *Australasian Institute of Mining & Metallurgy. Monograph Series* **7.**

MILLIGAN, E. N., SMITH, K. G., NICHOLS, R. A. H. and DOUTCH, H. F., 1966—The geology of the Wiso Basin, N.T. *Bureau of Mineral Resources, Australia—Record* **1966/47** (unpublished).

RAY GEOPHYSICS (AUSTRALIA) PTY LTD., 1967—Geograph seismic survey of the Hanson River area, Northern Territory, OP 119. Report *for* American Overseas Petroleum Limited (unpublished).

SMITH, K. G., STEWART, J. R. and SMITH, J. W., 1961—The regional geology of the Davenport and Murchison Ranges, Northern Territory. *Bureau of Mineral Resources, Australia —Report* **58.**

Uranium mineralization associated with late Palaeozoic acid magmatism in northeast Queensland

J. H. C. Bain

The late Palaeozoic acid igneous petrographic province, covering some 120 000 km² in the Cairns-Townsville hinterland, has associated uranium mineralization characterized by various combinations of uranium, fluorine, and molybdenum. Mineralization of this type has been described from other parts of the world, but is best known in the USSR. Information about the Australian deposits and occurrences is very limited, but it is apparent that the mineralization is mainly of hydrothermal origin and genetically related to extensive late Palaeozoic magmatism.

Zones of high porosity and permeability within 300 to 1500 m or so of the surface, which were accessible to mineralized hydrothermal fluids at temperatures of about 150°C to 300°C, appear to have been the most favourable sites for the deposition of uraniferous minerals. Suitable porosity and permeability may be of sedimentary, diagenetic, volcanic, hydrothermal, or tectonic origin, but flat, or gently dipping coarse sedimentary rocks at the base of acid volcanic sequences are possibly the most suitable hosts for layer-like and stockwork deposits. Intensely jointed rocks, hydrothermal alteration zones, breccia pipes, fault zones, unconformities, flow-top breccias, and faulted or fractured fold hinges, may also have sufficient porosity and permeability to host mineralization. Permeable basement fractures, dyke swarms, and intrusive contacts, as well as some of the potential hosts themselves may have provided channelways from the mineralizing source. Suitable channelways and deposition sites are common throughout the province, and offer the prospect of additional discoveries of uranium deposits of similar and related types.

Introduction

Airborne scintillograph and ground geological reconnaissance surveys by BMR in the 50's (Fig. 1) did not result in the discovery of any significant uranium deposits in the Georgetown Inlier. However, the general revival of interest in uranium prospecting in the late 60's, and the discovery in 1971 of the Maureen uranium-fluorine-molybdenum deposit 35 km north-northwest of Georgetown, have led to increased exploration activity in the Georgetown Inlier in the last few years (Fig. 1). This search is mostly for deposits of the Maureen type—a type not previously recognised in Australia, and apparently little known outside the USSR. The Maureen deposit, which lies within sediments at the base of a late Palaeozoic acid volcanic formation, is believed to be of hydrothermal origin and to be genetically related to an unexposed body of late Palaeozoic granite. The late Palaeozoic igneous rocks are part of a large petrographic province that extends throughout most of the Cairns-Townsville hinterland. In the USSR, deposits similar to Maureen represent only one of several different, but related, types of uranium deposit found in a variety of geological environments associated with petrographic provinces like that in northeast Queensland. Some of the controls of mineralization and many potentially mineralized geological environments within the Cairns-Townsville hinterland can be deduced from the regional and mineral deposit geology of both the Queensland and Soviet deposits. The late Palaeozoic acid volcanic petrographic province is a uranium province characterized by deposits of uranium-fluorine-molybdenum minerals.

Reports of uranium, fluorine, and molybdenum minerals associated with tin-bearing granites in similar acid volcanic provinces elsewhere in the Tasman Geosyncline (Ingram, 1974) suggest that this mineral association may be more common than hitherto suspected in Australia.

Regional setting

The Cairns-Townsville hinterland comprises a Precambrian and early Palaeozoic metamorphic and granitic infrastructure, and a late Palaeozoic acid igneous superstructure. Most uranium deposits in the region are genetically and spatially closely related to the latter.

Precambrian and early Palaeozoic rocks

The infrastructure consists of the Precambrian Georgetown Block to the west (White, 1965; de Keyser & Lucas, 1968; Oversby *et al.*, 1975), and early Palaeozoic rocks of the Tasman Geosyncline to the east (White, op cit.; de Keyser & Lucas, op. cit.)—separated by an irregular line of roughly colinear and en echelon faults known as the Tasman Line (Hill, 1951). There are several isolated patches of rocks of probable Precambrian age east of the Tasman Line (Wyatt, 1968; T. Bell, pers. comm., 1976), and similar rocks may underlie much of the early Palaeozoic part of the Tasman Geosyncline. Both provinces contain sedimentary and igneous rocks which have been multiply deformed and variably metamorphosed. The metamorphic rocks are predominantly fine to medium-grained quartzose, pelitic, feldspathic and calcareous sediments, with minor intercalated basic volcanics, intruded by basic sills and dykes. They have been complexly deformed by up to five episodes of folding and much brittle fracturing; their metamorphic grade ranges from low greenschist to granulite facies. The granitoids which intrude the metamorphics are mostly within the Georgetown Block, where they comprise both batholithic bodies and small aplite and pegmatite dykes. They include biotite and muscovite granitoids, which are commonly leucocratic porphyritic and foliated. The dominant fracture trends, as indicated by lineaments on Landsat imagery (Fig. 2), are similar in both provinces, despite differences in age and lithology. In particular, the dominant east-northeast-trending set of lineaments is common to both sides of the Tasman Line. Furthermore, similar trends are exhibited by segments of the Tasman Line, the distribution of late Palaeozoic igneous rocks and mineral deposits (especially tin), and significant post-Jurassic faults and flexures in the domed surface of the Georgetown Block (as indicated by structure contours of the base of the Mesozoic sequence—Fig. 2). Thus it is likely that many fault and fracture systems throughout the region have been active at least intermittently during a considerable period of time, and that some are deep structures that could have influenced the distribution and development of the late Palaeozoic igneous rocks, hydrothermal systems, and related mineral deposits.

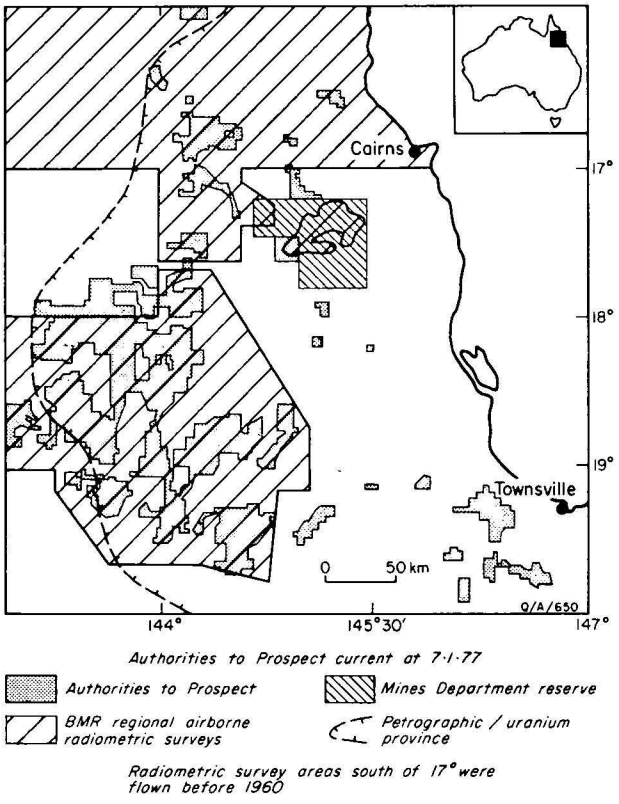

Figure 1. Cairns-Townsville hinterland, showing Authorities to Prospect, and areas covered by BMR regional airborne radiometric surveys.

Late Palaeozoic acid igneous province

The late Palaeozoic acid igneous province extends over at least 120 000 km^2, (Fig. 3), and contains many comagmatic calc-alkaline volcanic complexes, ring dykes, and granitoids (Branch, 1966; Sheraton & Labonne, in press) and areas of related hydrothermal alteration. It covers much of the Precambrian Georgetown Block and the early Palaeozoic rocks of the Tasman Geosyncline. Although the main area of these acid rocks lies in the hinterland of Cairns and Townsville, scattered late Palaeozoic granite plutons are known as far north as Cape Melville (320 km north of Cairns), and there are similar, probably comagmatic, acid igneous rocks of late Palaeozoic age around the northern end of the Bowen Basin 170 km southeast of Townsville. The chemical data required to establish that the rocks in the latter area are comagmatic with and hence part of this petrographic province are absent, and hence the southern extent of the province is not known. Outcrop of the acid igneous province is limited on the west by overlying Mesozoic and Cainozoic sediments, and on the east by the coastline.

The distribution of the granitoids, acid volcanic formations, and related sedimentary formations (Table 1) within the late Palaeozoic acid igneous province are shown in Figure 3.

Granitoids. The granitoids are mostly grey to pink, medium to coarse biotite and hornblende-biotite granite, adamellite. and granodiorite. Porphyritic, granophyric, and aplitic varieties are common, and there are some more basic rock types such as quartz gabbro and tonalite. Many are subvolcanic rocks, and grade through porphyritic microgranite into comagmatic acid volcanics which they commonly intrude.

Tourmaline, topaz, fluorite, apatite, allanite, and epidote are commonly accessory minerals; feldspars are usually zoned, hydrothermally or metasomatically altered, and typically hematitic. Undulose extinction, fine fractures, and slightly recrystallized quartz and feldspar, indicate that the rocks have undergone mild deformation.

Greisens are common, and in the most fractionated granitoids, such as the Elizabeth Creek Granite, they are especially common and generally contain cassiterite; many also contain molybdenite or wolframite.

Intrusions are mostly small, discrete, or overlapping, and circular or elliptical in plan, and have chilled margins and narrow thermal metamorphic aureoles. Many of the extensive granite units shown on the published 1:250 000-scale geological maps of the region are in fact composite bodies composed of many separate, but closely related, intrusions (Blake, 1972; Olatungi, 1975). The microgranites are mostly dykes and small irregularly shaped intrusions within the acid volcanics or the basement adjacent to them. The chemistry of the rocks is similar to other calc-alkaline intrusive suites, but their restricted compositional range is a notable feature—only 6 percent of the granitoids analysed by Sheraton (1974) contain less than 65 percent SiO_2, and about 80 percent contain more than 70 percent SiO_2. Trace-element abundances are close to values of Turekian & Wedepohl (1961) for average low-calcium granite, and of Taylor (1968) for average granite, although Sn, Th, and U are slightly higher than average, and Cu and Ba lower (Sheraton & Labonne, in press).

Many of the granitoids have element abundances indicating a high degree of fractionation—in particular marked, but variable depletion in Sr and Ba; and enrichment in Li, Be, Rb, F, Y, Sn, Th, U, and to some extent Pb and Ga (Sheraton & Labonne, in press). The most highly fractionated granitoids, such as the Elizabeth Creek Granite, probably exceed 5 000 km^3 in total volume, and contain about 11 ppm U (ranging from 3-28 ppm U), which is about three times the average amount of uranium in acid igneous rocks, values that are comparable with those of intrusives associated with uranium deposits in the Mount Isa and Pine Creek uranium provinces (Derrick, 1977, Table 5). Such extreme fractionation is believed to be a consequence of a longer crystallization history when compared with the extrusive rocks, resulting in more effective fractional crystallization (Sheraton & Labonne, op. cit). Late or post-magmatic processes such as greisenization may also have played a part in enriching the rocks in certain elements—especially F, Li, Rb, and Sn, and in depleting them in Ba, and Sr. Sheraton & Labonne have shown that low water pressures prevailed during crystallization of the granitoids, and calculated the depth of emplacement for Elizabeth Creek Granite. Their estimate of 2 km is comparable with observed minimum depths of emplacement within the Newcastle Range Volcanics of 1-1.5 km (B. S. Oversby, pers. comm., 1977).

D. Richards (pers. comm., 1976) notes that the granitoids comprise both 'S' and 'I' types as defined by Chappell & White (1974); most of the more siliceous rocks are corundum-normative (Sheraton & Labonne, op. cit) and thus probably 'S' types.

Volcanics. The volcanic sequences are dominantly grey to pink and purple rhyolitic ignimbrites, with intercalated acid lava, tuff, breccia, agglomerate and volcaniclastic sediments. Some sequences contain andesitic lavas, generally towards the base, and some—probably most—are underlain by scattered lenses of coarse, feldspathic epiclastic terrestrial sediments. Recent geological mapping of the Newcastle Range Volcanics (Fig. 4; Bain *et al.*, 1975,

Granitoids

Elizabeth Creek Granite, Cannibal Creek Granite, Almaden Granite, Herbert River Granite, Ixe Monzonite, Mareeba Granite, Lochaber Granite, Tiger Hill Microgranite, Tully Granite Complex, Oweenee Granite, Bagstowe Ring Complex, Pall Mall Adamellite, Purkin Igneous Complex, Prestwood Microgranite, Eva Creek Microgranite, Hales Siding Granite, Hammonds Creek Granodiorite, Nymbool Granite, Bakerville Granodiorite, Kabinga Granodiorite, Watsonville Granite, Atlanta Granite, Trevethan Granite, Gurrumba Ring Complex; unnamed units CPg, C-Pb, C-Pi, and Cg (Townsville 1:250 000 Sheet area), Cge, Cgb, Cgp (Ingham 1:250 000 Sheet area), Pgc (Innisfail 1:250 000 Sheet area), and Pzu (Mossman 1:250 000 Sheet area) and Pzug (Gilberton 1:250 000 Sheet area).

Volcanics

Sunday Creek Volcanics, Nanyeta Volcanics, Nychum Volcanics, Scardons Volcanics, Glen Gordon Volcanics, Kallon Volcanics, Walsh Bluff Volcanics, Featherbed Volcanics, Warby Volcanics, Boxwood Volcanics, Claret Creek Volcanics, Slaughter Yard Creek Volcanics, Gurrumba Volcanics, Gingerella Volcanics, Galloway Volcanics, Newcastle Range Volcanics, Cumbana Volcanics, Cumberland Range Volcanics, Agate Creek Volcanics, unnamed volcanics at Mt Tabletop, Bagstowe Ring Complex, Butlers Igneous Complex, Montgomery Range Rhyolite Porphyry, Hells Gate Rhyolite, Tareela Volcanics, Percy Creek Volcanics, Saint James Volcanics; also units Cuv, Cuy, C-Pp and C-Pv (Townsville 1:250 000 Sheet area), Cgp and Cp (Ingham 1:250 000 Sheet area), Pzu (Gilberton, Einasleigh, Clarke River, Atherton, Georgetown 1:250 000 Sheet areas).

Sediments

Montalbion Sandstone, Mount Mulligan Coal Measures, Silver Valley Conglomerate, Ringrose Formation, Gilberton Formation, Clarke River Formation, Bundock Creek Formation, Ellenvale Beds, Marsh's Creek Beds, Insolvency Gully Formation, Piccadilly Formation, Game Hill Beds, Star Beds, Hardwick Formation, Lollypop Formation, and unnamed units C and D-C (Townsville 1:250 000 Sheet area). Some older, Devonian and Silurian formations contain similar rock types and may also be prospective for uranium.

Table 1. Constituents of the late Palaeozoic acid igneous province as shown on published geological maps of the region.

1976, in press) has demonstrated that both basal epiclastic and intercalated volcaniclastic sedimentary layers are far more common than was indicated on earlier reconnaissance maps (White, 1962; Branch, 1966).

It is expected that most other similar volcanic sequences within the province will, when examined in more detail, be found to contain much the same proportion of sedimentary strata.

The ignimbrites are mostly welded, compact, and well jointed, generally with several intersecting sets of closely spaced fractures. Individual ignimbrites are distinguished mainly by colour, size and abundance of quartz and feldspar phenocrysts, and fractures. In general, groups of ignimbrite layers have cooled together, and some of these cooling units are much more fractured than others. Many joints clearly reflect basement fractures, possibly reactivated during cauldron subsidence. Some of the ignimbrites and other rock types are locally or extensively pyritic and kaolinized, silicified, recrystallized, or otherwise hydrothermally or metasomatically altered; certain epiclastic sedimentary layers are locally hematitic.

Many of the volcanic complexes and related intrusives are preserved in fault-bounded cauldron subsidence areas (Branch, 1966)—the thinner, more extensive distal parts of the volcanic strata, that once extended beyond the subsidence areas, have been removed by erosion. Dyke swarms, breccia pipes, and hydrothermal alteration systems are common associates of the volcanic complexes.

The more siliceous volcanic rocks are not as fractionated as the equivalent intrusives, and are only slightly enriched in Be, Rb, Y, Pb, Th, and U; and depleted in Sr, relative to the less siliceous rocks. Probably the most significant chemical difference between the volcanics and the granitoids is the greater variation in alkali contents of the volcanics; some have been depleted in K and enriched in Na, and vice versa; and some, although depleted in Na are not enriched in K. This is a result of alkali metasomatism, which Sheraton & Labonne (op. cit) consider to be a post-magmatic process that accompanied hydration of the rocks, possibly during devitrification. Some of the volcanics, especially the Newcastle Range Volcanics, appear to have deen depleted in uranium relative to the average composition (i.e. 2 ppm as against 5 ppm). This observation led Sheraton & Labonne (in press) to point out that elements such as U, Cu, Pb and Zn, removed from the volcanics by alkali-rich hydrothermal (metasomatic) solutions, may be re-deposited and concentrated to form economic deposits.

Sediments. The sedimentary formations are lithologically similar to, but usually thicker and more extensive than, the sedimentary interbeds of the volcanic formations. Most contain lacustrine and fluviatile feldspathic sandstone, siltstone, mudstone, and conglomerate, and some tuff and limestone; plant debris is common, but marine beds and acid volcanic interbeds are rare. Some formations are typical continental red-bed sequences, and all lie with angular unconformity on older Palaeozoic and Proterozoic rocks. Most lie east of the Tasman Line within the Tasman Geosyncline.

Uranium deposits

Several uranium prospects and many uranium occurrences have been found associated with the acid igneous rocks in the Cairns-Townsville hinterland, but little information has been published on them. The following is a summary of the known deposits and their distribution.

Maureen deposit

The deposit consists of lenticular stratabound concentrations of uranium-fluorine-molybdenum minerals conformable within a gently dipping conglomerate-sandstone-siltstone sequence at the base of late Palaeozoic Galloway Volcanics, which overlie high-grade Precambrian metasedimentary rocks on the northeastern edge of the Georgetown Inlier (O'Rourke, 1975).

The Galloway Volcanics are predominantly rhyolitic ignimbrites and agglomerates, with subordinate basalt and tuffaceous and sedimentary beds. The latter are unusually thick (320-400 m) in the vicinity of the deposit, and comprise feldspathic sandstone-conglomerate, siltstone-sandstone, limestone, and tuff. The lowermost 60 m of the sequence contains the mineral deposit (O'Rourke, op. cit) and consists of alternations of pebbly feldspathic sandstone, chloritic siltstone, and minor tuff, as well as a basal conglomerate.

The location of the mineralization has been strongly influenced by sedimentary diagenetic features such as porosity and permeability; nevertheless the mineralization is apparently of hydrothermal origin, albeit probably modified by subsequent groundwater action. It has cut across some sedimentary structures, and has filled fractures, and replaced the matrix, some clasts, and locally the entire rock; it is related to faults and joints, postdating some, and is commonly associated with hematitic alteration

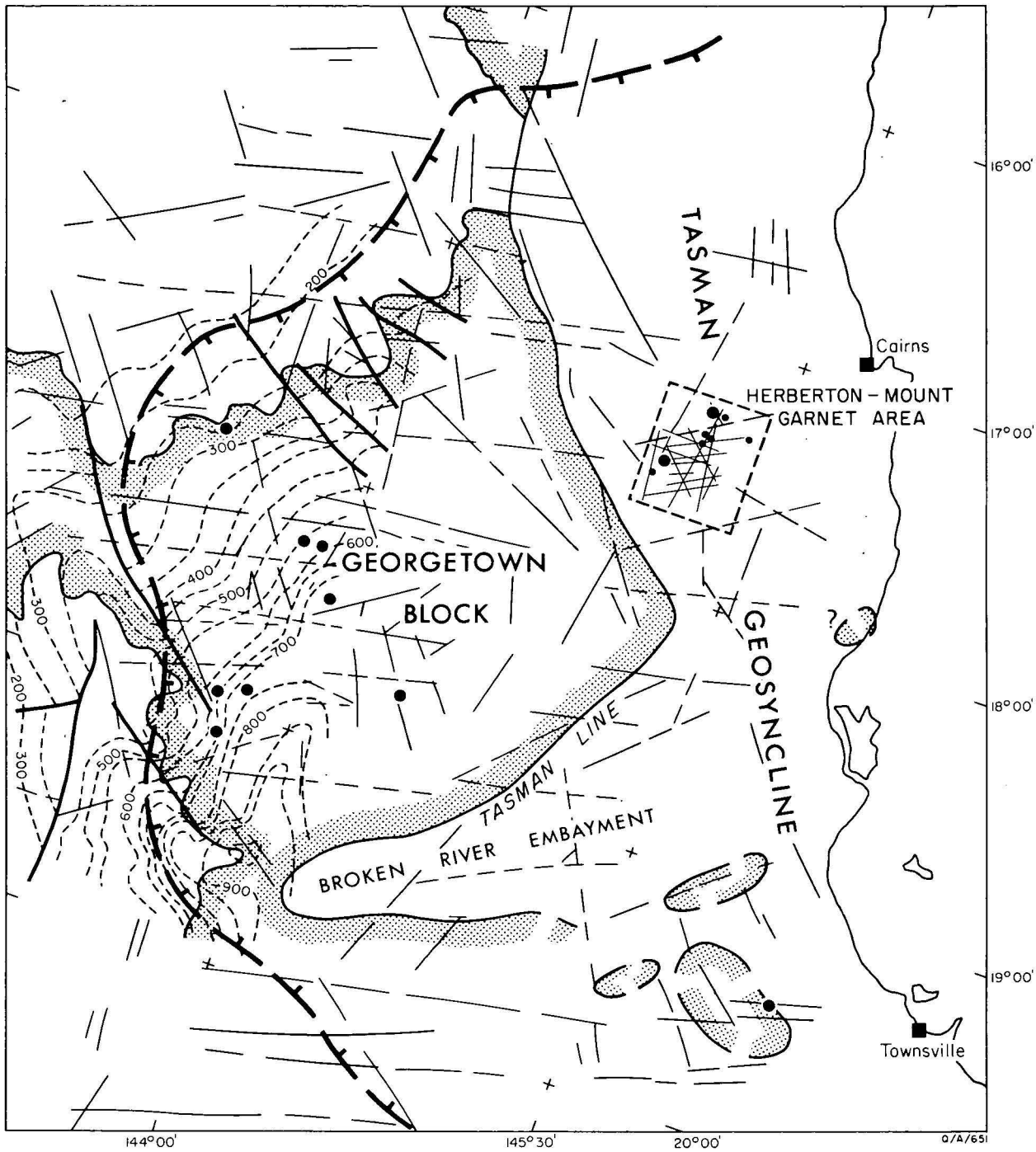

0 50 100 km

--200-- Structure contours (metres above sea level), base of Mesozoic sequence (from Doutch, Smart, Needham)

Fault or discontinuity indicated by structure contours

Precambrian basement

Late Palaeozoic Acid Igneous Province

Lineament, interpreted from Landsat imagery

Major Sn mine

Uranium occurence

Trend of tin and basemetal mines and mineral occurrences within the Herberton – Mount Garnet area (after Taylor & Steveson 1972, Blake 1974)

Figure 2. **Extent of outcropping Precambrian basement in the Cairns-Townsville hinterland. Also shown are the pattern of major lineaments interpreted from satellite imagery, trends of distribution of mineral deposits in the Herberton/Mount Garnet area, structure contours on the base of the Mesozoic sedimentary sequence, and the extent of the late Palaeozoic acid igneous province.**

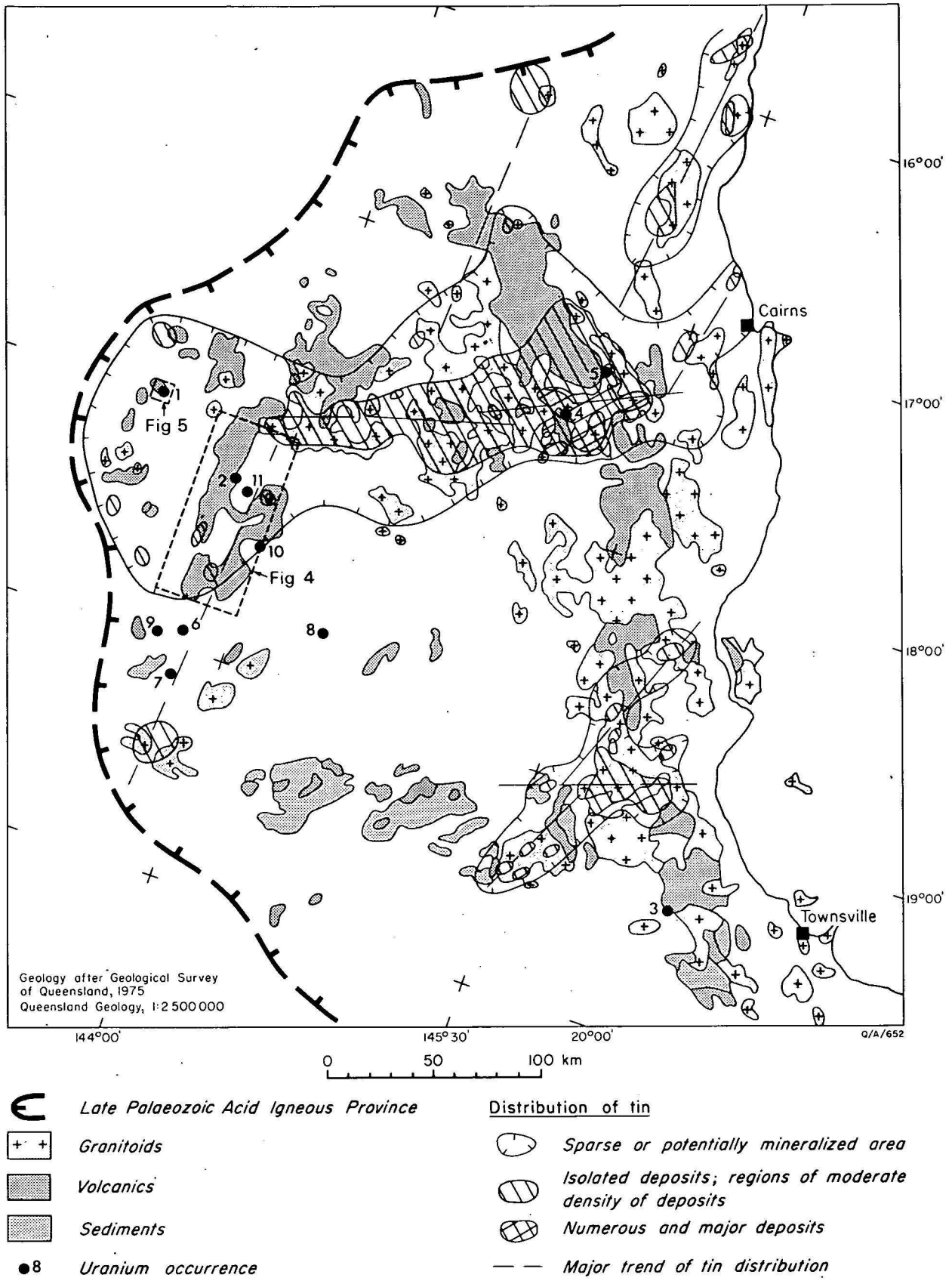

Figure 3. **Distribution of granitoids, volcanics, and related sediments, uranium occurrences, and tin deposits in the late Palaeozoic acid igneous province, Cairns-Townsville hinterland. Numbered uranium occurrences are: 1. Maureen, 2. Laura Jean, 3. Hervey Range, 4. Treasure, 5. Stannary Hills, 6. Limkins, 7. Mount Hogan, 8. Lynd, 9. Percyville, 10. Kaiser Bill, 11. Questend.**

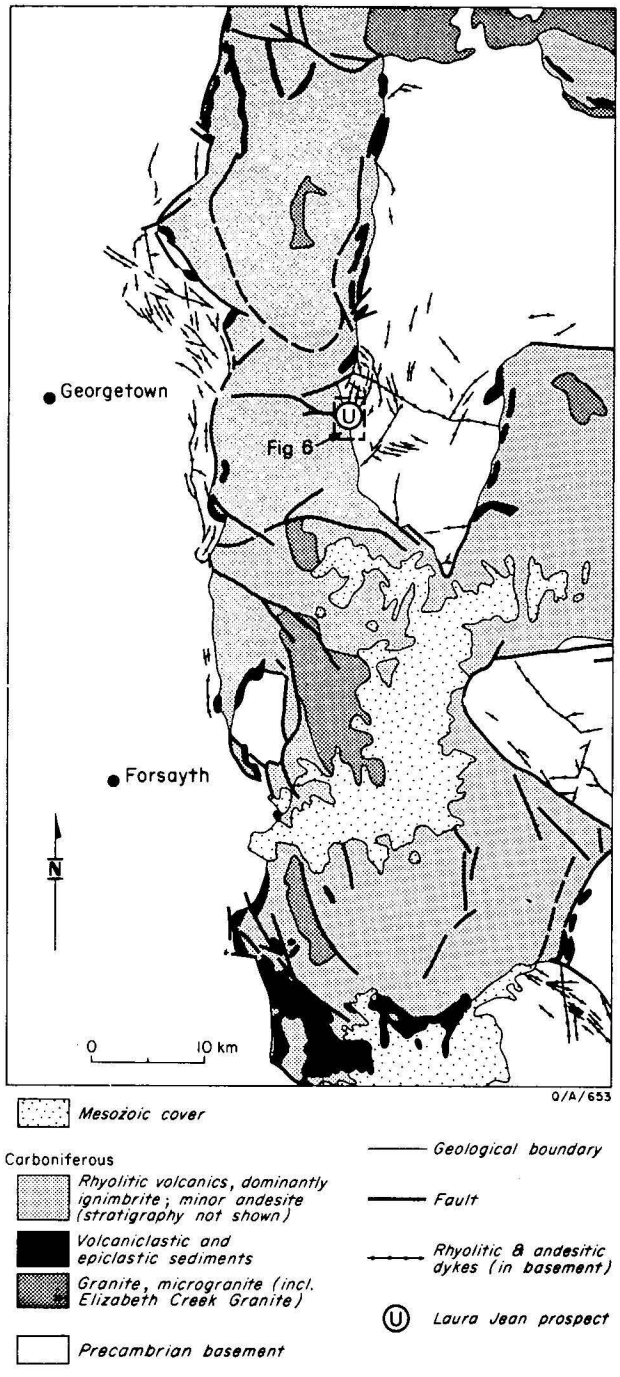

Figure 4. Distribution of sedimentary units in the Newcastle Range and Cumbana Volcanics (simplified, after mapping by B. S. Oversby, J. H. C. Bain and I. W. Withnall).

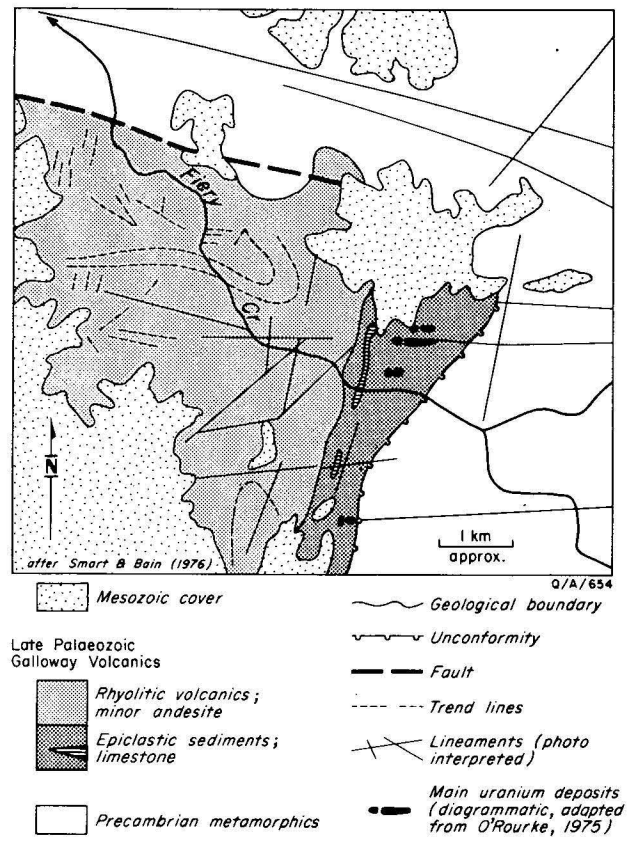

Figure 5. Maureen uranium-fluorine-molybdenum deposit.

and bleached wallrock. Linear, cigar-shaped 'mantos' of highest grade mineralization inside lower grade envelopes appear to lie on extensions of basement lineaments and O'Rourke (1975), states that they parallel a regional fold axis and shear, although he does not specify their age or location. High and low-grade mineralization within the metamorphic basement, or immediately over or near irregularities in it, as well as the mineralogy of the deposit, further attest to the hydrothermal origin of the ore fluids. Some late-stage veinlets of dickite and kaolinite cut the mineralization (O'Rourke, 1975). The deposit contains at least 3600 tonnes of U_3O_8 (Withnall, 1976); Fluorine and molybdenum contents have not yet been announced.

The uranium mineralogy is complex, particularly within the oxidized zone. It comprises renardite $Pb(UO_2)_4(PO_4)_2(OH)_4.7H_2O$, saleeite $Mg(UO_2)_2(PO_4)_2.8H_2O$, meta-uranocircite $Ba(UO_2)_2(PO_4)_2.8H_2O$, uranopilite $((UO_2)_6(SO_4)(OH)_{10}.12H_2O)$, autunite $Ca(UO_2)_2(PO_4)_2.10\text{-}12H_2O$), meta-autunite, meta-autinite II, undetermined calcium uranium phosphate, and uraninite. The last is the only primary uranium mineral. The largest and highest grade bodies of uranium are generally associated with abundant purple fluorite, which at a 0.05 per cent U_3O_8 cut-off constitutes about 13 percent of the rock and economically significant amounts of molybdenum. The molybdenum minerals comprise microscopic molybdenite, ferrimolybdite $(Fe_2(MoO_4)_3.8H_2O)$, umohoite $((UO_2)MoO_4.4H_2O)$, wulfenite $(PbMoO_4)$, powellite $(CaMoO_4)$ ilsemannite, $(Mo_3O_8.nH_2O)$, iriginite $(U(MoO_4)_2\text{-}(OH)_2.2H_2O)$, and an unnamed calcium iron molybdenum phosphate. Up to 1.5 percent strontium is present locally as goyazite $(SrAl_3(PO_4)_2(OH)_5.H_2O)$ and svanbergite $(SrAl_3(PO_4)(SO_4)(OH)_6)$, and titanium as altered rutile and ?anatase is also locally abundant. Pyrite is present (generally less than 0.1 percent) as a fracture filling and finely disseminated throughout the sedimentary sequence. Where uranium is associated with it the pyrite is very fine and generally more abundant (up to 20 percent). The deposit also contains minor amounts of barite, gorceixite $(BaAl_3(PO_4)_2(OH)_5.H_2O)$, gypsum, kaolinite, dickite, galena, sphalerite, chalcopyrite, arsenopyrite, trogerite $((UO_2)_3(AsO_4)_2.12\ H_2O)$, apatite and alunite, and traces of tin, tungsten and mercury (O'Rourke, op. cit).

O'Rourke has described the deposit as a metasomatic replacement, believing that it formed where hydrothermal solutions ascending along major fault and fracture systems from a non-outcropping intrusion of Elizabeth Creek Granite, encountered favourable conditions for deposi-

tion—the porous and permeable sediments at the base of the volcanic sequence.

Laura Jean prospect

The small Laura Jean fluorine-uranium prospect (Fig. 6) is in brecciated dacitic lava within a linear zone of multiple faulting and intrusion associated with the eastern edge of the Newcastle Range Volcanics about 25 km east of Georgetown; it is well exposed in a cutting on the northern side of the Gulf Highway.

The mineralized zone is a dark, purplish breccia of angular iron-stained fragments of porphyritic dacitic lava; cut by veins of sparsely porphyritic microgranite, veins of purple fluorite and chlorite containing some specular hematite and disseminated pyrite; and by later carbonate veins. Fluorite has extensively replaced the dacite and microgranite fragments in the most intensely mineralized parts of the breccia. Although the fluoritized breccia is relatively highly radioactive, averaging 5 to 10 times background radiation, with rare patches having up to 100 times background, neither primary nor secondary uranium minerals are visible in the outcrop. However, preliminary analyses of the rock indicate that it contains, in addition to fluorite and the other minerals noted above, 112 to 155 ppm uranium, 290 to 330 ppm thorium, 480 to 710 ppm molybdenum, and trace amounts of copper (10 to 30 ppm), lead (59 to 65), and zinc (36 to 48 ppm); tin has not been detected.

The breccia is flanked on the east by a sheared, fault-bounded dyke of intensely sericitized, silicified, and locally carbonated aphyric ?andesite, about one metre wide. The late-stage carbonate veins also cut this dyke. Faulted against the breccia on the west is a variably porphyritic microgranite dyke in which two dissimilar parts have been juxtaposed by a fault. The western part contains only sparse, small quartz and feldspar phenocrysts, whereas the eastern part contains much larger and more numerous phenocrysts. The country rock is Precambrian granodiorite.

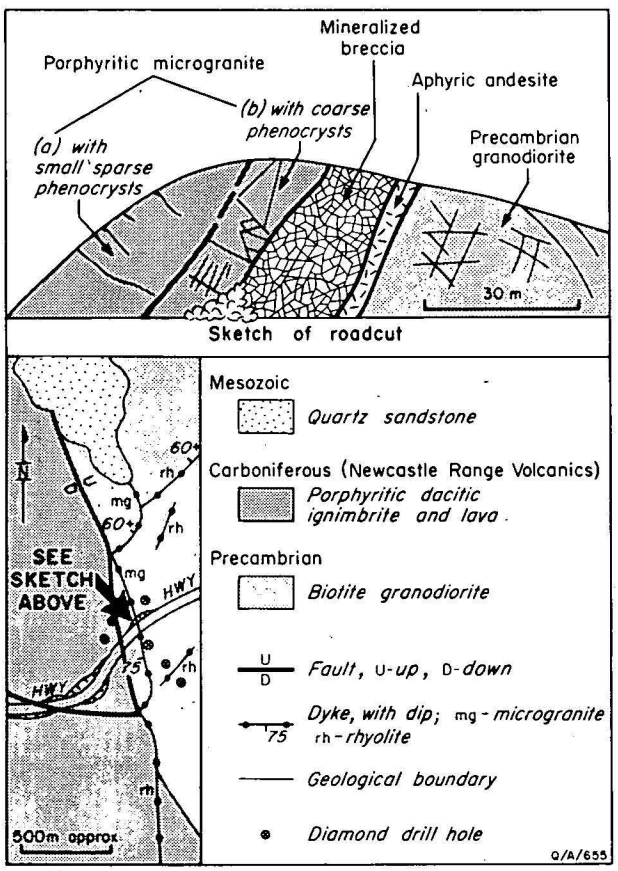

Figure 6. Laura Jean fluorite-uranium prospect (modified from a figure drawn by B. S. Oversby).

The Laura Jean deposit has had a complex history involving repeated faulting and intrusion. Oversby (*in* Withnall, in press) considers that the following sequence of events occurred: (1) emplacement and brecciation of a faulted slice of dacitic lava and other rocks, close to, but not at, the present level of exposure; (2) intrusion of microgranite along the fault and into parts of the breccia; (3) faulting and re-brecciation of the breccia accompanied by the introduction of fluorine (and uranium)-bearing fluid which locally replaced fragments; (4) emplacement of the ?andesite dyke; (5) carbonate veining; (6) relatively minor late-stage faulting and fracturing which emplaced the rocks in their present position. The mineralization probably represents a channelway used by mineralizing fluids similar to those which formed the Maureen deposit.

Hervey Range prospect

Uranium has recently been found in the Hervey Range area about 55 km west of Townsville (Jack, 1976), reputedly in the Upper Carboniferous Saint James Volcanics. The volcanics consist of about 100 m of andesitic and rhyolitic flows and pyroclastics, and subgreywacke, which have been intruded by late Palaeozoic porphyry and faulted against Upper Carboniferous subgreywacke, feldspathic sandstone, siltstone, mudstone, conglomerate, and chert of the Insolvency Gully Formation. Lying unconformably between the volcanics and ?Precambrian metamorphic basement are similar but older Palaeozoic sediments (Game Hill Beds). Other rhyolitic, dacitic and andesitic volcanic formations and comagmatic intrusives are present within a few kilometres to the north and east, and there are many faults in the area. Although the regional geological setting is very similar to that of the Maureen deposit, it is not known whether the mineralization is confined to, or even within, the sedimentary beds.

Herberton-Mount Garnet area occurrences

Torbernite is present in trace amounts in many wolframite/cassiterite lodes in the Herberton-Mount Garnet area (Ingram, 1974), as for example at the old Treasure mine in the Geebung Hill area 15 km north-northwest of Mount Garnet (Blake, 1972). There the lode, a greisen containing wolframite, cassiterite, and some molybdenite, fluorite, topaz and arsenopyrite, is in Elizabeth Creek Granite about 2 km north of the rhyolitic Nanyeta Volcanics.

Torbernite, meta-torbernite and purple fluorite have recently been found (G. Croft, pers. comm. 1976) in a hydrothermally altered, pyritic fault zone separating sandstone (Hodgkinson Formation) and porphyritic rhyolite (Featherbed Volcanics), from Elizabeth Creek Granite in the Stannary Hills area 18 km northwest of Herberton. There are several large and many small faults in the area, and innumerable abandoned small lode tin workings. This deposit may be similar to the Laura Jean.

Limkins prospect

The Limkins prospect, about 8 km east-northeast of Percyville, was virtually the only uranium occurrence of any note recognized before the recent resurgence of exploration. It is a very small, but rich deposit (about 10 tonnes of 2 percent U_3O_8), and not of commercial interest. Mineralization is confined to a 1 m wide fractured quartz vein, and adjacent fractured and hydrothermally altered parts of the wallrock—?Siluro-Devonian granodiorite (Wyatt, 1957).

Meta-torbenite, autunite, pyrite, and traces of galena are present in microveinlets and on fracture surfaces. No primary uranium mineral has been seen, and the grade decreases markedly with depth. Mineralization and alteration are structurally controlled as they are confined to an area of cross fracturing. The mineralizing fluids probably emanated from late Palaeozoic magma, but outcrops of intrusive or extrusive rocks of that age have not been identified nearby.

Mount Hogan occurrence

Disseminations, veinlets and fracture coatings of uraninite, pitchblende and phosphuranylite ($Ca(UO_2)_4(PO_4)_2(OH)_4.7H_2O$) (torbernite or meta-torbernite where oxidized) are present locally in the auriferous, fractured, and hydrothermally altered zones of a ?Precambrian biotite granite pluton 20 km south of the Limkins prospect. These fractured and altered zones are confined to the southeastern margin of the pluton, adjacent to a body of late Palaeozoic intrusive rhyolite. They are mostly outward-dipping sheets of fractured, sericitized, chloritized, and quartz-veined granite interspersed with relatively unaltered rock, and cut by several basalt or trachy-andesite dykes. The uranium is disseminated in the alteration zones, and associated with chloritic alteration along fractures, with gold and minor amounts of base metal sulphides in pyritic quartz veins, and with black fluorite veins; it is also present in a basalt dyke (Central Coast Exploration, pers. comm., 1977).

Lynd prospect

Yellow uranium minerals are present in a small roof pendant of biotite schist in Precambrian porphyritic granite, 15 km north-northwest of Lynd homestead. At this recently discovered prospect the schist contains several lit-par-lit lenses of granite, numerous thick stringers of white and iron-stained quartz, and a shear zone. Outcrop, however, is very poor, and the local geology is not well known (Hoyle, 1974).

Within the mineralized zone (about 12 x 80 m) meta-autunite, autunite, torbernite ($Cu(UO_2)_2(PO_4)_2.8\text{-}12H_2O$), sabugalite (HAL $(UO_2)_4(PO_4).16H_2O$), and bassetite ($Fe(UO_2)_2(PO_4)_2.8H_2O$) coat mica lamellae, and fill microfractures that cut the foliation in the schist. The highest grade mineralization (about 1 percent U_3O_8) is confined to an area of 2 m width and undetermined length, but most of the mineralized area contains at least several hundred ppm of uranium. Fine pyrite and traces of chalcopyrite accompany the uranium. Unlike most other uranium occurrences in the region, there is no obvious link with the late Palaeozoic magmatism.

Other occurrences

Anomalously high levels of radioactivity, and, locally, green secondary uranium minerals, are present in the mullock from the lowest levels of some old gold workings in the Percyville area; and in copper-silver workings near Einasleigh (Kaiser Bill), and 35 km east of Georgetown (Quest End). The mineralization at these localities is probably, at least in part, of Palaeozoic age.

Similar uranium deposits in the USSR

Deposits of the uranium-fluorine-molybdenum association have been reported from several other parts of the world (Staatz & Osterwald, 1956; Radusinovic, 1974; Mittempergher, 1974; Assereto *et al.*, 1976; Smirnov, in press) but those of the USSR appear to be most numerous and to have been most comprehensively investigated (Shcherbakov, 1966; Vol'fson, 1968).

The Soviet deposits are mostly associated with acid igneous provinces, and have been classified on the basis of ore-type, rock association, and geological environment, as follows (Smirnov, in press):

(1) andesite/diorite associations
a. hydrothermal uranium associated with dyke belts
b. hydrothermal molybdenum-uranium in palaeovolcancoes and 'exocontacts' of minor intrusions.
(2) rhyolite/granite associations
a. hydrothermal uranium in volcanic depressions
b. hydrothermal molybdenum-uranium in subvolcanic massifs.
c. hydrothermal molybdenum-uranium in explosion pipes and necks.
(3) andesite/rhyolite associations
a. hydrothermal fluorite-uranium deposits in erosional tectonic basins.

In deposits that are analogous to the Maureen deposit (type 3a) the following paragenetic sequence has been observed: quartz, albite; carbonate, hydromica; sulphide, carbonate; jordisite-pitchblende; fluorite-carbonate. It is believed that the ore minerals were deposited at a depth of 300-1500 m below the surface, and at about 150-200°C (pre and post-ore fluids had temperatures of 300-350°C and 80-150°C respectively). Points of particular interest are the importance of flat-dipping faults, and especially intersections of them, in localizing ore, and the commercial importance of fluorine.

In the group of deposits related to rhyolitic/granitic rocks. (type 2), stockwork and, to a lesser degree, vein deposits of either simple or complex mineralogy are the most important. Most are localized in depressions of volcanic origin, and only a few are located along major faults in the basement of depressions which have filled with the vent facies of palaeovolcanoes. All are related to intrusive/extrusive complexes of rhyolitic/granitic composition, and formed as a result of post-volcanic hydrothermal activity, under 'semi-platform' conditions— after the cessation of intense volcanic eruptions and intrusion of hypabyssal bodies. The position of the deposits is believed to have been determined by the fields of discharge of hydrothermal systems. These are restricted most commonly to open faults and zones of intense jointing in the volcanics, explosion pipes and necks, marked depressions in the surface during the period of ore formation, and the most permeable layers in flows. Tuffite, tuffogenic sandstone, and agglomerate below dome-like flows of quartz porphyry overlying andesitic lava and agglomerate, and areas topographically above and close to concealed felsite dykes, are also favourable sites. Ore bodies are accompanied by hydrothermally altered zones from which much Na_2O and SiO_2 have been removed. They are confined to rocks with high effective porosity (more than 10 percent), high permeability (more than 0.5 md), low compressive strength (less than 200 kg/cm^2), and an elastic modulus of less than 5×10^5 kg/cm^2. Conversely, compact, poorly permeable rocks with high compressibility and low porosity do not contain ore (Smirnov, in press). The nature, orientation, and abundance of fractures, especially joints, in normally non-permeable rocks such as lava and welded tuff, is of great importance. Generally speaking, vein-type mineralization is confined to an upper zone 300-500 m below the surface, and does not contain much sulphide material, whereas stockwork and layer-like bodies are confined to a lower zone 1000-1200 m below the surface, which contain molybdenum and lead sulphides in addition to pyrite. The molybdenum content

appears to be of commercial significance. Following is an example of the sort of paragenetic sequence in these types of deposits: (1) quartz-hematite-feldspar veins; (2) albite, calcite, fluorite, apatite, quartz, pyrite (barytes); (3a) pitchblende, coffinite, calcite, pyrite; (3b) pitchblende, molybdenite, galena, sphalerite, and sericite.

Formation and preservation of mineralization

Source

It is apparent from the chemistry and volume of the igneous rocks in the northeast Queensland province, and their close relations with uranium deposits, that late Palaeozoic magmatism, directly and indirectly, was capable of mobilizing considerable quantities of uranium. Sheraton & Labonne (in press) have shown that some of the igneous rocks, particularly some granitoids, are enriched in uranium relative to normal crustal abundances, and that some acid volcanics have apparently been leached of uranium, possibly by late-stage metasomatic fluids. Furthermore, there is abundant evidence of late Palaeozoic hydrothermal activity throughout the province, much of it associated with tin and base-metal mineralization. It seems likely, as demonstrated by Bohse *et al.* (1974), and Smorchkov (1966), that at least some of these hydrothermal fluids, particularly those derived from the most highly fractionated magma, would have been even more enriched in uranium than the enriched granitoids that crystallized from these magmas. They were probably the most important source of uranium during the late Palaeozoic. The Maureen and Laura Jean deposits have apparently formed from such sources, as have most uranium-fluorine and uranium-molybdenum deposits in the USSR (Shcherbakov, 1966; Smirnov, in press).

Other potentially important sources of uranium are metasomatic fluids that leached alkalis, uranium, and possibly base metals from the acid volcanics during hydration and devitrification of the cooling volcanic pile after addition of groundwater (Sheraton & Labonne, in press). The volume of volcanics thus affected can be estimated at hundreds of cubic kilometres, and the quantity of uranium leached could have been enormous, even if the volcanics were depleted by only a few parts per million.

Groundwaters that passed through (1) the highly fractionated granitoids with their high background uranium content; or (2) the volcanics and granitoids with lower background uranium; or (3) either hydrothermally or metasomatically formed concentrations; could also have provided uranium for re-concentration under appropriate conditions at any time since the late Palaeozoic. For some deposits the uranium could have been derived from all three sources, either sequentially or simultaneously.

The distribution of potential source areas of uranium-enriched hydrothermal fluids—the most highly fractionated granitoids within the igneous province—is not known precisely. However, as these rocks are also enriched in, and apparently the source of all, or most, lode tin, tungsten and molybdenum deposits, the distribution of the tin (Fig. 3) may be taken as a rough guide to their distribution, although the uranium, which is more mobile than tin, probably has a wider distribution. Potentially, a very much greater area could contain uranium deposits. This is because the volcanic rocks extend beyond the area of highly fractionated granitoids, as do suitable host rocks that are effectively connected with possible source regions. Mineralization is apparently not confined to one side of the Tasman Line—thus the type of basement appears not to be of critical importance. The entire late Palaeozoic acid igneous province is therefore *a priori* a uranium province.

It is not known whether all similar acid igneous provinces contain associated uranium deposits, and if not, why not. However it seems likely that one essential control is the degree of fractionation achieved by the acid magma. Possibly only the most highly fractionated magmas will mobilize sufficient uranium for the formation of ore deposits. The presence of significant quantities of tin within any such petrographic province may be an indication that fractionation has proceeded to an adequate degree.

Channelways

The existence of physical connections or channelways between sources of mineralizing fluids and potential mineral deposit hosts must be a critical factor in determining the distribution of mineralization. The type and nature of suitable channelways would depend to a certain extent on the nature and location of both the source and host of the mineralization. Vertical and steeply dipping channelways may provide the mineralizing fluids with direct access to overlying hosts (e.g. Maureen deposit, Fig. 5) or to less steeply dipping channelways that permit lateral movement to a more distant host. In general, permeable fault and fracture zones, particularly those with considerable depth and strike length, and with long, complex histories could be the most effective of the 'vertical' channelways; breccia pipes, dykes, and short fractures in the contact zones of intrusives would be less so. It is likely that the wall-rocks of those structures that have been traversed by metalliferous fluids will be hydrothermally altered (Omel'yanenko, 1966), and that there will be mineral deposits in some (e.g. Laura Jean). Unfortunately such structures crop out poorly unless filled with a later dyke, and little is known of their nature or distribution within the province. However, as discussed earlier, the Landsat imagery of the Cairns-Townsville hinterland reveals a pattern of lineaments (Fig. 2), indicating that major basement fracture systems extend across the Tasman Line and throughout the province. Furthermore, many of these fractures were apparently active at least intermittently during a considerable period of time, and probably influenced the shape and distribution of various igneous bodies, and also the passage of hydrothermal fluids. Flat-lying permeable structures, such as unconformities, flow-surface irregularities, hydrothermally altered zones, gently-dipping faults and joints, and permeable sedimentary beds can also be important in directing the movement of ore fluids as well as being favourable sites for the deposition of ore. Such structures are common in the volcanic complexes of the province.

Deposition sites (Fig. 7)

Zones of high porosity and permeability within 300 to 1500 m or so of the surface, which were accessible to mineralized hydrothermal fluids at temperatures of about 150 to 300°C, appear to have been the most favourable sites for the deposition of uraniferous ores of the types described, and which are represented in northeast Queensland by the Maureen deposit. The physical properties of such rocks in the USSR have been measured (Smirnov, in press), and were provided earlier. High porosity and permeability are necessary in potential host rocks for the inwards flow of mineralizing fluids and the subsequent entrapment of the minerals by precipitation in voids, and by replacement of some of the rock constituents. Such porosity and permeability may be of sedimentary, diagenetic, volcanic, hydrothermal, or tectonic origin, but flat or gently dipping, porous and permeable sedimentary rocks at the base of acid

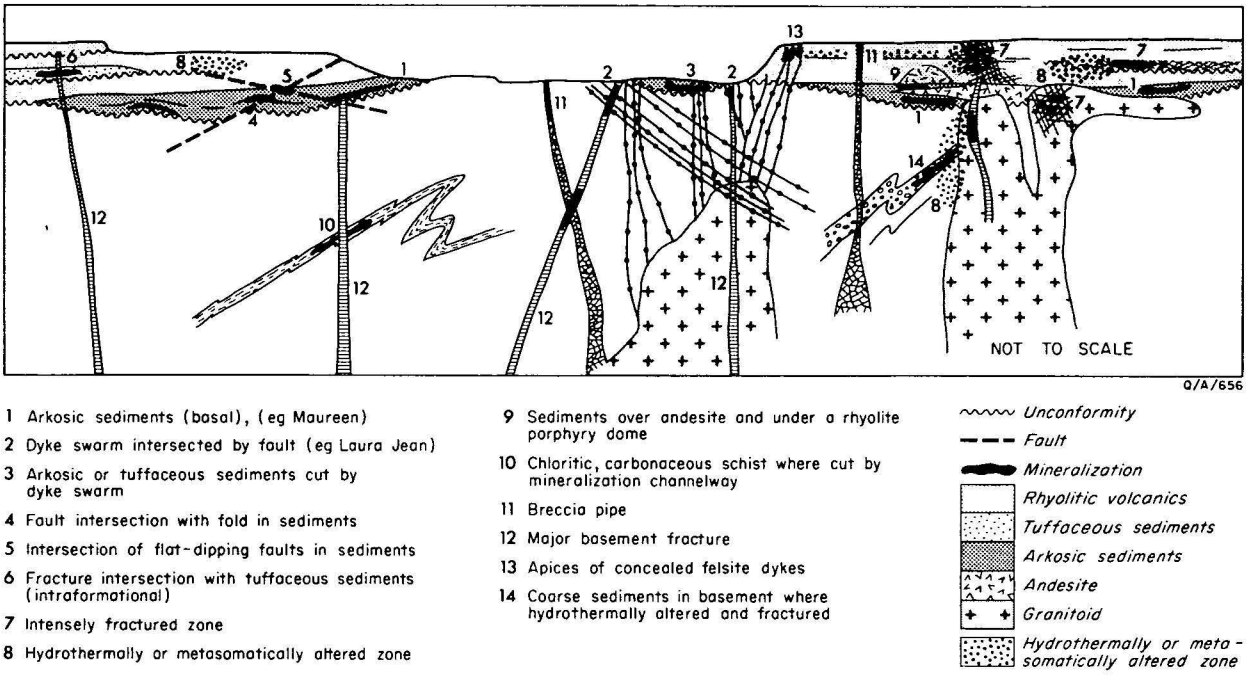

Figure 7. Some possible sites for concentrations of uranium (± fluorine ± molybdenum).

volcanic piles (e.g. Maureen deposit) are possibly the most suitable hosts, especially for layer-like and stockwork deposits. The orientation, width, and spacing of multiple joint sets can combine to give high porosity and permeability normally absent in otherwise compact, poorly permeable rocks. Hydrothermal alteration zones (Omel'yanenko, 1966), breccia pipes, fault zones (especially the intersections of flat-dipping faults), unconformities, flow-top breccias or irregularities, and fold hinges where faulted or fractured, may, besides providing channelways for mineralizing fluids, provide suitable conditions for the formation of deposits or the localization of the highest grade ore, in basement, volcanics, or granitoids. Some of the criteria discussed by Grutt (1971) in relation to sandstone-type uranium deposits probably apply to the deposition of uranium within the sedimentary units in the province, especially groundwater sources of uranium, or modifications to existing concentrations by groundwater movement. In particular, the presence of alternations of permeable and non-permeable beds, pyrite, and carbonaceous material in these sediments can be regarded as favourable factors in the determination of suitable hosts.

Preservation and exposure

The absence of major post-Palaeozoic tectonic activity or metamorphism, decreased groundwater movement —through climatic or structural changes, and burial by later volcanics or sediments—could have contributed to the preservation of the deposits. Such conditions have all operated locally or regionally, temporarily or continuously, throughout the province since the late Palaeozoic, resulting in generally low, but locally variable, rates of erosion and flushing.

It is likely that many deposits have been preserved but not yet exposed, or only poorly exposed, because many of the most suitable sites for deposition of economic concentrations of ore minerals lie at the base of, or deep within, thick piles of acid volcanics.

Furthermore, much potentially mineralized ground lies buried beneath Mesozoic and Cainozoic sediments in the west and northwest of the area of interest, and there are large areas within the province where mineralization could be concealed beneath Cainozoic basalt or terrigenous sediments, and others where it may be equally hard to find because of deep weathering and laterite.

Acknowledgements

I gratefully acknowledge the assistance of many colleagues, in particular, Brian Oversby, whose painstaking mapping and study of the Newcastle Range has indicated the variety of potentially mineralized environments that exist within the volcanic formations of the region; John Sheraton for geochemical and petrological data; Ian Withnall (GSQ) for assistance in the acquisition of various data; Robert Melsom and Andrew Retter for drafting the figures; Lee Ranford, Ian Lambert, Stewart Needham, Dick Dodson, Geoff Derrick, Ian McLeod, Brian Oversby, and John Truswell for helpful suggestions for the improvement of the text; and my wife Peta for encouragement, and for typing the manuscript drafts.

I am especially grateful to Professor D. A. Brown for permitting access to a preprint of the English Language edition of 'Ore Deposits of the USSR' edited by I. V. Smirnov, and to Dr A. A. Opik and Mara Murnieks for translating various passages of the Russian Language edition of 'The Geology of Hydrothermal Uranium Deposits' edited by D. I. Shcherbakov.

References

ASSERETO, R., BRIGO, L., BRUSCA, C., OMENETTO, P., & ZUFFARD, P., 1976—Italian ore/mineral deposits related to emersion surfaces, a summary. *Mineralium Deposita*, **11**, 170-9.

BAIN, J. H. C., OVERSBY, B. S., & MACKENZIE, D. E., in press—Georgetown Project; *in* Annual summary of activities 1976, Geological Branch. *Bureau of Mineral Resources—Report.*

BAIN, J. H. C., OVERSBY, B. S., & WITHNALL, I. W., 1975—Georgetown Project, 80-85; *in* Annual summary of activities 1974, Geological Branch. *Bureau of Mineral Resources—Report* **189.**

BAIN, J. H. C., WITHNALL, I. W., & OVERSBY, B. S., 1976—Geology of the Forsayth 1:100 000 Sheet area (7660) north Queensland-Georgetown Project Progress Report. *Bureau of Mineral Resources—Record* **1976/4** (unpublished).

BLAKE, D. H., 1972—Regional and economic geology of the Herberton-Mount Garnet area, Herberton tinfield, north Queensland. *Bureau of Mineral Resources—Bulletin* **124.**

BLAKE, D. H., 1974—An analysis of metal distribution and zoning—the Herberton tinfield, north Queensland, Australia: discussion. *Economic Geology*, **69**, 557-62.

BOHSE, H., ROSE-HANSEN, J., SORENSEN, H., STEENFELT, A., LOVBORG, L., & KUNZENDORF, H., 1974—On the behaviour of uranium during crystallization of magmas—with special emphasis on alkaline magmas, 49-61; *in* FORMATION OF URANIUM ORE DEPOSITS. *International Atomic Energy Agency, Vienna.*

BRANCH, C. D., 1966—Volcanic cauldrons, ring complexes, and associated granites of the Georgetown Inlier, Queensland. *Bureau of Mineral Resources—Bulletin* **76.**

CHAPPELL, B. W., & WHITE, A. J. R., 1974—Two contrasting granite types. *Pacific Geology*, **8**, 173-74.

DE KEYSER, F., & LUCAS, K. G., 1968—Geology of the Hodgkinson and Laura Basins, north Queensland. *Bureau of Mineral Resources—Bulletin* **84.**

DERRICK, G. M., 1977—Metasomatic history and the origin of uranium at Mary Kathleen, northwest Queensland. *BMR Journal of Australian Geology and Geophysics*, **2**, ...—...

DOUTCH, H. F., INGRAM, J. A., SMART, J., & GRIMES, K. G., 1970—Progress report on the geology of the southern Carpentaria Basin. *Bureau of Mineral Resources—Record* **1970/39** (unpublished).

GEOLOGICAL SURVEY OF QUEENSLAND, 1975—Queensland Geology, Scale 1:2 500 000. *Department of Mines, Brisbane.*

GRUTT, E. W., Jr., 1972—Prospecting criteria for sandstone uranium deposits, 47-78; *in* BOWIE, S. H. U. (Editor), URANIUM PROSPECTING HANDBOOK. *Institution of Mining and Metallurgy, London.*

HILL, DOROTHY, 1951—Geology, 13-24; *in* HANDBOOK FOR QUEENSLAND. *Australian Association for the Advancement of Science, Brisbane.*

HOYLE, M. W. H., 1974—Final report for year ended 31st December 1973, Authority to Prospect 1166M, Australian Anglo American Limited. *Geological Survey of Queensland Library* (unpublished report) CR4974.

INGRAM, J. A., 1974—Uranium deposits. *Bureau of Mineral Resources—Mineral Resources Report* **6.**

JACK, P. D., 1976—Queensland uranium discovery: *The Australian Financial Review* **3965** September 2, 1.

MITTEMPERGHER, M., 1974—Genetic characteristics of uranium deposits associated with Permian sandstones in the Italian Alps; 299-312; in FORMATION OF URANIUM ORE DEPOSITS, *International Atomic Energy Agency, Vienna.*

NEEDHAM, R. S., 1971—Mesozoic stratigraphy and structure of the Georgetown 1:250 000 Sheet area, Queensland. *Bureau of Mineral Resources—Record* **1971/100** (unpublished).

OLATUNGI, J. A., 1975—The geology and mineralization of west Herberton district, north Queensland. *James Cook University of North Queensland*, PhD Thesis (unpublished).

OMEL'YANENKO, B. I., 1966—Changes in the rocks immediately surrounding the hydrothermal deposits, (in Russian) 275-321; *in* SHCHERBAKOV, D. I., (Editor), GEOLOGY OF HYDROTHERMAL URANIUM DEPOSITS, *Akademiya nauk SSSR, Nauka, Moscow.*

O'ROURKE, P. J., 1975—Maureen uranium-fluorine-molybdenum prospect, Georgetown, 764-9; *in* KNIGHT, C. L., (Editor), ECONOMIC GEOLOGY OF AUSTRALIA AND PAPUA NEW GUINEA, Monograph **5**, 1: Metals, *Australasian Institute of Mining and Metallurgy, Melbourne.*

OVERSBY, B. S., PALFREYMAN, W. D., BLACK, L. P., COOPER, J. A., & BAIN, J. H. C., 1975—Georgetown, Yambo and Coen Inliers—regional geology, 511-16; *in* KNIGHT, C. L., (Editor), ECONOMIC GEOLOGY OF AUSTRALIA AND PAPUA NEW GUINEA, *Australasian Institute of Mining and Metallurgy, Melbourne.*

RADUSINOVIC, D., 1974—Zletovska Reka uranium deposits, 593-601; *in* FORMATION OF URANIUM ORE DEPOSITS *International Atomic Energy Agency, Vienna.*

SHCHERBAKOV, D. I., (Editor), 1966—GEOLOGY OF HYDROTHERMAL URANIUM DEPOSITS (in Russian), *Akademiya nauk SSSR, Nauka Moscow.*

SHERATON, J. W., 1974—Chemical analyses of acid igneous rocks from northeast, Queensland. *Bureau of Mineral Resources—Record* **1974/162** (unpublished).

SHERATON, J. W., & LABONNE, B., in press—Petrology and geochemistry of acid igneous rocks of northeast Queensland. *Bureau of Mineral Resources—Bulletin* **169.**

SMART, J., & BAIN, J. H. C., in press—Red River, Qld—1:250 000 Geological Series. *Bureau of Mineral Resources, Australia—Explanatory Notes* **SE/54-8.**

SMIRNOV, V. I., (Editor), in press—ORE DEPOSITS OF THE USSR, in 3 volumes, translated by D. A. Brown. *Pitman, London.*

SMORCHKOV, I. E., 1966—The significance of magmatic processes in the origin of hydrothermal uranium deposits, 119-46 (in Russian); *in* SHCHERBAKOV, D. I., (Editor), GEOLOGY OF HYDROTHERMAL URANIUM DEPOSITS, *Akedmiya nauk, SSSR, Nauka, Moscow.*

STAATZ, H., & OSTERWALD, F. W., 1956—Uranium in fluorspar deposits of the Thomas Range, Utah. *United States Geological Survey—Professional Paper* **300.**

TAYLOR, S. R., 1968—Geochemistry of andesites, 559-583; *in* AHRENS, L. H., (Editor), ORIGIN AND DISTRIBUTION OF THE ELEMENTS, *International Series of Monographs in Earth Sciences*, **30.** *Pergamon Press, Oxford.*

TAYLOR, R. G., & STEVENSON, B. G., 1972—An analysis of metal distribution and zoning in the Herberton tinfield, north Queensland, Australia. *Economic Geology*, **67**, 1234-40.

TUREKIAN, K. K., & WEDEPOHL, K. H., 1961—Distribution of the elements in some major units of the Earth's crust. *Geological Society of America Bulletin* **72**, 175-92.

VOL'FSON, F. I., (Editor), 1968—GEOLOGY AND PROBLEMS OF GENESIS OF ENDOGENIC URANIUM DEPOSITS (in Russian), *Akademiya nauk SSSR. Institut Geologii Rudnylch Mestorozhdenii Petrografic, Mineralogic i Geokhimii, Nauka Moscow.*

WHITE, D. A., 1962—Georgetown, Qld,—1:250 000 Geological Series. *Bureau of Mineral Resources, Australia—Explanatory Notes* **SE/54-12.**

WHITE, D. A., 1965—The geology of the Georgetown/Clarke River area, Queensland. *Bureau of Mineral Resources, Australia—Bulletin* **71.**

WITHNALL, I. W., 1976—Summary of mineral exploration in the Georgtown area *Queensland Government Mining Journal* **77**, 583-99.

WITHNALL, I. W., in prep.—Mines and mineral deposits of the Georgetown 1:100 000 Sheet area. *Geological Survey of Queensland—Report.*

WYATT, D. H., 1957—Limkins uranium prospect, Percyville. *Queensland Government Mining Journal*, **58**, 40-43.

WYATT, D. H., 1968—Townsville, Qld.—1:250 000 Geological Series *Bureau of Mineral Resources, Australia—Explanatory Notes* **SE/55-14.**

Geophysical response of heavy-mineral sand deposits at Jerusalem Creek, New South Wales

D. F. Robson and N. Sampath

Introduction

BMR has started evaluating how geophysical methods might assist in exploration for deposits of the heavy minerals rutile, zircon, ilmenite, and monazite.

Historically, exploration for these heavy minerals has concentrated on the search for high-grade onshore beach-sand deposits, and has employed surface sampling and shallow drilling. However there is a growing awareness that future exploration targets are likely to be low grade and perhaps either deeply buried or located offshore. Exploration directed towards these targets will require new exploration methods, particularly those which offer remote sensing capabilities.

BMR has begun a program of test surveys and laboratory investigations to establish the geophysical response of heavy-mineral deposits. As the first stage of these investigations, airborne and ground geophysical surveys were made over heavy-mineral deposits in the Jerusalem Creek area of NSW during 1975. Jerusalem Creek was chosen for the initial field investigations because of the variety and extent of heavy-mineral deposits in the area. The airborne survey (Fig. 1) was carried out over an area of 200 sq km of coastal plain south of Evans Head, and used magnetic and gamma spectrometer methods.

Ground surveys were conducted over the Evans West and GL 10 deposits, using magnetic, radiometric and induced polarization methods. The locations of the Evans West and GL 10 deposits are shown in Figure 1. The Evans West deposit is 2 km in length, 3 m thick, 30 m wide, and is covered by 3 m of overburden. The deposit has a fairly sharp grade cut-off at its boundaries, and averages about 10 percent heavy minerals comprising 36 percent zircon, 35 percent rutile, 25 percent magnetics, minor monazite and other minerals. The magnetic fraction is largely ilmenite. The GL 10 deposit has a similar mineral composition but the deposit consists of several parallel leads up to 40 m wide. The average grade of the deposit is only 1-5 percent, and the deposit is buried under only 0.5 m of cover. The magnetic, radiometric and induced polarization methods were used because the mineral assemblage of the Jerusalem Creek deposits suggests susceptibility, radioactivity and induced polarization contrasts between ore and the surrounding sands. The Evans West and GL 10 deposits were chosen as ground survey sites because extensive mine development drilling provided excellent geological control for the interpretation of geophysical results.

To establish the physical properties of heavy-mineral ores and to assist interpretation of the geophysical surveys, laboratory measurements of susceptibility, induced polarization and radioactivity were made of ore and sand samples collected from the Evans West deposit. The surveys at Jerusalem Creek were carried out in close co-operation with Associated Minerals Consolidated (AMA), whose assistance in the planning and carrying out of the survey is gratefully acknowledged.

Jerusalem Creek airborne survey

The main objective of this survey was to seek broad changes in the radioactivity and magnetic intensity of the sand ridges associated with heavy-mineral deposits.

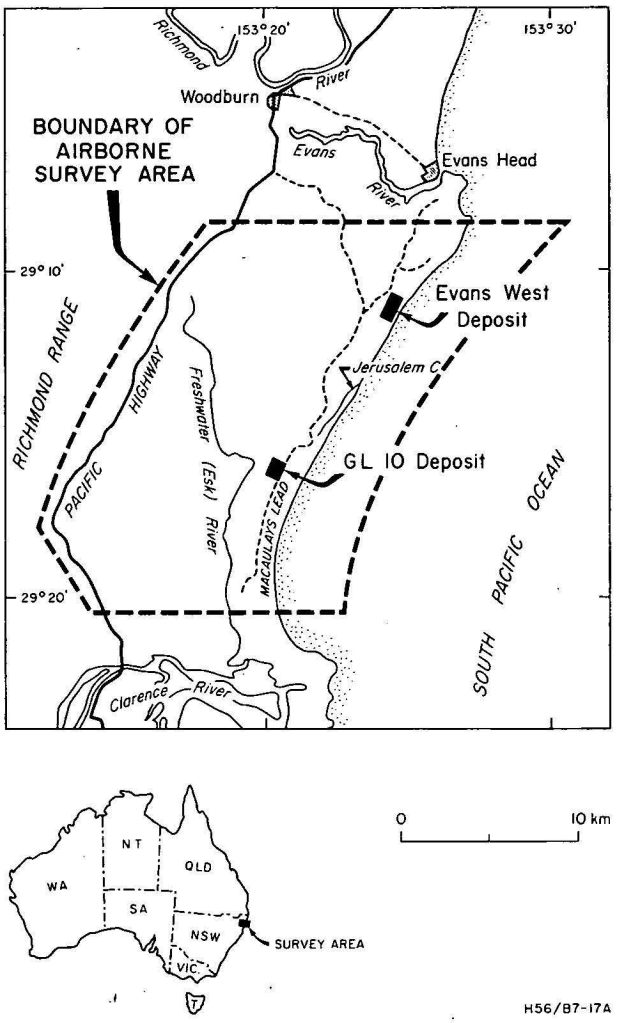

Figure 1. Locality map.

The survey was flown at an altitude of 100 metres, a traverse spacing of 400 metres and a speed of 180 km/hr. The radiometric survey was made with a differential 4-channel 3700 cm³ Hamner Harshaw gamma-ray spectrometer; and the magnetic survey used a BMR-designed fluxgate magnetometer with a sensitivity of 1 nT. The survey specifications were adequate to locate the broad sources sought, but were not suitable for detecting small isolated sources.

Radiometric results

Figure 2 shows the results of some total count radiometric traverses, which are superimposed on the geology (Nicholson, 1974) of the Jerusalem Creek area. The heavy-mineral leads are cross hachured. The radiometric results show a few large and some small radiometric anomalies on a low background of less than 3 μR per hr. Thorium anomalies with a radioactivity of up to 20 μR per hr were recorded over heavy-mineral stockpiles (area A), and smaller anomalies were observed over mining sites (area B) and along some sand ridges (area C). The results indicate

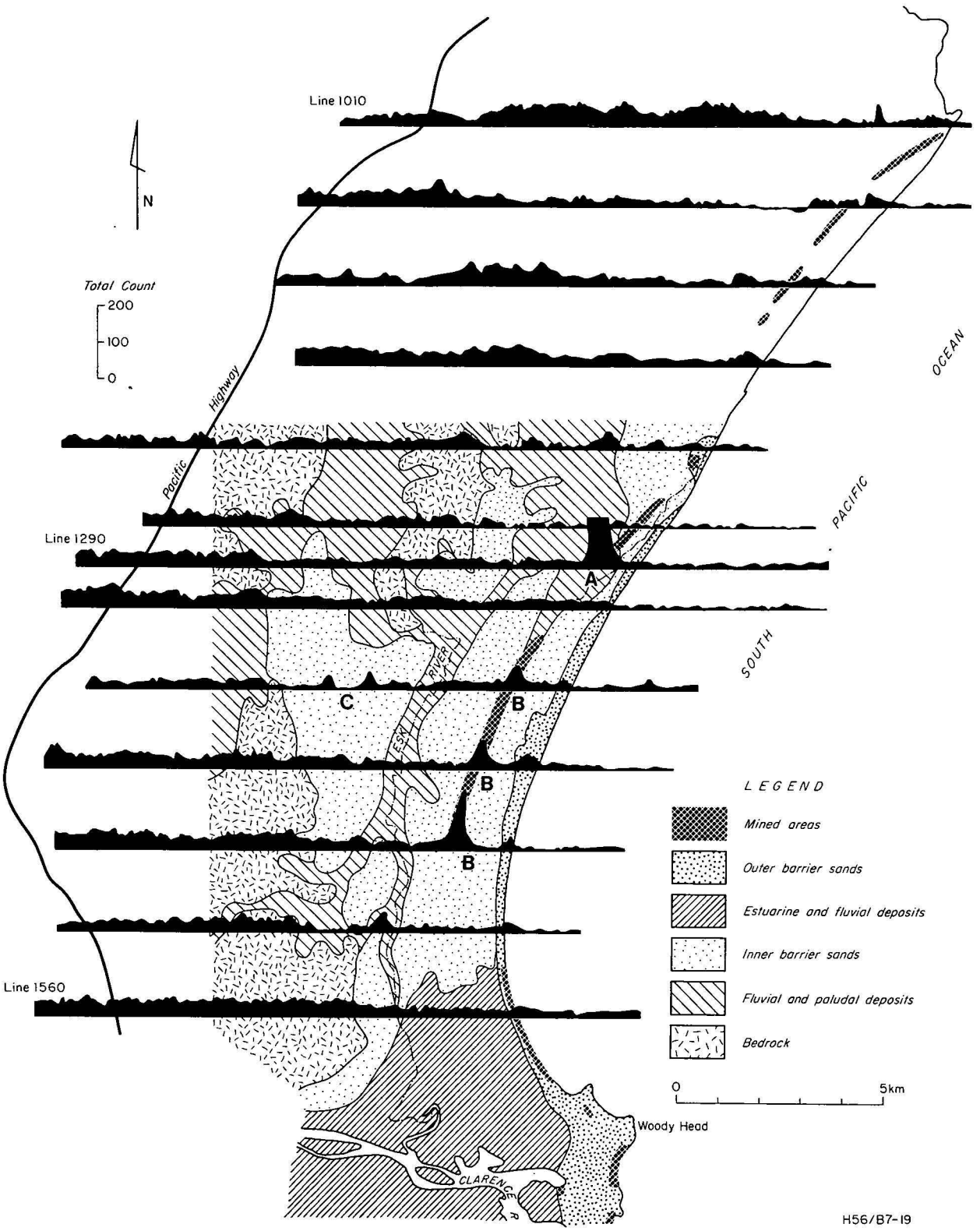

Figure 2. Airborne radiometric results.

that the heavy-mineral deposits at Jerusalem Creek are radioactive but that the radioactivity is easily masked by overburden.

Magnetic results

The results of the airborne magnetic survey show a positive, magnetic gradient of about 3 to 5 nT per km. The sources of all magnetic features are deep, and there is no indication of magnetic sources within or at the base of the beach sands.

Ground surveys at Evans West

Ground geophysical surveys employing magnetic, radiometric and induced polarization methods were made over

the Evans West deposit. Samples were also collected for laboratory measurements.

Figure 3 shows the results of averaging the heavy mineral concentrations in the Evans West area over a depth of 10 metres. The gap in the orebody between 600 N and 300 N is due to a large sand dune which has prevented drilling of the deposit in this area.

Magnetic survey

Magnetic surveys employing intensity, gradient and susceptibility measurements were made. The surveys were designed to detect small anomalies caused by the susceptibility contrast between the ore and the surrounding sands. The Evans West deposit contains about 0.01 percent magnetite and would probably have a susceptibility contrast of around 0.0005 SI units. Depending on the size and geometry of the orebody such a contrast might produce intensity anomalies of up to 5 nT if the deposit were buried no deeper than one or two metres.

The intensity survey was made with a proton-precession magnetometer of 1 nT sensitivity, and involved about fifty traverses across the orebody. Traverses were up to 300 m in length, were from 10 to 50 m apart, and used a station interval of 5 m. The results of the intensity survey show a variation of less than 15 nT over the survey grid, and indicated that there were no magnetic trends or anomalies associated with the ore deposit. Because of the low susceptibility and the considerable depth of overburden these results are not surprising.

A magnetic gradient survey was made along two traverses using sensors with a 4 m vertical separation and a proton-precession magnetometer of 0.1 nT sensitivity. This survey was designed to enhance the magnetic response of the orebody by measuring the rapid attenuation in intensity with distance from the magnetic body. No anomalies were detected on any of the traverses.

In situ susceptibility measurements on sand and ore were made throughout the survey area with a Bison susceptibility meter. No contrasts in susceptibility were observed.

Radiometric survey

The ground radiometric survey was carried out with a Geometrics DISA 400A, 4-channel gamma-ray spectrometer. About 30 traverses were made across the orebody, including several traverses where the overburden had been removed. The radiometric data were processed by removing non-geological background, and 'stripping' to separate the contributions to count rates from each of the radio-elements thorium, uranium and potassium. The results show that the radioactivity in the area is predominantly caused by thorium; anomalies up to 50 times background occur over exposed mineralization. The results only reflect the ore zone where the overburden was stripped.

Monazite accounts for 0.2 percent of the heavy minerals and is presumably the radioactive source. Although the ore is highly radioactive, 3 metres of overburden completely blankets the response.

Electrical survey

The electrical surveys used magnetic induced polarization (MIP) and electrical induced polarization (EIP). They were designed to detect a possible electrical property contrast between the ore and silica sands. MIP (Seigel, 1974) was used as the main technique because it offered easier resolution of small shallow sources and could overcome the problem of the high contact resistances expected. Few EIP traverses were made over the orebody.

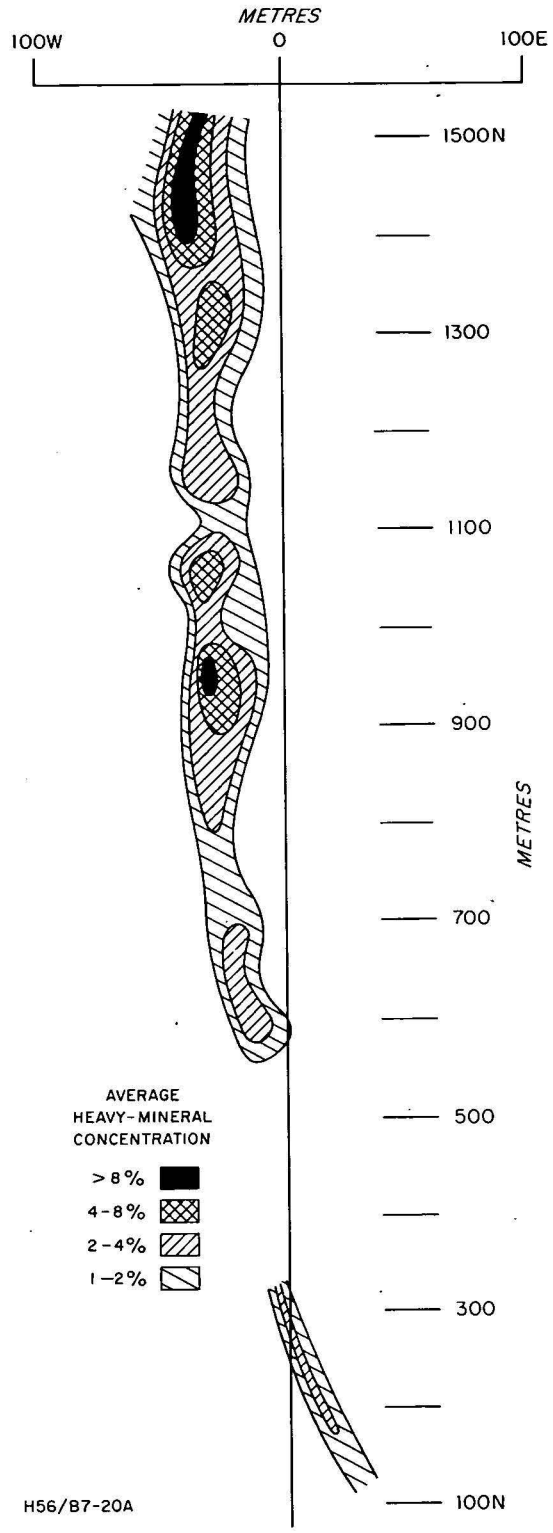

Figure 3. Average heavy mineral concentration Evans West.

MIP. Figure 4 shows stacked profiles of the MIP chargeability. Anomalous values are shaded in black, and non-anomalous zones dotted. Black lines show the outline of the orebody as known from auger hole sampling.

Overall there is good correlation of anomalous MIP chargeability with concentrations of heavy minerals. Westerly extensions of four northern lines and easterly extensions of four southern lines show typical background responses.

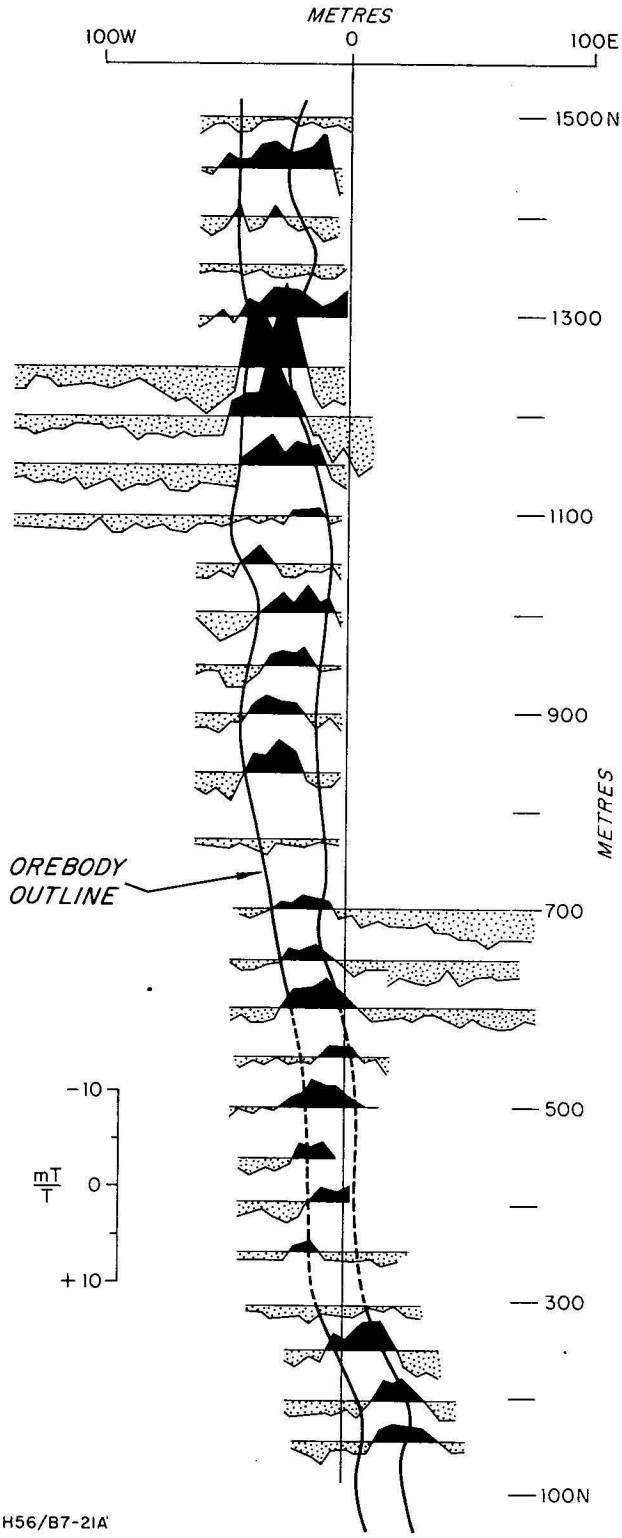

Figure 4. Chargeability.

The anomalous responses average −3 mT/T and the background level is from 2 to 3 mT/T. The chargeability response indicates that the ore zone is continuous between 600 N and 300 N, where auger sampling was not possible.

At every chargeability measurement, the normalized magnetic field strength is also determined. This parameter is similar to a measurement of relative conductance and can be used to detect changes in the resistivity of the ground. At Evans West this parameter was fairly uniform and the results indicate that the heavy-mineral deposits have a similar resistivity to the unmineralized sands. This deduction was substantiated by subsequent laboratory measurements.

There was no information on the nature or location of heavy-mineral concentrations in the shape of the MIP decay curve.

EIP. EIP traverses were made across the Evans West deposit using the dipole-dipole array, with a dipole spacing of from 5 m to 10 m. Too few traverses were made to allow a satisfactory comparison with the MIP results, but small anomalies were recorded over the heavy-mineral zone which were less well defined than the MIP anomalies.

Physical property measurements

Samples of ore, overburden and unmineralized sand were collected from the Evans West area, and laboratory measurements of susceptibility, resistivity, IP effect and radioactivity were made. The results of the measurements are summarized in Figure 5.

Susceptibilities of all samples were low; resistivities showed no apparent contrasts between mineralized and unmineralized sand. The most significant physical property was the IP effect and the largest effects were associated with the magnetic fraction of the ore which contains 70 percent ilmenite. The ore was highly radioactive, and spectral analysis shows that thorium daughter-elements were the main source of radioactivity.

PHYSICAL PROPERTY MEASUREMENTS OF BEACH SANDS JERUSALEM CREEK, NSW

DESCRIPTION	SUSCEPTIBILITY	RESISTIVITY (ohm-m)	IP EFFECT (mV/V) AT 50 ms	RADIOACTIVITY ($\mu R/h$)
DUNE SAND	LOW	300-400	< 5	2 - 5
ORE	LOW	300-500	10 - 30	40-60
MAGNETIC FRACTION OF THE ORE	LOW	100-300	80-100	< 5

H56/B7-22A

Figure 5. Physical property table.

Ground surveys at GL 10

Ground geophysical surveys using magnetic, radiometric and MIP methods were made along four traverses to the north and four traverses to the south of the GL 10 deposit.

Magnetic and radiometric survey

As at Evans West the magnetic results show no trends or anomalies associated with the heavy-mineral leads. The radiometric survey results were also similar to those recorded at Evans West. Where heavy minerals were exposed at the surface a high thorium count rate was detected, but in undisturbed areas a low uniform count rate was recorded.

MIP survey

Figure 6 shows the results of the MIP survey at GL 10 as stacked chargeability profiles superimposed on the heavy-mineral concentrations. The outline of the heavy-mineral concentrations has been determined by averaging the heavy-mineral grade over a 3 m interval; boundaries of the heavy-mineral concentrations are defined as 0.5 percent. Small but

persistent MIP anomalies appear to correlate with the known heavy-mineral leads.

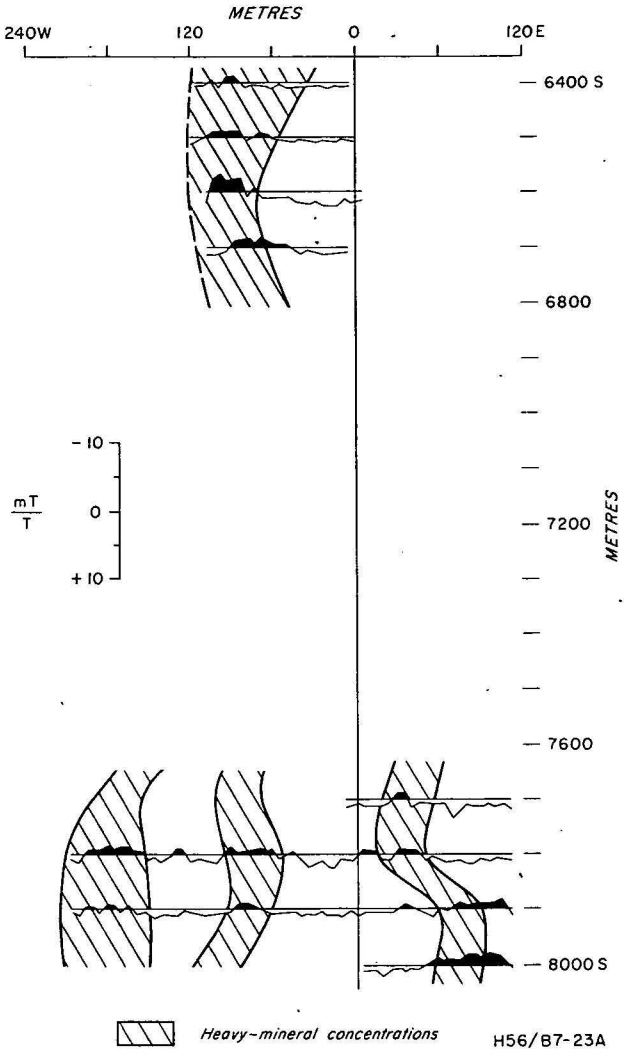

Figure 6. GL 10 chargeability results.

IP survey over heavy-mineral stockpiles

The source of the IP anomalies detected by the MIP and EIP surveys at Evans West and GL 10 was investigated by IP surveys over three heavy-mineral stockpiles at the Jerusalem Creek processing plant. The surveys were carried out using an EIP, dipole-dipole array with an electrode spacing of 5 m. The first stockpile (a) contained heavy-mineral concentrations after the removal of silica; the second (b) consisted of heavy-mineral concentrates after the removal of silica and magnetic products; and the third (c) stockpile contained the magnetic fraction of the heavy minerals and consisted of over 70 percent ilmenite. Results are shown in Figure 7. The traverse across the mineral dump with the silica removed recorded a peak chargeability response of about 32 ms with background of about 7 ms; and over the dump of heavy minerals with both silica and magnetics removed a low chargeability response of about 5 ms. However chargeabilities in excess of 120 ms were measured over the dump containing the magnetic fraction.

The results of the short traverses over these stockpiles show that the IP effect recorded is due to the magnetic fraction of heavy-mineral sands. This conclusion was supported by laboratory measurements.

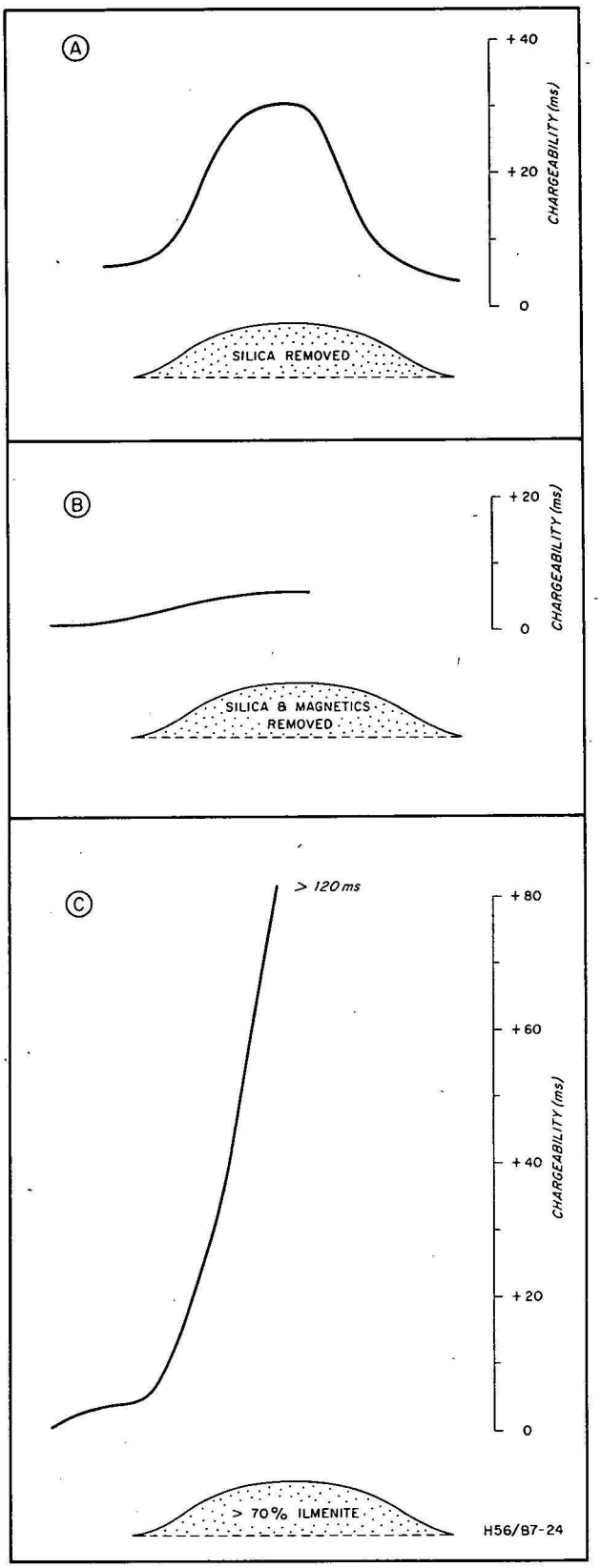

Figure 7. IP results over stockpiles.

Discussion and conclusions

Geophysical surveys over heavy-mineral deposits in the Jerusalem Creek area, NSW, were made with the magnetic, radiometric and induced polarization methods.

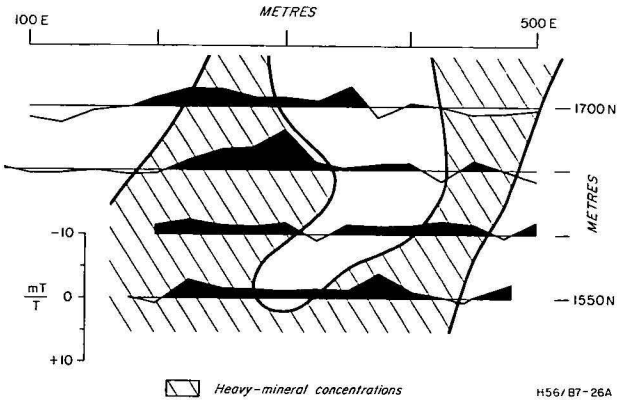

Figure 8. Lanherne Beach MIP results.

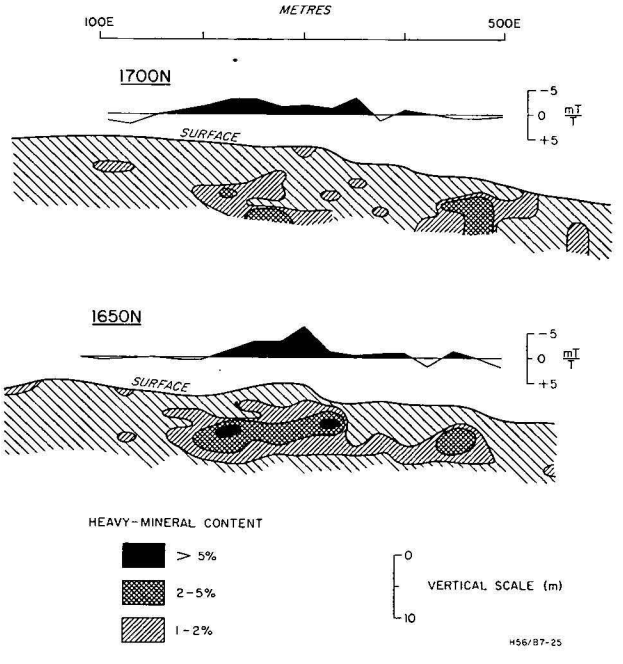

Figure 9. Lanherne Beach MIP results.

Induced polarization and in particular the MIP method is capable of detecting and outlining both high and low-grade deposits. Laboratory and field measurements show that the IP response of the heavy-mineral deposits in the Jerusalem Creek area is due to the ilmenite content of the deposits.

Magnetic surveys did not produce a response which could be directly related to heavy-mineral concentrations. This observation can be explained by the low susceptibility of the ore at Jerusalem Creek.

Measurements made in the laboratory and in mine workings show that the heavy-mineral deposits are highly radioactive, but owing to the blanketing effects of overburden no radioactivity anomalies were recorded over *in situ* deposits.

Induced polarization, in particular magnetic induced polarization, and radiometric methods, may prove to be useful tools for prospecting for heavy-mineral deposits. However further work is necessary to establish in what environments, and in what operational modes, the methods could be used.

Following the MIP surveys in the Jerusalem Creek area, similar surveys have been made over a variety of heavy-mineral deposits by private companies. AMDEX Mining Ltd have kindly made available the results of MIP test surveys over heavy-mineral deposits at Lanherne Beach, King Island, Tasmania, and the results are shown in Figures 8 and 9.

Figure 8 shows the results of the MIP survey superimposed on the heavy-mineral concentrations at Lanherne Beach. The average of this deposit is about 1.5 percent; the hachured area outlines a zone of greater than 0.5 percent heavy minerals, averaged over a depth of 5 m. A reasonable correlation exists between MIP chargeability and the heavy-mineral concentrations.

Figure 9 is also from Lanherne Beach and shows that although the mineralization in cross-section is patchy and sporadic, the MIP chargeability gives a clear indication of the presence of heavy-mineral sands.

References

NICHOLSON, D. A., 1974—Selected onshore heavy mineral deposits—Jerusalem Creek Area; *in* THE MINERAL DEPOSITS OF NEW SOUTH WALES (Editors, MARKHAM, N. L., & BASDEN, H.,) *Geological Survey of New South Wales, Sydney*. 615-6.

SEIGEL, H. O., 1974—The magnetic induced polarization (MIP) Method. *Geophysics*. **39**, 321-39.

NEW ZEALAND JOURNAL OF GEOLOGY AND GEOPHYSICS

Publishes the results of research in the earth sciences in New Zealand, Antarctica and the South Pacific. It also includes research by New Zealand workers in other areas, and other studies which have particular relevance to earth science in New Zealand. The dissemination of information about earth science literature is seen as an important function and bibliographic studies, within the general scope of the Journal, are welcomed.

Since 1975, six numbered issues have been published in each annual volume. The *New Zealand Journal of Geology and Geophysics* forms an integral part of the DSIR exchange system. It can also be bought on subscription from the Publications Officer, Science Information Division, DSIR, P.O. Box 9741, Wellington, New Zealand. Subscription costs NZ$6.00 per volume, post free (surface mail).

Price of single copies NZ$2.00.

NEW ZEALAND JOURNAL OF GEOLOGY AND GEOPHYSICS

Vol.	No.			Per Issue NZ$	Per Vol. NZ$
15	1—4	1972	Mar, Jun, Sep, Dec	2.00	6.00
16	1—4	1973	Apr, July, Sep (INQUA), Dec	2.00	6.00
17	1—4	1974	1, 2, 3, 4	2.00	6.00
18	1—6	1975	1, 2, 3, 4, 5, 6	2.00	6.00
19	1—6	1976	1, 2, 3, 4, 5, 6	2.00	6.00

THE GEOLOGICAL SOCIETY OF AUSTRALIA

The Geological Society of Australia Incorporated has for its object the advancement of the geological sciences, and membership of various categories is open to individuals, institutions, and companies.

The *Journal of the Geological Society of Australia* contains general and specialized papers concerned mainly with Australasia. Some sections of the Journal are devoted to reviews of the geology of the various States. In addition, there are *Special Publications* and a *Tectonic Map of Australia and New Guinea*, available from the Society.

The Journal is issued quarterly, and subscription rates are as follows:—

To Members:	Included as part of annual membership fee	$Aust. 25.00
To Subscribers:		$Aust. 30.00 p.a.
	OR	$Aust. 7.50 per issue (post free).

The following publications may be obtained from the Honorary Administrative Officer, Geological Society of Australia Incorporated, 39 Hunter Street, Sydney. N.S.W. 2000—

Journal of the Geological Society of Australia*

Volumes 8-15	Each volume consists of two parts, each part costs $4.00 except for Volume 9 (2), the price of which is $7.00
Volume 16 (1)	Hard covered edition, $15.00 Soft covered edition, $7.50
Volumes 16 (2), 17 (1), 17 (2)	Each part costs $5.00
Volumes 18-20	Each volume consists of four parts, each part costs $5.00
Volumes 21-23	Each volume consists of four parts, each part costs $6.25, except for volume 22(1) which is out of print.

*Volumes 1-7 are out of print.

Special Publications

1. A survey of Geoscientists in Australia $0.30
2. Proceedings of Specialists' Meeting $6.75
   a. The Permian of Australia
   b. Palaeovolcanology
   c. Environmental Analysis in Sedimentology
   d. Granulite Facies
3. Symposium on Archaean Rocks
   Members $ 6.00
   Non-Members $12.00
4. Mesozoic and Cainozoic Palynology
   Members $ 8.50
   Non-Members $12.00
5. The Geology of Victoria $25.00
6. Dynamic Metamorphism: processes and products in Devonian carbonate rocks, Canning Basin, Western Australia.
   Members $10.00
   Non-Members $15.00
7. Tectonic Map of Australia and New Guinea (scale 1:5 000 000) $5.00

Contents

Page

P. J. Cook, J. B. Colwell, J. B. Firman, J. M. Lindsay, D. A. Schwebel, and C. C. Von der Borch
The late Cainozoic sequence of southeast South Australia and Pleistocene sea-level changes 81

B. R. Spies
Absolute electromagnetic scale modelling and its use in interpretation of TEM response 89

J. Draper
Environment of deposition of the Carlo Sandstone, Georgina Basin, Queensland and Northern Territory 97

L. P. Black
A Rb-Sr geochronological study in the Proterozoic Tennant Creek Block, central Australia 111

G. M. Derrick
Metasomatic history and origin of uranium mineralization at Mary Kathleen, north-west Queensland 123

P. J. Kennewell, S. P. Mathur, and P. G. Wilkes
The Lander Trough, southern Wiso Basin, Northern Territory 131

J. H. C. Bain
Uranium mineralization associated with late Palaeozoic acid magmatism in northeast Queensland 137

Notes

D. F. Robson and N. Sampath
Geophysical response to heavy-mineral sand deposits at Jerusalem Creek, New South Wales 149